Data-Driven Demand Management for Smart Grid

by

Mikhak Samadi Kouhi

Thesis submitted to the University of Ottawa
in partial fulfillment of the requirements for the
Doctorate in Philosophy degree in
Electrical and Computer Engineering

School of Electrical and Computer Engineering
Faculty of Engineering
University of Ottawa

Abstract

The concept of the smart grid has been proposed to modernize the power grid with efficient and comprehensive monitoring systems as well as autonomous and self-healing technologies. Demand response (DR) and demand side management (DSM) are two aspects of the smart grid. The first is used to control the demand and supply, and the peak-to-average ratio (PAR) of a distribution network, and the second is used to manage a site's energy consumption efficiently. This thesis focuses on reducing the need for importing extra electricity from resources outside the local distribution network using DR, DSM. First, a demand management model is described to optimize customer energy usage and consider their comfort within a sequential optimization model. A multi-layer and multi-objective optimization system is proposed at the energy consumption level to consider customer comfort and experience. The cluster-based sequential management approach is presented to improve customer comfort via appliance scheduling. To quantify thermal comfort, a thermodynamic solution is used for the heating ventilation, and air conditioning (HVAC) system to schedule thermal load and eliminate customer inconvenience on room temperature. Customer inconvenience refers to a condition that the use of an appliance does not meet the preferences of the customer. Moreover, the satisfaction of electric vehicle charging, constrained by minimum cost, and the preferred usage time for the non-interruptible deferrable loads are considered in this model.

Due to the uncertain demand profile of users, stochastic solutions for demand response problems enable utility companies to address the uncertainties in the customers' energy consumption. A stochastic DR approach is presented between an aggregator and residential customers during peak load periods, and the optimal outputs of customers and aggregator are determined. This probabilistic demand response management model uses a mixed-strategy Stackelberg game to maximize the profit of total energy reduction for the aggregator and to maximize the reward of demand reduction for customers. The proposed solution reduces the demand, PAR, and the overall energy costs for both customers and the grid while maintaining customer comfort. To perform a secure and robust energy

trading model with high scalable decentralized supervision, a mixed-strategy stochastic game model is integrated with energy blockchain to address uncertainties in DR contributions. This model utilizes the processing hardware of customers for block mining, stores customer DR agreements as distributed ledgers, and offers a smart contract and consensus algorithm for energy transaction validation. A novel consensus algorithm compatible with a DR problem is presented to incentivize customers to contribute to DR events and collaborate in block mining to gain monetary profits. The results demonstrate the security and robustness of the consensus algorithm for detecting malicious activities. In summary, this thesis proposes schemes that control grid demand and minimize energy usage while preserving user comfort, security, and economic fairness.

Acknowledgements

I would first like to express my gratitude to my supervisors Prof. Melike Erol-Kantarci and Prof. Henry Schriemer, for their valuable advice, kind supervision, continuous support, and patience during my Ph.D. study. I am thankful to Prof. Schriemer for engaging me in industrial projects and providing me a chance to collaborate with IEMS Ltd. in an internship program. Absolutely without Prof. Erol-Kantarci's motivation and continuous support, it would not have been possible to complete this work.

With many thanks to my doctoral committee members, I would like to show my gratuitous also to Prof. Kebriaei, Prof. Ruj, and Dr. Fattahi, who shared their expertise and knowledge unconditionally with me.

Dedicated to my parents

Table of Contents

List of Tables

List of Figures

List of Abbreviations

Term	Description
ADM	autonomous demand side management
AHP	analytic hierarchy process
AP	access point
API	application programming interface
ASHRAE	American Society of Heating, Refrigerating and Air-Conditioning Engineers
BPSO	binary particle swarm optimization
BFT	Byzantine fault-tolerant
CA	control agent
CBL	customer baseline load
CSM	cluster sequential management
DApp	distributed application
DER	distributed energy resources
DERMS	distributed energy resource management system
DG	distributed generation
DMS	distributed management system
DPoS	delegated proof of stake
DR	demand response
DRA	demand response aggregator
DS	distributed storage
DSA	digital signature algorithm
DSM	demand side management
DSO	distribution system operator
EMC	energy management center
EMS	energy management system

Term	Description
EV	electric vehicle
FERC	Federal Energy Regulatory Commission
G2V	grid-to-vehicle
GA	genetic algorithm
GUI	graphical user interface
HEMS	home energy management system
HVAC	heating ventilation and air conditioning
ID	identity
IEEE	Institute of Electrical and Electronics Engineers
IESO	Independent Electricity System Operator
IIoT	industrial internet of things
IoT	internet of things
LP	linear programming
LSA	load shed availability
MAS	multi-class appliances scheduling
MHO	multi-objective household appliance optimization
MILP	mixed-integer linear programming
MIMO	multi-input multi-output
MINP	mixed-integer non-linear programming
ML	machine learning
MLP	multilayer perceptron
MSG	mixed-strategy Stackelberg game
MTU	master terminal unit
NB	Naïve Bayesian
NE	Nash equilibrium
NLP	non-linear programming
NN	neural network

Term	**Description**
OEB	Ontario energy board
OSR	optimal stoping rule
PAR	peak-to-average ratio
PBFT	practical Byzantine fault-tolerant
PB	private blockchain
PK	public key
PLC	programmable logic controller
PLP	peak load periods
PMV	predicted mean vote
PoA	proof of authority
PoB	proof of benefit
PoE	proof of energy
PoEC	proof of energy consumption
PoEG	proof of energy generation
PoEM	proof of energy market
PoES	Proof of energy saving
PoL	proof of learning
PoS	proof of stake
PoW	proof of work
PPD	predicted percentage dissatisfaction
PSO	particle swarm optimization
PV	photovoltaic
QBPSO	quadratic binary particle swarm optimization
RTU	remote terminal unit
SaaS	software-as-a-service
SCD	smart consumer devices
SCADA	supervisory control and data acquisition

Term	Description
SE	Stackelberg equilibrium
SEP	smart energy profile
SHA256	secure hash algorithm 256
SK	secret key
SoC	state-of-charge
SVM	support vector machine
TDR	transactive demand response
ToU	time-of-use
V2G	vehicle-to-grid
V2V	vehicle-to-vehicle
VN	vehicular network
VPP	virtual power plant

List of Symbols

N	number of customers/players
i	index of customer
a	index of household appliance
T	number of time slots in a day
t	time index
M	total number of elastic and deferrable loads
$\mathcal{A}_i$	set of appliances belongs to customer i
$\|A_i\|$	total number of appliances of customer i
l_a^t	energy consumption of appliance a at time slot t
T_a	number of time slots appliance a operates
τ_a^t	appliance a status (ON/OFF) at time slot t
x_a^t	optimized consumption of appliance a at time slot t
χ_i^t	total optimized demand of customer i at time slot t
$\mathcal{A}_E$	set of essential loads
$\mathcal{A}_{El}$	set of elastic loads
$\mathcal{A}_D$	set of deferrable loads
$\mathbf{I}_a$	permissible interval for appliance a
t_a^s, t_a^f	starting and finishing time slots of appliance a
ρ_a	priority coefficient of appliance a
Δ	positive value
p^t	time-of-use pricing signal at time slot t
Q_{power}	thermal power
θ_{inside}	room temperature
$\theta_{preferred}$	preferred room temperature
$\frac{d\theta_{room}}{dt}$	variation of θ_{inside} and $\theta_{preferred}$

C_{room}	room thermal capacity
Q_{leak}	power leakage
$\theta_{outside}$	outdoor temperature
R	room thermal resistance
r	AHP priority value
m	number of criteria
n	number of alternatives
A_k	relative matrix for criteria k
i, j	index of alternatives
k	index of criteria
α_{ij}	relative rate
w_i^k	alternative i's weight in criteria k
w^k	criteria weight
ρ_i	priority of alternative i
N_A	number of aggregators
N_C	number of customers/clusters
H	number of time slots in a day
h	time index
$\boldsymbol{\tau}_{PLP}$	peak load periods
k_h	reward value from aggregator/CA at time slot h
r_h	reward value from DSO at time slot h
k_h^{min}, k_h^{max}	minimum and maximum boundary for k_h
l_h^i	load shed availability of customer i at time slot h
x_h^i	power consumption of customer i at time slot h
p_h^i	baseline load of customer i at time slot h
U_c^i	utility function of customer i
U_a	utility function of aggregator
E^i	minimum total consumption of customer i
M_h^i	maximum consumption of customer i at time slot h

β	profit function
Γ	game definition
$\mathcal{N}$	set of players
n	index of player
S^n	space of pure strategies of player n
d^n	index of pure strategy of player n
m_h^n	number of pure strategies of player n at time slot h
$s_{d^n}^n$	pure strategy of player n
U^n	payoff function of player n
$\rho_{d^n}^n$	probability value of a pure strategy of player n
σ_h^n	probability distribution of customer n at time slot h
s^*	best strategy
s^{-1^*}	space of best response strategies of customers except aggregator
itr	number of iterations
s_{itr}, f_{itr}	starting and finishing points
w_{itr}	window size at iteration itr
a^i	distance between point i and other points in the same cluster
b^i	distance between point i and other points in neighboring clusters
sil^i	the Silhouette value
N_d	number of CAs
E	number of DR events
e	index of DR event
A_i	availability value of customer i
R_i	reputation value of customer i
ρ_i	compliance ratio of customer i
arc_i	consensus value of customer i
χ	required mining energy
x_{i1}^{PV}	PV generation of customer i used for mining
x_{i1}^{demand}	demand of customer i used for mining

x_{i1}^{EV}	EV capacity of customer i used for mining
c_i^e	actual demand reduction of customer i at event e
r_i^e	desired demand reduction of customer i at event e
x_{i2}^{PV}	PV generation of customer i used for household demand
x_{i2}^{demand}	household demand reduction of customer i
x_{i2}^{EV}	EV capacity of customer i used for household demand
α	profit price of DSO
G	desired minimum energy reduction
l_i	minimum available reduction of customer i
β	reward value for customer demand reduction
A	scaling parameter
γ	reward value for block mining
θ	profit price of charging EV through PV
x_{i3}^{EV}	extra PV generation of customer i used for EV charging
P_i	total PV generation of customer i
$B_i^{current}$	EV current capacity of customer i
B_i^{min}, B_i^{max}	EV minimum and maximum capacity of customer i
d_i	essential household demand of customer i
σ_i	EV status of customer i
S_n	space of pure strategies of player n
U_n	payoff function of player n
U_d	utility function of DSO
U_c	utility function of customer
$\boldsymbol{\tau}_{Sup}$	network supervision time slots
N_{Cu}	number of customers
λ	security parameter
σ	HEMS signature
a_h^i	availability of customer i at time slot h
r_h^i	reputation of customer i at time slot h

c_h^i	compliance ratio of customer i at time slot h
arc_h^i	consensus value of customer i at time slot h
$\boldsymbol{r}_h^{-i}$	reputation vector customer i submits for other customers at time slot h
x_h^i	energy consumption of customer i at time slot h
w_h^i	PV generation of customer i at time slot h
e_h^i	EV discharging of customer i at time slot h
b_h^i	minimum required demand of customer i at time slot h
α_h^i	EV status of customer i at time slot h
δ^i	summation of demand reduction of customer i
p_h^i	predicted demand of customer i at time slot h
$\overline{r}$	trust threshold
rep_h^i	historical reputation value of customer i at time slot h
d_h	demand reduction reward value from DSO
q_h	mining reward value
T_h	EV minimum discharge capacity at time slot h
β_h^i	profit function of customer i at time slot h
U_{Cu}^i	utility function of customer i
U_{CA}	utility function of CA

Chapter 1

Introduction

1.1 An Overview of the Transition to the Smart Grid

Decades ago, the population was smaller in proportion to energy resources, and a smart distribution network with distributed functionality was not a serious concern. The traditional grid was fed from generators (such as natural gas, coal, nuclear and hydro) outside the urban areas, and the energy was brought into the cities by transmission lines. This centralized architecture is prone to wide-scale blackouts due to interruptions in some parts of the system and suffers from the lack of online solutions, communication platforms, and intelligent services to efficiently monitor and manage the electricity network. Smart grid was born out of the need for better use of distributed renewable resources, better management of demand, accurate metering, and fewer energy losses in distribution lines [1]. The smart grid is an interoperable system that enables bidirectional flows of energy and uses cyber-secure two-way communication and control capabilities to create new functionalities and applications [2]. Using smart grid technologies, the utility company can better control the peak demand and manage resources to avoid shutdowns and damages.

The transition from the traditional grid architecture to the smart grid architecture starts with demand side management approaches. Afterward, with the increase of distributed resources in networks and the need for communication and monitoring technologies, more smart grid features are developed to bring new and efficient controlling services. Demand reduction is an efficient approach in the smart grid that has emerged in the past few years. In this technique, the utility company reduces the likelihood of blackouts and network damage. It also eliminates the pressure on generation and saves on resources.

Technology convergence, in communications, computation, and control in distributed energy resources has led to the transformation of the grid, and its management [3]. We could extend this description to smart grid applications that supervise the distribution network. Regarding the requirements mentioned above, ancillary services, as defined by the Federal Energy Regulatory Commission (FERC) (Order 888), use the technologies and assets needed to make a reliable platform in both conventional and modern grids. The order addresses the required services in predefined time responses and latency boundaries [4]. Based on this standard, any open access transmission system must include scheduling and controlling features, voltage and frequency control, and necessary adjustments for power systems. Furthermore, with the smart grid's progress and high-demand management penetration, latency and processing time are becoming critical. Therefore, a high-speed processing and autonomous demand management system is needed to control consumption in the shortest available time. The utility company also needs to implement a distributed energy resource management system (DERMS) in the distribution network to control all the agents involved in demand, supply, and resource management.

Studies show that residential and commercial customers consume a significant portion (almost 75% [5]) of generated electricity. Based on this, the involvement of residential customers in demand reduction could benefit network control. Their contributions to demand reduction, injecting their renewable resources into the grid, and even sharing their energy profile information are examples of cooperation in the demand-supply balance program. Therefore, any solution with the engagement of customers on appliance load scheduling is categorized as a demand side management (DSM) technique that helps control energy consumption and may reduce the peak-to-average ratio [6, 7]. Consequently, the initial requirement for using consumers to participate in distribution network management is to install a home energy management system (HEMS) at their premises. HEMS is an intelligent device that uses a communication protocol to exchange messages such as pricing signals, load profiles, and peak load periods with some third party such as an aggregator or utility company. As a programmable unit, HEMS can implement different optimization models and algorithms for load scheduling.

Demand response (DR) solutions mainly focus on demand and supply balance in a distribution network. Frequently, the demand response model is implemented between the utility company and its consumers to control the distribution network and increase the profit of the users. Consumers can only minimize their consumption to reduce their expenses. The utility company can generate a demand response request to ask users to change their consumption preferences regarding an incentive-based profit function. Within the development of renewable energy generators and storage equipment (such as photovoltaic systems, wind turbines, battery storage, and electric vehicles), residential customers can generate their required energy and reduce their demand from the grid. This approach can reduce the customers' costs and lower the demand on the grid. Using distributed energy resources (DER) is another solution for demand response control. Prosumers are the consumers who own such DER and can sell their surplus generation to the grid and make money in return. Therefore, DER solutions can reduce electricity imports and avoid energy loss on the transmission lines.

The solutions mentioned above require fully connected infrastructure to link all the agents and exchange grid data such as electricity usage, pricing signal (if employing real-time or dynamic pricing), and distribution line load in a robust and secure platform. In addition, the utility company needs a secure data storage technology to keep a copy of the data and transactions for analyzing and processing the distribution network situation. In the traditional grid, the collected data were stored in a centralized data center but the process of storing data in and extracting data from a centralized data center was time-consuming, and the probability of losing data was high. To this end, blockchain technology is an appropriate solution that provides a distributed ledger architecture to connect smart agents and guarantees the security and privacy protection of demand response transactions. Moreover, distributing the computational cost in the blockchain is a unique feature suitable for smart grid applications.

1.2 Motivation

According to the Independent Electricity System Operator (IESO), Canada [8], peak time slots usually happen in the afternoons and evenings, once residential customers come back from work and start to use their high load devices such as their oven and dishwasher. Therefore, the total demand increases, and the utility company must supply extra energy for load balance. This comes with extra dispatch costs. Thus, increasing the supply to meet the demand during peak times requires over-provisioning of generation assets. Consequently, the solution would be to incentivize the customers to flatten demand. Household demand management must be aligned with the comfort factors and economic concerns of customers. This goal is achieved by enabling consumption profiles and establishing utility functions for demand optimization that incorporate these factors and concerns.

In the smart grid, the process of directly controlling all the agents through the utility company is a massive data processing burden and increases the processing time. Establishing a hierarchical structure between the utility company and customers would make it feasible to pass some control requests to aggregators. An aggregator is an agent that manages a local area, monitors its connected customers, controls supply and demand, and reports critical situations to the utility company. The aggregator is rewarded when it reduces the demand of its supervised local area during peak periods. For instance, in a high-demand situation, the aggregator can use a transactive energy model and offers demand reduction to the utility company and rewards to the customers. Usually, this approach involves a negotiation between the aggregator and customers in which both parties consider the reduction quantity and price. Therefore, an automated bidding strategy is required to handle real-time decision-making by minimizing the interactions and maximizing profits.

Low latency communication, data accuracy, customer privacy, and cyber security are the requirements of transactive demand response (TDR) [9]. TDR mainly focuses on the interoperability between the distribution network agents and applies smart grid standards and protocols for high-performance outputs. The purpose of the TDR in the digitized electricity grid is to implement a consistent hierarchical architecture connecting all sensing and actuating nodes, which supervise demand and energy resources. In the smart grid, grid stability (dynamic balance of supply and demand) is an increasingly sophisticated energy management problem that includes cyber security concerns, user privacy issues, and energy settlement processes [10]. For addressing these, a distributed, secure, and highly available data exchange architecture such as blockchain is required to increase the reliability of both electricity and data exchange in transactive networks.

1.3 Proposed Solutions

DERMS is an appropriate solution for large-scale systems with energy resources, demand management control, and monitoring techniques in a distributed infrastructure [11]. Advances in demand management in the smart grid have shown that demand response can significantly benefit the customers and the utility companies [6, 12]. Utility companies as principal agents have pursued various demand control approaches, including direct load control [13] and incentive-based indirect methods [14, 15]. To develop an incentive-based indirect model, the utility company relies on the aggregator [15] as the local energy community to supervise the transactions and control the balance [16]. Then the aggregator can offer monetary rewards to customers to reduce their demand at peak times.

In this thesis, we propose a DERMS system that has intelligent demand management techniques, smart agents, and a secure data exchange platform. Our proposed hierarchical transactive model is shown in Figure 1.1. The control model starts from the customer level (lower level), where we design a DSM system to implement a household demand scheduling model constrained by the comfort factors of the customer (such as temperature, appliance usage time, and cost). The following layers belong to the aggregators and distribution system operator (DSO). The aggregator as intermediary works between the DSO and customers to transfer the consumption data and control signals to reduce the processing load on the DSO. The DSO and aggregators are two entities that work together with distinct goals and payoff functions.

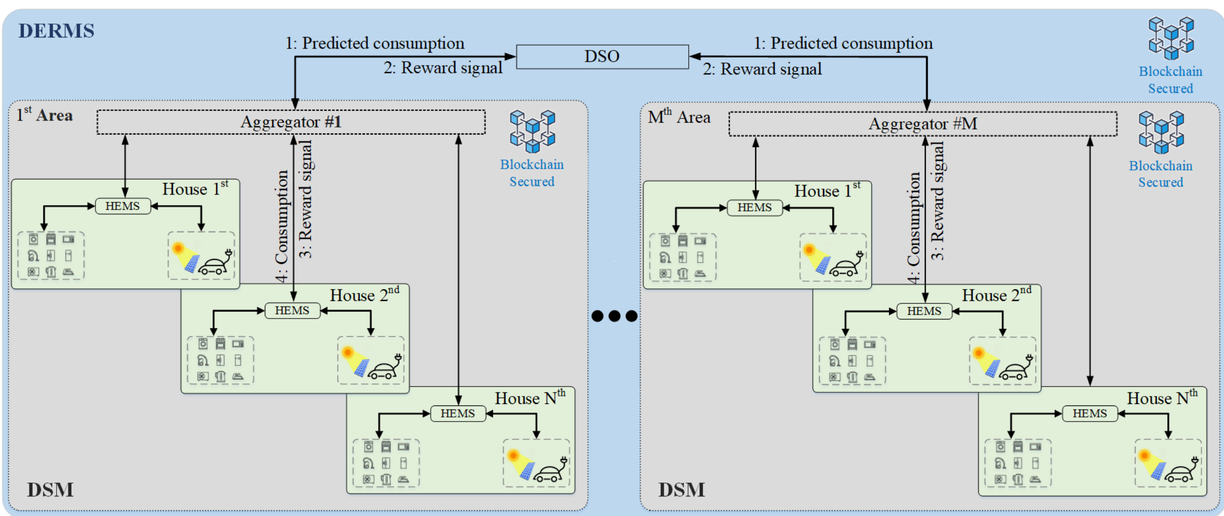

Figure 1.1: An overview of our proposed architecture.

A demand response model is presented in our DERMS to describe the ability of the DSO to manage the consumption of customers in response to distribution network load variations. Due to the uncertain energy consumption of customers and their unpredictable reactions to demand response offers, we take a stochastic demand response approach. Stochastic approaches can mitigate demand uncertainties through the use of probability distribution functions [17]. Finally, to have all these components working together, a secure and robust data exchange architecture is implemented to guarantee the performance of demand response transactions in our designed system. Accordingly, our collaborative demand response model is empowered by blockchain technology to secure energy transactions among customers and the DSO to address cyber security concerns, user privacy issues, node failure, and processing time of smart grid applications.

Most of the research on DSM, including residential level demand control, explores how to reduce the customer bill and the distribution network peak-to-average ratio [18]. Therefore, the first step in this demand management system is to start from the customer level to reduce and/or efficiently organize the customers' energy consumption. The residential demand management model is a trade-off between demand reduction and user comfort that alters the usage profile and reduces the peak usage. [19]. Customer comfort could be associated with appliance usage performance, delays in responding to utility company demand response requests, room temperature, etc.

Our proposed DSM approach preserves customer comfort using a multi-objective sequential optimization model to minimize the energy cost of appliance usage and distribute demand over time. The model is generalized by categorizing loads into clusters of load types to determine the effect of different categories on demand optimization. By equipping a house with a HEMS, appliance management allows residents to prioritize their appliances and adjust their settings based on their comfort factors. Then we maximize the customer convenience on thermal load according to the household thermal standards, increase their satisfaction on electric vehicle optimal charging constrained by minimum cost and time, and reach the optimal schedule time for the non-interruptible deferrable loads constrained by permissible intervals.

A TDR scheme emphasizes interoperability between the agents in a transactive energy architecture. Our proposed TDR scheme is designed to provide privacy and maximize customer participation and rewards so that they will comply with demand reduction. A demand response request is initiated by the utility company and allocated to the HEMS.

The HEMS implements a multi-input multi-output fuzzy controller to address negotiation and optimal reduction. The proposed architecture is compatible with the IEEE 2030.5 standard, which brings smart grid interoperability within a cyber-secure smart energy profile (SEP) context. The standard helps to transfer the control data using the RESTful application programming interface (API) in a specific data exchange format.

Among the various approaches in demand management, game-theoretic methodologies [20] are particularly appealing as they provide a conceptual framework for the formal description of the complex interaction between independent rational players. From the demand response game theory perspective, customers have typically been seen as agents interacting with the utility company and playing multiple independent (non-cooperative) games. Usually, demand response approaches consider day-ahead power consumption decision-making that brings uncertainty on demand management of the next day. So, a mixed-strategy game model, a probabilistic method, has the advantage of better managing the distribution network since it is a multi-level game theory model. We implement a probabilistic demand response approach using a mixed-strategy Stackelberg game between an aggregator and aggregations of customers in a local area. The game incorporates both customer lifestyle preference and fiscal incentives, as well as aggregator strategies for demand response. This is a sequential model in which the aggregator and customers are treated as a leader and followers in the game, respectively. The outcome is a Stackelberg equilibrium for the recommended strategies in that individual customers reach the optimal demand response reduction point constrained by their availability. The aggregator maximizes its profit due to its efforts in consumption reduction. Furthermore, forecast models allow load rescheduling and enable demand reduction while accommodating customer preferences. Consequently, this model reduces the total peak-to-average ratio of the grid and maintains user comfort and satisfaction.

The proposed multi-level architecture requires a flexible and fast converging distributed platform to develop a reliable transactional demand management system. Since a demand response offer is created, updated, or accepted by an agent, the transaction data must be stored on a secure and robust platform without a failure. An energy blockchain provides a distributed storing mechanism and enables rapid automated DERMS control. This scheme can validate the transactions before storing them on the blockchain and provides cyber security. We develop a demand response technique that uses the blockchain for DER saving [21] and data storage to incentivize the customers to maximize their demand reduction profit and energy savings. The blockchain solution brings a secure and robust demand response model, with high scalability, system management, and control without centralized supervision, that is useful to reduce the number of transactions at the DSO. In our energy blockchain, HEMSs are considered nodes of blockchain, following the design of the incentive-based energy management model, to engage the customers in the data storing process [22]. Therefore, we propose a demand response Stackelberg game between the DSO and customers empowered by the energy blockchain where the control agent (CA) as an intermediary agent monitors and controls the contributions of customers within a private blockchain. Our model incentivizes customers to maximize their demand reduction profit value, charge and discharge electric vehicle efficiently, and maximize their chance to gain rewards through block mining. We design an energy blockchain to store the energy transaction data securely and use the surplus household DER for the block mining process to reduce the waste of energy (unlike the traditional proof-of-work Bitcoin platform).

Both demand response and energy blockchain are random systems [23] that allow us to apply a stochastic model to examine the strategy scenarios of customers. Continuing our prior work, we propose a collaborative demand response model empowered by blockchain technology and game theory to reduce the randomness of customers participation and balance distributed demand and generation resources. We develop a mixed-strategy Stackelberg game model to achieve the best demand response contributions and maximize the profit of customers. This stochastic system provides a demand response settlement between the CA as the leader and customers as followers while considering possible demand response contributions (strategy scenarios) of players with different probability values. Rewards are allocated to the customers who reduced their demand and succeeded in block mining. Additionally, it enables customers to invest surplus energy (e.g., extra photovoltaic generation) and the processing hardware in block mining.

Here is a list of our published and submitted articles:

A . **M. Samadi**, J. Fattahi, H. Schriemer, M. Erol-Kantarci. Demand Management for Optimized Energy Usage and Consumer Comfort Using Sequential Optimization. *Sensors*, 21(1):130-146, 2021.

B . J. Fattahi, **M. Samadi**, M. Erol-Kantarci, H. Schriemer. Transactive Demand Response Operation at the Grid Edge using the IEEE 2030.5 Standard. *Engineering*, 6(7):801-811, 2020.

C . **M. Samadi**, H. Kebriaei, H. Schriemer, M. Erol-Kantarci. Stochastic Demand Response Management using Mixed-Strategy Stackelberg Game. *IEEE Systems Journal*, accepted in Feb 2022.

D . **M. Samadi**, S. Ruj, H. Schriemer, M. Erol-Kantarci. Energy Blockchain for Demand Response and Distributed Energy Resource Management. *IEEE Internet of Things Journal*, submitted in Dec 2021.

E . **M. Samadi**, H. Schriemer, S. Ruj, M. Erol-Kantarci. Energy Blockchain for Demand Response and Distributed Energy Resource Management. 12^{th} *IEEE International Conference on Communications, Control, and Computing Technologies for Smart Grids (SmartGridComm)*, 1:425-431, 2021.

In the following, we summarize our contributions.

- In [A], we present a DSM approach to optimize household demand using a multi-objective sequential optimization model to minimize the energy cost of appliances, distribute the demand over the time horizon, smooth the demand curve, and provide customer comfort.

- To process a transactive DR scheme between the utility company and customers [B], a probabilistic demand response approach using a mixed-strategy Stackelberg game between an aggregator and customers is presented in [C] to find the optimal energy reduction of customers constrained by their demand reduction availability and maximize the profit function of the aggregator on total demand reduction.

- In [D], we introduce a secure and robust demand response model that uses the mixed-strategy Stackelberg game integrated with energy blockchain to control demand at peak periods, maximize demand response profit for customers, increase their winning probability of block mining, and use the distributed processing hardware of the customers for the block mining. This model is a new DER saving mechanism using energy blockchain to develop a collaborative distributed storage system and interactive demand reduction in a residential area [E].

Chapter 2

Background and Literature Review

2.1 Introduction

In the past decades, supervisory control and data acquisition (SCADA) enabled remote monitoring, supervising, and controlling the electric network equipment, and it remarkably helped to improve the reliability of electricity flow throughout the network. SCADA employs a central controller, master terminal unit (MTU), and multiple outstation hardware including remote terminal units (RTUs) and programmable logic controllers (PLCs) distributed in the network [24]. RTU is an analog-to-digital converter that converts the sensors' signals and sends them to the controller. SCADA enables collecting a large amount of operational data from electric substations [25] and then monitoring and controlling the electric network. This technology accommodates the requirements of the distribution management system (DMS) [26] but it might not be a suitable solution for a low voltage distribution network (demand management approaches).

In the last twenty years, utility companies have started to obtain solutions for monitoring their distribution networks and reducing the damage and cost before the failure. In

2007, the smart grid concept emerged to modernize the grid [27,28]. Communication technologies give the ability to remotely meter the electricity usage of an individual house using smart meters and to integrate different parts of the distribution network to enhance monitoring with the help of two-way communications. Thus, all these developments provide a reliable and robust network with minimum loss of energy.

To deploy an intelligent energy management network, we need sufficient technologies and distributed infrastructure to work together simultaneously. In smart infrastructure, a utility company would be able to control the equipment in real-time and predict faults before they happen. This infrastructure calls for smart meters, energy resources, secure communication infrastructure, standard data protocol, and retailers. Due to our focus on demand management solutions in this thesis, we discuss smart grid management methods and review the existing technologies and projects in this section.

2.2 Distributed Energy Resource Management Systems (DERMS)

A modern grid should support four aspects: economics (forecasting and scheduling of resources and market operation); reliability (system assurance and security); resiliency (microgrid design and distributed architecture); and customer services (incentive models for customer coordination and transactive energy) according to [29]. Therefore, DERMS is an efficient solution that can consider all of these. DERMS is a large-scale distributed energy resources (DER) that may include renewable resources and storage devices to efficiently manage distributed infrastructure [30]. DERMS architecture should be transparent and able to monitor and control the system in real-time. It consists of optimization and management approaches for DER to bring a scalable system with maximum benefit and lower operational costs. Thus, DERMS technology can increase energy efficiency, reduce distribution loss, improve power quality, and provide market services for customers, self-organization, and storage optimization [31]. Figure 2.1 shows a DERMS model including DER.

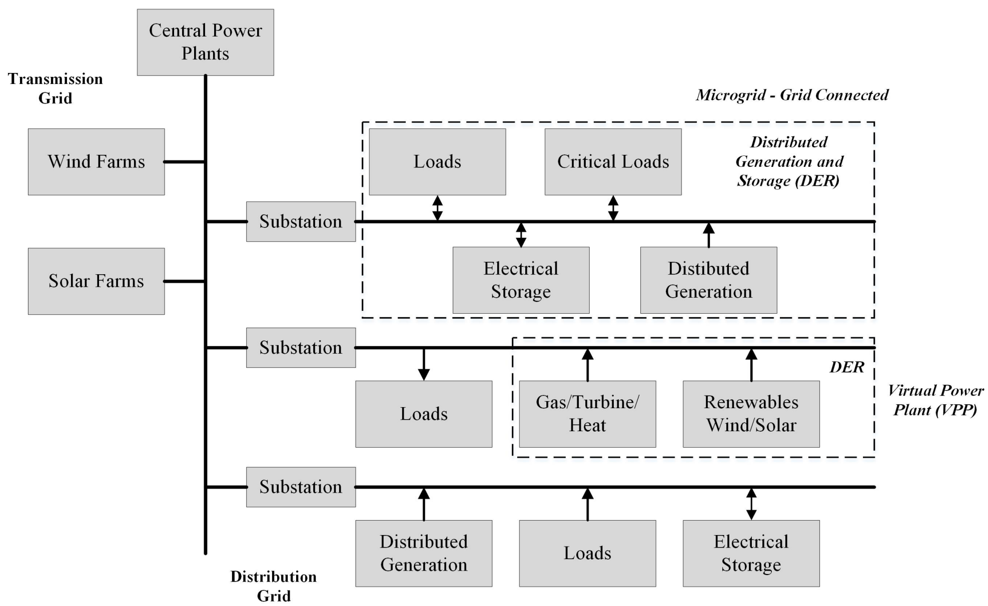

Figure 2.1: DER in transmission and distribution grid [11].

A DERMS is a software and hardware based mechanism to manage and control DER to enhance the performance of the electric distribution network [32, 33]. According to [34], DERMS consists of distributed generation, distributed storage, and demand response approaches. DERMS should have the ability to control and manage DER in an optimal way to improve the reliability of the grid and quality of service and be capable of predicting the grid demand profile based on the history and weather forecast [35]. To control the grid components and prioritize them to apply maintenance solutions in DERMS, the authors of [36] proposed an analytic hierarchy process (AHP) merging with fuzzy sets and called Fuzzy AHP. They solved a multi-criteria decision-making problem for asset management, and their defined criteria are the total number of components, total number of component failures, component repair duration, component investment cost, and component repair and maintenance cost.

In the article [29], the authors identified the aspects and applications that a modern grid should support, such as forecasting models, virtual power plant (VPP) (including renewable generators, storage system, and customer demand), and economic aspects. VPPs and microgrids are components of the DERMS system. An electricity network is connected microgrids if the agents (consumers and producers) be able to manage their load and generation independently using smart technology [37]. The principal idea of presenting microgrids is to increase the quality of services [38]. According to the article [39], a microgrid is a combination of demand, distributed generation, and distributed storage that are connected to other parts of the distribution network. VPP is an architecture that controls dispatching, applying demand management, and optimizing generation and resources with the software programming solutions [38]. In the article [40], the authors clustered a distribution network into microgrids and multi-microgrids based on the Monte Carlo algorithm and called it an active distribution network. The idea was to control the strategies of microgrids and increase reliability and management control. Additionally, they tested the accuracy of the microgrid system and determined its efficiency, voltage profile, and reliability. They found that as the microgrid shrank, the demand side management (DSM) capacity increased significantly, and demand and generation converged quickly. Based on [41], a multi-agent system is a system with smart agents that all collaborate for a specific goal. The authors in [42] developed a multi-agent system to control a microgrid distributed energy resources and loads using non-cooperative game theory to optimize the renewable energy resources (such as photovoltaic systems, wind turbines, battery storages systems, etc).

Notably, Duke Energy and Alstom Grid implemented a DERMS testbed project in Charlotte, NC in the US with 17,000 customers [43]. The architecture consisted of a demand response program, storage devices, photovoltaic systems, electric vehicles, sensors, and communication lines. They controlled the household heating, ventilation, and air conditioning (HVAC) systems using a forecasting model for the demand response. They equipped the grid with one 750 kW and two 25 kW storage substations and two different transformers. They installed one 50 kW and seven 2.37 kW photovoltaic systems in substations and roofs. They provided five electric vehicles and charging stations in the area. For network monitoring, they installed sensors working with Wi-Fi technology while electric vehicle charging stations, photovoltaic systems, batteries, and smart meters transfer their data through the power lines. The system is easily controlled and monitored with a dedicated graphical user interface (GUI).

In [44], the authors presented a decentralized monitoring project that increased reliability and reduced communication delay and single points of failure. System resiliency or a self-healing system is another feature they considered to return the system to the normal mode of operation after a fault. The authors developed a hardware-in-the-loop platform to control the grid, mainly by distributing the monitoring demand among the agents in the grid.

The following subsections present the solutions for DR, DSM and DER that are parts of DERMS technology.

2.2.1 Home Energy Management System (HEMS)

Due to the increase of residential energy consumption, smart home energy management system is one of the successful demand management solutions in smart grids. A HEMS can monitor and control various home appliances based on user preferences to minimize the electricity cost and enhance energy load profile [45]. On a large scale system (such as a residential area), by equipping houses with HEMS, we can improve distribution network efficiency, control energy usage, and reliability, as well as provide energy for distributed systems [46]. To this end, DERMS solutions could be integrated with home energy management systems to control the demand and supply better while residential customers can react (via their HEMSs) to the utility company's supervisory decisions. Therefore, HEMS allows customers to participate in energy markets and power saving activities by rescheduling the load profile constrained to cost and comfort [46, 47].

A home energy management system installs at the customer's place and executes demand management programs autonomously while enabling the customer to control and monitor the demand [48]. Based on the article [49], a home energy management system is designed for devices control with the assistance of ZigBee technology to bring a wireless solution with a high-level communication protocol and active sensors. There are uncertainties about the quality of services provided by different home energy management technologies for demand management. Thus, authors in [50] studied 308 different home energy management products to recognize their functionalities and algorithms for load control, energy saving, demand shifting, customer comforts, and security. In the article [51], the authors focused on equipping a house with renewable energy resources and battery storage while the HEMS charge the battery with grid electricity at off-peaks and discharge the capacity for the house demand at peaks. Furthermore, the HEMS schedules appliances usage to optimize the energy cost and reduce the peak-to-average ratio. This model allows customers to sell the surplus energy into the grid and earn profits.

2.2.2 Demand Response (DR) Solutions with Game Theory

In this subsection, we concentrate on DR models using game theory tools, mainly to control the total energy consumption in a grid (a residential, commercial, industrial, or mixed-use area). Game theory becomes an efficient solution for demand response problems because players can reach their best strategies and maximize their profits. Game-theoretic approaches for demand response have accelerated in the past decade. The initial game theory demand response models presented peak-to-average ratio (PAR) control and cost management [14,52]. According to [53], end-users have a significant effect on improving the energy efficiency in demand response problems using their energy resources and demand schedule. Therefore, we study different projects and determine the system performance of proposed demand response systems and end-users participation in demand response programs.

A cooperative game was played by the utility company and its customers to minimize cost and PAR based on power consumption and price signal strategies [14]. In [52], the authors reduced the peak and electricity bills using a time-based pricing system with a non-cooperative game. A two-level game was played in [54] to reduce the peak, where a non-cooperative competitive game was played among the utility companies and an evolutionary game between residential customers. At level one, the utility companies competed on electricity price, then the data aggregation unit broadcasted the price information to the customers, and they chose a utility company and bought electricity from it. In a non-cooperative manner in [55], first, the customers sent their vector of demand to the energy provider, and then the provider responded by forecasting the price signal. Here, the goal of customers was to reduce costs, and the energy provider wanted to maximize its profit and minimize PAR. In the article [56], the authors minimized cost and PAR using a convex cost function in the game model. The players were customers, and their strategies were their power consumption, which is the output of the particle swarm optimization (PSO) algorithm implemented in a residential place. Their objective was to reduce PAR and customer bills using household appliance scheduling.

Despite the non-cooperative game popularity in demand response models, some researchers looked into cooperative attitudes between players. The authors of [57] implemented a cooperative game energy consumption scheduling model between N customers and one energy provider; their goal was to reduce the bill of the customers and decrease PAR. In this game, the customers shared their strategies (energy consumption), but they could only discover the accumulated energy consumption. In other DR solutions, a demand response contract is signed between the utility company and customer [15]. In [15] a contract-based demand response solution was implemented between customers and an aggregator. The aggregator randomly chose a group of customers to collaborate in demand response events, and customers reduced their consumption in return.

Demand response approaches can be formulated as a leader-followers game (a Stackelberg game). A game is known as Stackelberg when one player (the leader) has the power to choose the first movement and all other players (the followers) move after that [58]. The idea of transactive energy is presented to connect different agents and provide a trading market between the sellers and buyers. The Stackelberg game model is one of the popular tools for solving these transactive energy problems. This model is well-described in [59], where a one-leader, N-follower game was implemented to achieve the optimal demand control level by forming a virtual electricity-trading process using real-time pricing. Real-time pricing is a utility rate structure that vary hourly or sub-hourly. Earlier leader-follower demand response approaches are described in [60–63]. The authors of [59] presented a real-time pricing demand response approach using virtual electricity trading to find the optimal demand of appliances. They used a Stackelberg game model between Energy Management Center (EMC) as a leader and smart appliances as followers. EMC is a virtual electricity retailer which allocates different prices to different devices based on the real-time pricing received (every hour) from the utility company. Each device responds to the price and chooses its optimal demand. A Stackelberg game between demand response aggregator (DRA) as a leader and the generators as followers was presented in [60]. The leader and followers try to maximize their profits on demand response events while DRA minimizes the dissatisfaction of customers (or maximizes their social welfare) and minimizes their consumption. In another demand response Stackelberg model, the game was played between the utility company and customers to maximize payoffs of players [61]. They proposed a multi-utility company and multi-user game and tried to find the Stackelberg equilibrium (described in appendix A). In this scheme, the utility companies present their prices, and the customers reply with their usage profile. Additionally, they designed a non-cooperative game between utility companies to find the optimal offering price. In [63], there is a Stackelberg game between the retailer and customers, and the main goal is to find the optimal points of customer bill reduction and the maximum payoff for the retailer. They used a genetic algorithm (GA) to maximize the payoff of customers and linear programming to minimize the customer bill. In the article [64], the authors presented an energy transactive multi-level DERMS model with a fair allocation of financial resources among the prosumers, aggregators, and DSO using a reverse Stackelberg solution. They proved the existence of a Stackelberg equilibrium by dividing the game into sub-games and then finding the Nash equilibrium (NE) point for each sub-game. In the paper [65], a Stackelberg game was played between the aggregator, who owned a wind farm, and consumers to reach the maximum matching between the demand of consumers and wind farm generation by offering a bonus to the consumers to change their demand profile. A Bayesian game (a non-cooperative game with incomplete information) was presented in [66] to find the optimal day-ahead bidding strategy for the energy market. The game is between aggregators and a system operator who collects the bids of aggregators, and in return, the aggregators receive rewards. Customers sign a contract with the DR aggregator, and the aggregator controls the usage of customers with dynamic pricing. The system operator can buy electricity from the grid or the aggregators. The operator offers rewards to aggregators, and aggregators ask their customers to reduce their demand and compensate for their reduction. There is no penalty for the customers if they do not contribute to a demand response program.

The goal of demand response papers has changed, and now most studies focus on satisfaction factors of agents. For instance, in the article [67], there was a competitive game on customer power consumption scheduling where customers seek to satisfy their load usage before the total demand exceeds an energy threshold. Also, a similar approach was presented in [68] to decrease the bills of customers and increase their satisfaction using the demand schedule. From the perspective of customer satisfaction, in [69], the authors presented a demand optimization for selected buildings in a decentralized model. They controlled consumption, PAR, thermal comfort, and electricity cost factors. In their proposed game, the players are the buildings, and their strategy is the optimal inside temperature. They transformed the game into an optimization model using the Nikaido-Isoda algorithm. In [68], the authors encouraged customers to shift their demand from peak to off-peak times and gain cost reduction using an incentive-based model for demand control. In their model, the peak tariff is unique for customers based on their consumed energy.

They applied the Shapely value method for the game part and focused on distributing the generation cost fairly among the customers. In another customer satisfaction and demand response approach, a Stackelberg game was implemented in [70]. The game was played between the retailers and consumers; the leader proposed the electricity price, and the followers replied with consumption. The authors considered two categories for retailers and users (two leaders and two followers). One category of users was equipped with a photovoltaic system and sold their extra generation to the grid. In the other user category, the consumption of users was optimized based on the price signal. One category of retailers provided power, heating, and cooling energy for the customers, and the other only allowed the customers to buy energy equal to their contract value. Meanwhile, if the customer needed extra energy, they could request more from the first retailer. Customer satisfaction depended on energy consumption; the more they consume, the greater their satisfaction.

To control the distributed source of electricity, some solutions focused on energy generation monitoring models [70, 71]. In [71], the aggregators sold the extra generation of the community to the grid, and in the opposite, in [70] customers controlled their usage using a game model to balance the demand and generation of retailers. An energy management system for smart building [72] was presented to reduce the peak by fairly allocating the building's photovoltaic generation among the rooms. Their approach employed a multi-agent clustering model (to categorize customers' consumption), supervised learning (to forecast the energy demand), and a Minority game including load profile uncertainties to improve the cost savings. In another paper, authors modeled a competition between aggregators for selling their extra energy to the grid [71]. The model was developed using an i-game where players do not have complete information about the bids of others. The aggregators are the players, and their strategies are their selling price. The research in [73] presented a Stackelberg game model between an aggregator and customers where the former offers price and the latter reply with the quantity of energy to buy from or sell to the aggregator. In [74], the authors presented new price-based and incentive-based demand response models where a real-time price model is implemented in a three-level Stackelberg game between the power grid operator, retailers, and customers sequentially. For every five minutes, the power gride operator releases demand reduction prices to retailers, and retailers offer new prices to users while their profit values are considered.

Recently, demand response studies focused on merging optimization and game theory models with stochastic solutions to consider possible actions of agents and achieve optimal and realistic results. Most of the stochastic demand response research has modeled renewable generation, storage system management, risk of system operation, and electrical vehicle mobility pattern in microgrids [75]. A demand response bidding strategy game with an uncertain wholesale market price was modeled in [76, 77]. To cope with uncertainties, a demand control stochastic programming problem was represented in [78]. The authors classified customers and applied a pricing scheme to encourage customers to participate in demand response using a Bayesian model to minimize costs. In the article [79], authors presented an energy model using the Stackelberg game played between the customers and a community energy storage system. A non-cooperative mixed-strategy game was played between the customers to determine their uncertain consumption behavior. In another work, the authors implemented a two-stage non-cooperative energy trading model between the aggregator and electric vehicles [80]. First, they found the conventional amount of charging or discharging for electric vehicles and then investigated the probabilistic behavior of aggregators using a non-cooperative mixed-strategy game to select proper charging time slots. In the case of integrating a learning-based game theory model with a probabilistic method, the article [81] presented a competition between power companies to sell energy to customers. A customer selects a serving company using reinforcement learning based on the offered price and electricity quantity. The probability for power company selection depends on its reputation value and competitiveness.

Table 2.1 shows a summary of the studied articles in this section that are categorized based on their functionalities.

Table 2.1: Categories of studied DR solutions with game models.

Category	Articles	Game model
PAR and cost control	[14, 57]	Cooperative game
	[15]	Stochastic game
	[52, 54–56]	Non-cooperative game
Energy trading	[59–65]	Stackelberg game
	[66]	Bayesian game
Customers Satisfaction	[67, 69]	Cooperative game
	[68]	Shapely value
	[70]	Stackelberg game
Distributed energy control	[70, 71, 73, 74]	Stackelberg game
	[72]	Supervised learning in a minority game
Stochastic demand control	[75, 77]	Stackelberg game
	[76]	Non-cooperative game
	[78]	Bayesian game
	[79, 80]	Mixed-strategy non-cooperative game
	[81]	Reinforcement learning and non-cooperative game

2.2.3 Demand Side Management (DSM) and Demand Response (DR) Solutions with Optimization Tools

According to the energy internet paradigm, monitoring technologies play a fundamental role in the modern grid [82]. DSM focuses on users demand management for load scheduling and cost minimization, but demand response is an approach that incentivizes customers to control their demand in response to a price signal [83]. Load shifting, load reduction, and peak clipping push the load down till it reaches the boundaries. Examples of household demand management are represented in Figure 2.2 [84]. Most demand response and DSM papers use a mathematical model to minimize or maximize objective functions with different constraints on demand.

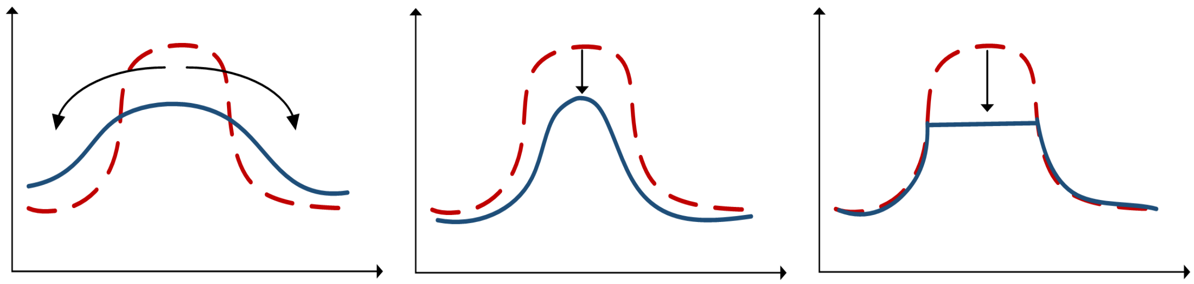

Figure 2.2: Demand management techniques [84].

A demand response control collaborating model in [85] is delineated among the near-zero buildings that share their renewable generation. The authors predicted the supply, clustered the buildings based on their profiles, and minimized the buildings' bills using an iterative non-linear programming model. A non-linear programming model with a dynamic pricing method was used to increase the building performance, reduce the electricity bill, and reduce the peak and computational costs. This model stores the extra renewable energy in the battery storage of neighbors or sells it to the grid. Finally, the authors compared their scheme with a non-cooperative game theory model and discovered that the amount of energy imported by a non-cooperative model is more than their collaborative model. The authors of [86] implemented a forecasting model to predict household renewable generation and demand. They applied an optimization model to schedule the appliance usage profile based on increasing electric vehicle charging, reducing the total cost, and maximizing the benefit of selling renewable energy.

With the increasing penetration of renewable energy at the residential level, some previous works on DSM proposed appliance scheduling based on energy generation from renewable resources. A hierarchical model was proposed in [87] to maximize DER usage and reduce the grid demand. In this model, the customer consumption is scheduled to follow the available renewable resources pattern. This approach reduces the demand on the grid and the cost to the customers. In [88], the authors decided to reduce the cost and keep the energy consumption of a building under a certain threshold. They shared the generated electricity among the building residents for cost minimization.

Most of the research on DSM is intended to reduce either the cost to the customer or the PAR of the grid operators [18]. For instance, in [28], the authors integrated a sensor network with a HEMS and determined the energy consumption, cost reduction, and PAR utilizing a household communication network. In [48], the authors proposed a smart home analysis using a HEMS to minimize the bill by scheduling time-shiftable and thermal loads using photovoltaic generation and battery storage. Their proposed algorithm optimizes the cost of electricity usage by switching between the grid and battery resources subject to price signal and comfort. Paper [89] presented a multi-objective demand response model to minimize the cost to the utility company and give a bonus to the aggregators who reduced the demand. The demand response aggregator acts as an intermediary and sends demand response requests to the customers to reshape their demand profile and allocate compensation in return. One of the popular DSM solutions is to categorize loads and then apply a suitable objective function with relevant constraints to schedule the demand [90]. In [91] authors classified appliances into two categories, essential demand and flexible demand, and then defined a consumption order for the appliances to minimize their costs. In another article [92], authors studied the scalability and acceptability of appliance load scheduling in a DSM strategy by categorizing and prioritizing their usage profile constrained by the time intervals. Authors in [93] presented a load scheduling model for a house using a multi-dimensional PSO approach to maximize the customer's rewards on demand reduction subject to appliance time constraints and user preferences. This model categorized the appliances based on their energy consumption and operating time. In [94], the authors clustered the loads to find a trade-off between the processing cost of the energy management system (EMS) and response time (delay) to achieve the demand and supply balance point. The authors of [95] concentrated on minimizing the household bill based on different categories of appliances and dynamic pricing tariffs using the genetic algorithm to find the optimal operating parameters for each device. In [96] the authors minimized the total energy cost by rescheduling the appliances and decreasing customer discomfort.

A smart meter plays a crucial economic role in an intelligent house where customers have the ability to adjust their usage profile. The authors of [97] designed an intelligent meter for residential usage to reduce the bill of the customer and keep the total consumption less than a threshold. This model works with two pricing schemes, flat and real-time pricing. The authors categorized the appliances as follows: 1) non-interruptible and non-schedulable, 2) interruptible and non-schedulable (such as the water heater and air conditioner), and 3) schedulable load (such an electric vehicle and dishwasher). They developed linear programming cost minimization within appliance usage priority. In [98] and [99], the authors presented a prioritized scheduling model based on appliance types to minimize the costs. DSM can be improved by a machine learning prediction model [100]. In [101], the authors performed day-ahead scheduling using a real-time pricing and prediction model to forecast the demand and minimize the cost of generation. In this case, the authors increased customer satisfaction by using an incentive-based model.

The temperature of a living area is one of the essential comfort factors for the residential customer. Most of the studies in this area have tried to minimize thermal load while maintaining customer comfort. In [102] the main goal was to minimize the cost of HVAC energy usage and maintain customer comfort. Therefore, the authors determined different parameters that affect the room temperature, such as the number of occupants, indoor and outdoor temperatures, and customer preferences. They used a nonconvex formulation to trade-off cost and thermal comfort. The authors of [103] presented a mixed-integer linear programming (MILP) model based on dynamic pricing to optimize the thermal load in a smart house and maintain customer comfort. In [104], the authors addressed HVAC system energy conservation and wastage using a machine learning approach, using internet of things sensor data to establish consumer consumption patterns.

In many articles on thermal load management, the authors took a thermal standard as an index and addressed temperature in that context. In [105], the authors employed the ISO standard on residential comfort temperature and minimized predicted percentage dissatisfaction (PPD). To ensure customer dissatisfaction remained less than a specific

Table 2.2: Categories of studied DSM and DR solutions with optimization tools. Optimal stopping rule (OSR), non-linear programming (NLP), genetic algorithm (GA), mixed-integer linear programming (MILP), linear programming (LP), colorpower (CP), binary particle swarm optimization (BPSO), machine learning (ML), mixed-integer non-linear programming (MINP).

Category	**Articles**	**Tools**
Distributed energy control	[85–87]	NLP
	[88]	GA
Load Scheduling	[18, 91, 100]	NLP
	[28, 48, 96, 97]	LP
	[89]	Priority scale CP controller
	[90]	Convex optimization
	[92]	OSR
	[93]	PSO
	[94]	Dynamic-priority optimization
	[95]	GA
	[98]	Priority vector
	[99]	BPSO
	[101]	MILP
Customer Comfort	[102]	Nonconvex optimization
	[103, 106, 107]	MILP
	[104]	ML
	[105]	PSO
	[108]	NLP
	[109]	MINP

value, they used the PPD function to measure the dissatisfaction of customers regarding the room temperature [105]. Then they applied a direct load control model with PSO to reduce thermal load. Other approaches optimized both thermal and non-thermal loads to increase system efficiency, as noted in [106, 108]. To optimize non-thermal loads, a mixed-integer non-linear programming approach was used in [109] to control cost and schedule appliance operation to increase customer comfort on appliance usage using mixed-integer nonlinear programming (MNLP) model. The multi-objective MILP in [107] was proposed to control PAR, cost, and customer inconvenience while using the time-of-use tariff. The idea of using MILP in DSM is to find optimal time slots for demand profiles.

Table 2.2 shows a summary of the studied articles in this section that are categorized based on their functionalities.

2.2.4 Distributed Energy Resources (DER)

In this section, we mainly focus on DER that provides the grid's required electricity in a distributed manner. Electricity sources such as storage systems, renewable resources (wind turbines, photovoltaic systems), and customer controllable loads are known as DER. Distributed energy technologies in power systems have a key role in compensating the local electricity requirements according to financial considerations for network sustainability. [110, 111].

The idea of energy trading within microgrids can help satisfy the demand of another microgrid using the surplus energy of one microgrid. Based on [112], this transaction is done through electric vehicles due to their ease of use and increasing rate. The authors presented an uncertain coalition using the Bayesian game, allowing the microgrids and electric vehicles to work together and keep the power loss less than the threshold. The authors of [113] minimized transmission losses by implementing a game between the distributed generators using the Shapley value. The Power Potential project was developed by the UK power network and National Grid Electricity System Operator [114]. This is a connected DER project with services and control features to provide high-speed and less expensive virtual power plant (VPP) to make a flexible system with a low operating cost. They used a remote terminal unit telemetry system for distribution network signal exchange. The platform was implemented on Microsoft Azure cloud computing, and they control the network through a web interface. The article [115] implemented a real-time distributed energy management model with advanced metering infrastructure to control electric vehicle charging. The article looked into a real-time simulation model for electric vehicle demand control to keep the cost of energy transmission down and use local DER instead. The authors used a fuzzy logic model to schedule electric vehicle charging time based on local energy resources. A DER project presented in [116] mainly focused on implementing a supervised model to control distributed renewable generation systems using GridLAB software. GridLAB was designed by the US Department of Energy for distributed energy management.

The authors of [34] represented a microgrid with both electrical and thermal grids, supported by the utility company as well as internal distributed generators (DGs) and distributed storage (DS). Their overview highlighted the differences between microgrids and large power systems. A smart energy management system was presented in [117] to optimize the microgrid operational cost. It mainly focused on predicting renewable resources, energy storage capacity, and cost models to find optimal operating solutions. To predict the stochastic distributed generation, the authors applied a neural network for photovoltaic systems and wind turbines using weather forecast data and modeled energy management and battery charging and discharging based on time-of-use pricing. Another DER forecasting model was elaborated in [118]; the authors used an artificial intelligence technique for a microgrid to reduce the cost, limit greenhouse gas emission and control the efficiency of components. First, they predicted photovoltaic and wind turbine generation using the neural network ensemble prediction model. Then they used fuzzy logic to schedule battery charging and discharging based on the electricity price, fuel price, state-of-charge, and time of day.

The authors of [119] presented mixed-integer nonlinear programming and a stochastic model to design an optimal bidding strategy regarding the uncertain amount of provided energy by DER. They considered load scenarios and amounts of renewable generation to design a robust bidding strategy. The paper [120], presented optimal scheduling for a VPP model to control DER. The proposed solution was a stochastic day-ahead forecasting model for storage devices and distributed generators. The idea of using VPP was to provide some reserve power for ancillary services and demand. The results illustrated that with a high electricity price, the VPP works as a power plant and attempted to balance demand and supply in the grid.

The authors of [121] implemented a real-time energy market to moderate the system efficiency and profits using bidding strategies and marketing functions. They simulated the operation of the microgrid market and assumed that the microgrid has photovoltaic systems, wind turbines, and storage devices. They developed microgrid central control and a distributed management system (DMS) for the control part. In their model, a DER can join the bidding strategy considering its operating cost, and customers can shift or shed their demand to help the grid while the market is trying to minimize the operational cost and maximize the overall profit. A fuzzy model was implemented as an EMS in a residential area to reduce the demand fluctuation [122]. The authors assumed a microgrid with renewable generation, demand, storage device, converters, weather station to forecast the distributed generation, and a control station to supervise the network [122]. In recent work, an energy market mechanism was proposed in [123] that defined an energy transaction model among microgrids while they send their offers and prices to the operator to find the optimal match. In this designed microgrid, the customers had renewable energy resources and storage systems, and with an incentive-based demand response model, they could be encouraged to participate in the market. In [124] a demand response management model was presented to manage an electricity bidding market and schedule DER to meet the network demand while DER and real-time pricing are engaged. Table 2.3 shows a summary of the studied articles in this section that are categorized based on their functionalities.

Table 2.3: Categories of studied DER articles within their tools. neural network (NN), fuzzy logic control (FLC), mixed-integer linear programming (MILP), linear programming (LP), mixed-integer non-linear programming (MINP).

Category	Articles	Tools
Transmission control	[112]	Bayesian Game
	[113]	Shapley value
	[114]	Optimization
	[115]	FLC
	[116]	Supervised learning
Resource control	[117]	NN
	[118]	NN and FLC
	[119]	Stochastic MINP
	[120]	Stochastic MILP
Demand control	[121]	LP
	[122]	FLC
	[123]	Stochastic cooperative game and MILP
	[124]	Stochastic LP

2.3 Customer Experience

Customer experience in the smart grid concept relates to the factors tangled with customer comfort and energy consumption. For example, room temperature, electric vehicle state-of-charge, appliance time of usage, and others are the factors affecting customer experience. According to that, different works have minimized/maximized customer discomfort/comfort.

The goal of the article [125] is to find optimal appliance scheduling constrained to pricing signal and photovoltaic and battery capacity. The paper classified the appliances into shiftable and non-shiftable loads, minimized the difference between buying and selling the electricity, reduced time discomfort (when the scheduling time differs from the desired usage time), and minimized the peak. The authors of the paper [126] presented a residential demand response model using a reward function to reduce the peak. They calculated the reward based on the amount of load shifting and voltage improvement and ranked the houses according to their voltage improvement. Their model required customers to fill out a survey to prioritize their appliance usage in different operating time slots (off-peak, mid-peak, and peak). An appliance with the minimum priority value on that survey was more likely to be shifted. A transactive demand response scheme is presented in [127] where a multi-input multi-output (MIMO) fuzzy controller decides on the compliance level of customers on demand reduction and maximizes their contribution and reward.

The authors of [96] optimized appliance usage time slots using a binary vector to illustrate the device working time slots. They minimized the customer bill and discomfort by delaying the appliances, considering their preferred usage time. In another time-sensitive approach, [91], the loads were categorized as essential or flexible. The flexible loads contain delay-sensitive and delay-tolerant loads. The delay-sensitive loads were higher priority than the delay-tolerant. The algorithm put the appliances into low and high priority queues while optimizing the high priority first. The authors minimized the cost and operating delay for flexible devices and implemented a neural network to reduce errors and faults. Like the previous work, the article [94] balanced the supply and demand inside a neighborhood using EMS and smart consumer devices (SCDs). The EMS was located centrally to control the demand of customers, reduce the network computational cost, and minimize the delay in responding to appliance scheduling. The SCD device sent the usage profile of the customer to the EMS and prioritized the load based on the communication time and delay. Thus, the authors tried to find a trade-off between the computation cost and the delays the customers experienced. They determined the effect of delay and the processing rate of high and low-priority events in their designed system.

The article [84] categorized loads as controllable, semi-controllable, and uncontrollable, and addressed thermal comfort management. The research determined demand management and customer comfort in residential and industrial places. It mainly focused on HVAC (controllable appliances) due to HVAC's direct effect on customer comfort. The authors found that HVAC performance related to four factors: the number of occupants, solar irradiance, heat transmission through the walls and windows, and heat convection; these cause the difference between the inside and outside temperature. They used a predicted mean vote (PMV) value, taken from the American Society of Heating, Refrigerating and Air-Conditioning Engineers (ASHRAE) standards [128], to measure the thermal comfort for customers. In other thermal research [129], the authors implemented a multi-objective function to optimize comfort parameters such as thermal, illumination, and air quality in a building. They found a balance point that maximizes customer comfort and energy consumption reduction. For thermal comfort, they used the ASHRAE standard features and kept the temperature between $20°C$ to $24°C$. For the simulation part, they developed genetic algorithm and PSO models with the same comfort assumption and found out that the genetic algorithm reduces the power consumption significantly more than PSO. In a same optimization model, the authors of [130] implemented a consumption scheduling model using day-ahead pricing and the solar energy generation of a house. They minimized cost, dissatisfaction, and CO_2 emission. They categorized the loads as shiftable (classified into flexible start time, flexible power, and plug-in hybrid electric vehicle) and non-shiftable and applied a collaborative multi-swarm PSO and a mixed-integer non-linear optimization model. They found that peak, total demand, cost to customers, and carbon dioxide emission all decreased. In [131], the author deployed a new binary quadratic function PSO called a quadratic binary PSO (QBPSO). They determined the customer comfort in real-time pricing and time-of-use pricing models; their defined utility function was multi-objective and the sum of cost and discomfort factors. A hierarchical multi-agent control system using PSO for building demand management was presented in [132]. The authors mainly focused on building demand, renewable energy generators, and storage systems in a microgrid. Their proposed PSO model controlled the energy flow and reduced consumption by maximizing customer comfort (such as temperature, illumination, and air quality).

In their proposed architecture, the microgrid operated in two modes: grid-connected and islanded. For the grid-connected, the PSO maximized the comfort and reduced the usage without shedding the demand. For the islanded mode, the PSO acted similarly, but when the comfort was low, it shed unnecessary demands to increase the comfort. They also controlled a microgrid using a graphic user interface platform to monitor the interactions of customers.

An advanced version of the comfort function was presented in [133] that reduced customer frustration and increases appliance efficiency. This solution was called a realistic scheduling mechanism, which depended on the appliance time of usage, user activity, residential unit features, and appliance settings. The authors categorized the appliances as activity dependence appliance (requires the activity of customer at home such as TV), occupancy dependent appliance (influenced by the presence of customer such as HVAC), and occupancy independent appliance (works without the presence of customers such as a washing machine). Afterward, they applied binary PSO to each appliance category, and analyzed the electricity usage and comfort in the realistic scheduling mechanism with and without battery storage. The realistic scheduling mechanism with battery storage gave more comfort and used less energy than realistic scheduling mechanism without battery storage. In [134], the authors predicted customer preferences and comfort using supervised learning models. The algorithm used time-of-use pricing to reduce customer bills by learning user preferences and predicting their comfort level. They used three algorithms, support vector machine (SVM), multilayer perceptron (MLP), and Naïve Bayesian (NB). For the data collection, they asked the customers to fill in a questionnaire and rank their comfort for different devices, including their usage time. They compared the performance and prediction accuracy of these algorithms and found out that SVM, MLP, and NB present accurate results, respectively. Table 2.4 represents customer experience studied articles and specifying their comfort functions.

Table 2.4: The utility factors of studied customer experience articles.

Articles	Delay Experience	Bill reduction	Load reduction	Appliance comfort	Thermal	CO_2 emission	Illumination
[84]		✓			✓		
[91]	✓	✓					
[94]	✓	✓					
[96]	✓	✓					
[125]	✓	✓					
[126]			✓	✓			
[127]		✓	✓				
[129]			✓		✓	✓	✓
[130]	✓	✓				✓	
[131]	✓	✓					
[132]			✓		✓	✓	✓
[133]	✓	✓		✓			
[134]		✓		✓			

2.4 Blockchain

Integrating the concept of smart grid with the communication technologies created the idea of interconnecting smart meters, aggregators, DSO, and DER to facilitate system control [135]. A centralized architecture faces a single point of failure, vulnerability to cyber attacks, long processing times, delay in communication lines, and other problems that led researchers to consider distributed architecture instead [135]. Besides, distributed architecture has some issues such as node synchronization, communication security, and trust authority between the nodes. Blockchain seems to be the proper trusted solution for a fully connected electricity network while providing a distributed and secure network with high reliability and support. According to [136], blockchain is a distributed, secure, fast, transparent, and immutable system that is well suited for management systems.

2.4.1 Fundamental Concepts in Blockchain

Blockchain is mainly used for its distributed architecture. It focuses on network trust and security enhancement. In a blockchain platform, a ledger is securely distributed among the network nodes, and its content cannot be modified. A block contains network transactions, and it will be generated when the mempool reaches a threshold. The mempool in blockchain architecture is a pool that accumulates the submitted transactions. A block contains data, the previous block hash value, and the current block hash value (used to prevent data modification). When a new block is generated, it replicates between all the nodes in the network [137]. Smart contract and distributed application (DApp) are programs deployed in blockchain to check and validate transactions [138]. The main idea is to prevent posting fraudulent transactions or incorrect data on the chain [139]. A smart contract is saved in a centralized place, and each node triggers it while posting a new transaction. DApp is a distributed version of the smart contract in that each node has a copy, and no centralized access is required. To this end, a DApp is faster than a smart contract.

To generate a block, a consensus algorithm is required in a blockchain. A consensus mechanism is an agreement level used to select a block miner among the nodes. Hence, there are popular consensus algorithms such as proof of work (PoW) and proof of stake (PoS). In PoW, each entity tries to solve a complex SHA256 (Secure Hash Algorithm) mathematical problem to find a hash value (random number) less than the defined difficulty threshold [140]. The SHA256 hash function works with eight 32-bit words that use different shifts and constants. In this scheme, all the nodes start to solve the SHA256 puzzle, and the node with more powerful hardware solves the problem quickest [141]. The node that finds the solution before the others and propagates the result first will generate the block and receive rewards. The PoS only allows the stakeholders to mine the block, but proof of authority (PoA) uses a voting mechanism to select the proper miner among others [142]. PoS was presented to reduce the PoW energy consumption by eliminating the number of extra miners. The miner would be the node with the highest stake value [141]. In an article, Siano et al. presented the proof of energy (PoE) consensus algorithm that is a peer-to-peer energy trading model and fundamentally was taken from PoS [141]. In this model, a node with energy generation equal to the consumption value would be the block miner. The authors of [143] presented the proof of learning (PoL) consensus mechanism. They developed a neural network mechanism to train the nodes in a local area. Each local node tries to mine a block using its learning mechanism, and the node with minimum loss function wins the block mining while its learning algorithm is being shared with other nodes.

Different consensus algorithms have been proposed to increase the system performance, reduce computational resources and energy consumption, and decrease the consensus time. Asheralieva et al. presented a consensus mechanism that works in a voting process in which only high-reputation peers are eligible to vote [144]. They formulated a collation game among nodes to maximize their reputation and payoff. The reputation of peers in a cluster varies according to the votes they submit for each other. For identification, any new node in the system submits a digital signature key and deposit currency without the need for a central authority. To reduce the probability of selecting a malicious node, they randomly checked the vote of clusters. When a cluster vote on appending a block to the blockchain, the maximum capacity of the node cluster plus one should have the same voting opinion. The authors of [140] determined an improvement model on delegated PoS (DPoS). DPoS has a node selection mechanism different from PoS. In DPoS, each node with a token is a candidate for block mining, and the candidates can vote for each other to select the final candidate. Hence, the authors improved the idea by considering the effect of vague and abstention votes using a fuzzy logic model.

Besides focusing on the consensus algorithm, in [145], the authors provided a coalitional game between the miners to maximize their payoffs and increase their chance for block generation. They proposed a mining pool method which a group of miners collaborate on a mining procedure and share the monetary reward. A miner can switch among the pools to find one with higher reward payments. Every pool has a manager, and whenever a miner finds a block mining solution, the result will be shared with the manager and other miners.

In another aspect, some articles work on trust and assurance among the nodes for blockchain security enhancement. For instance, the article [146] presented data trust and node reputation aspects in a private blockchain and proposed node registration using public and private keys and reputation values while a node's trustworthiness is calculated with reputation, confidence value, and observation. Similarly, the article [147] mentioned the functionality of private and public keys and coins deposited at registration level for nodes authentication. It presented a fair consensus algorithm that selected nodes for block generation based on a sequence. For security enhancement, the authors of [148] presented a two-stage security solution in which miner selection is based on node reputation and history. A node with the highest reputation is detected as active, and any of the rest with a reputation more than the threshold are known as standby miners (block validators). In another work, authors developed a trust model with reputation, endorsement, and confidence factors to evaluate transactions [149]. In their model, a node with a lower trust value is considered suspicious, and has to be validated by more verifiers.

2.4.2 Blockchain in Smart Grid

Recently, the advances of blockchain in smart grid technology have brought forth the idea to utilize distributed block mining as an electricity storage system. The authors of [21] presented the side effects of negative electricity pricing in markets caused by surplus generation. They elaborated cryptocurrency mining as a demand response mechanism to solve this issue. Cryptocurrency mining could be utilized as energy storage when the distribution network demand is less than the generation; the extra energy could be used for mining and saved as cryptocurrency instead. In high-demand time slots with the low generation, the utility company can buy electricity from retailers and pay the cost with the cryptocurrency. In [150], the authors introduced the idea of storing a wind farm's surplus generation as cryptocurrency. The extra energy can be used for Bitcoin mining, and during high-demand, they can buy electricity with their earned cryptocurrency. They determined the mining revenue, mining difficulty, and energy consumption. Another cryptocurrency storage system was implemented in California to reduce the waste of renewable energies [151].

A consensus protocol specifies the rules to select block miners and block generation in a blockchain network. In the case of energy blockchain, in the article [141], the authors presented a proof of energy consensus protocol for an energy trading model between customers where VPPs control the interactions. The miner is the VPP with the minimum variation on consumption and production. A similar study presented an energy trading model carrying a double auction between the customers and DER where VPPs handle the trading [152]. The authors' proposed proof of energy market (PoEM) selects the VPPs with maximum traded energy as block miners. Another proof of energy consensus algorithm, described in the article [153] manages the demand and supply at peak times when prosumers sell and buy electricity. The authors proposed two consensus algorithms: proof of energy generation (PoEG) to increase energy production and proof of energy consumption (PoEC) to incentivize customers to reduce energy consumption at peak. A different consensus algorithm, proof of benefit (PoB), was presented in [154] where an electric vehicle with the maximum benefit value was selected as a miner. The benefit value of an electric vehicle is measured according to its charging and discharging influences on the grid performance.

In a vehicular network described in the article [155], the authors integrated the internet of vehicles and a blockchain platform to store the data in a distributed manner. They categorized the collected data into vehicle surveillance, insurance, and charging stations, where each is stored on separate blockchains. In this proposed architecture, a moving vehicle exchanges data with nodes near the road through 4G technology. The authors compared the results of average delay, the average number of retransmissions due to connection loss, throughput, and blockchain transmission delay. They found that to keep the blockchain at a high-performance level, the number of moving vehicles should be less than an average value, and when the moving vehicles increase, the network connection loss rises likewise.

The work in the article [156] is a probabilistic approach to estimate the charging demand of charging stations. The blockchain platform distributes the data and validate the charging transactions with a smart contract. It is an auction and offer-based energy model among the charging stations to exchange their energy. The model was implemented on the Etherium blockchain platform. Another energy trading model for electric vehicle fleet was illustrated in [157], considering electric vehicle charging and discharging in a distributed energy market. In this scheme, the consumer can join the trading market and bid in the network directly while it reduces the convergence time and eliminates the intermediate participant (third party).

The authors of [158] designed a smart contract to evaluate vehicle transactions by determining their assigned reputation. In another work, a blockchain-based framework was presented to provide a secure charging system for electric vehicles that can reserve charging time and bring secure services employing smart contracts [159]. A publisher/subscriber method was implemented to inform subscribers (electric vehicles) when there are charging time slots available at the closest charging stations. The article [160] describes a blockchain energy trading scheme in which electric vehicles are both the providers and consumers. A vehicle-to-vehicle (V2V) and vehicle-to-grid (V2G) architecture is proposed in [161] to implement a two-way auction model based on the Bayesian game.

A demand response model illustrated in [162] that uses a blockchain architecture for an automated energy model where all the entities collaborate without DSO supervision. The idea is to store transactional data on the blockchain and establish smart contracts to check the prosumers' demand response compensation. In another demand response research, a pricing-based game theory model was presented in [163]. This involves a trading market between the prosumers to find prices using the Stackelberg game and blockchain platform. The authors developed a rule-based iterative pricing algorithm to solve the game by pruning the search area. They applied the practical Byzantine fault-tolerant (PBFT) consensus protocol where block mining depends on multi-iterative validators voting. The seller broadcasts its desired price to all the nodes, and buyers negotiate and bid on the price. Gallo et al. described a demand response mechanism that uses blockchain and smart contracts to develop a decentralized peer-to-peer communication network between the system operator and customers [164]. Before a demand response happens, the system operator sends the DR reduction signal to the customers. Then, the EMS at the customer's place finds the optimal appliance schedule for flexible loads and saves the data on the blockchain. The system operator allocates rewards (tokens) to the customers for their contributions. Each customer can only see its stored data on the blockchain using a private key, and cannot read or modify other information.

An implemented blockchain platform for energy trading was presented in [165]. The project was designed to provide a secure, transparent, flexible, distributed, autonomous, and highly efficient data storage system for the energy market. The prosumers interact to sell their extra generation or buy electricity from the market. The machine learning method helps the customer obtain the optimal decision (the amount of selling and buying energy) in the market. The article [166] developed a double-auction mechanism between prosumers to incentivize participants for bidding, eliminate market control, and maximize social welfare. Residential energy trading systems let the customers with DER join the market and reduce the total demand [167]. They developed a permission-based residential energy trading system utilizing blockchain to validate the bids of customers using a smart contract. In the article [168], a demand response model was implemented to determine the load shedding availability of customers at peak times, in addition to utilizing blockchain for transparent communication and a secure platform.

Some energy management approaches mainly use blockchain technology to handle security and user privacy simultaneously. For instance, articles [169, 170] proposed game-theoretic models for blockchain to detect attacks and discover honest and selfish miners. In the article [171], an extensive form game was presented to detect data collisions of transaction submissions in blockchain. The extensive model defines a game in the form of a game tree, which gives a practical solution for system monitoring to detect all possible movements of users. Articles [172, 173] have determined the cheating actions among the prosumers using a game model. The authors of [159] determined different security attacks in blockchain and presented solutions to confront them. They asserted that data is forged when a malicious node tries to modify a submitted transaction or block information, but the attack could be easily detected with the help of smart contracts. The data spoofing can change the identity of nodes; this can be resolved by employing initial node registration. The authentication attack occurs when one node tries to forge another's identity, which can be controlled using private and public keys. The authors in [147] studied other security concerns such as an appending attack, which occurs when a registered node in the network tries to submit a fraudulent transaction, and a 51% attack, when 51% of customers are attackers. These can be stopped by smart contract algorithms.

Table 2.5 presents the studied consensus algorithms in this document. Moreover, Table 2.6 presents a summary of the studied articles in this section that are categorized based on their functionalities.

Table 2.5: Studied consensus algorithms.

Category	**Articles**	**Method**
Consensus algorithm	[140]	Delegated PoS (DPoS)
	[141]	Proof of energy (PoE)
	[143]	Proof of learning (PoL)
	[152]	Proof of energy market (PoEM)
	[153]	Proof of energy generation (PoEG) and proof of energy consumption (PoEC)
	[154]	Proof of benefit (PoB)

Table 2.6: Categories of studied energy blockchain articles. vehicular network (VN), demand response (DR), distributed energy resources (DER).

Category	**Articles**
Blockchain and DER	[21, 141, 150–153]
Blockchain and VN	[154–161]
Blockchain and DR	[162–168]
Blockchain and cyber security	[147, 159, 169–173]

Chapter 3

Demand Management for Optimized Energy Usage and Consumer Comfort Using Sequential Optimization

3.1 Introduction

The energy-efficiency of demand management technologies and customer experience has emerged as important issues as consumers have begun to adopt these technologies heavily. In this regard, the electrical demand imposed on the smart grid by residential users needs to be optimized while exploiting customer comfort parameters such as thermal comfort and preferred appliance usage time interval. This work proposes a multi-layer architecture that uses a multi-objective optimization model in terms of energy consumption, consumer comfort, and experience. The solution shows how our proposed cluster sequential management (CSM) approach could improve consumer comfort via appliance scheduling. To quantify thermal comfort, we use thermodynamic solutions for a heating ventilation and air conditioning (HVAC) system and then apply our scheduling model to find the best time slot for such thermal loads, linking consumer experience to power consumption. In addition to thermal loads, we also include non-thermal loads in the cost minimization and the enhanced consumer experience. This hierarchical algorithm classifies appliances by their load profile, including degrees of freedom for consumer appliance prioritization. Finally, we schedule consumption within a time-of-use (ToU) pricing model. In this model, we use mixed-Integer linear programming (MILP) and Linear Programming (LP) optimization for different categories with different constraints for various loads. We eliminate the customer inconvenience on thermal load considering American Society of Heating, Refrigerating and Air-Conditioning Engineer (ASHRAE) standard, increase the satisfaction on electric vehicle (EV) optimal chagrining constrained by minimum cost and achieve the preferred usage time for the non-interruptible deferrable loads. The results show that our model is typically able to achieve cost minimization almost equal to 13% and peak-to-average ratio (PAR) reduction with almost 45%.

3.2 System Model and Problem Formulation

With the advances in smart appliances, home appliances are now a part of the internet of things (IoT) ecosystem while the smart grid positions itself as an ideal example of an industrial IoT (IIoT) system [174]. Figure 3.1 illustrates the significant elements of this ecosystem. At the top level, we have generators based on conventional or renewable energy sources. Then, the produced energy is transported through transmission lines to the distribution system transformers. Each transformer agent (TA) balances the voltage for residential usage at the energy distribution level by stepping up/down the voltage. At the residential level, a home energy management system (HEMS) as an IoT device communicates with TA to send customer usage data to the utility. The household IoT devices (HVAC, EV, washing machine, etc.) communicate with HEMS through Wi-Fi or

ZigBee and create a small network inside the house.

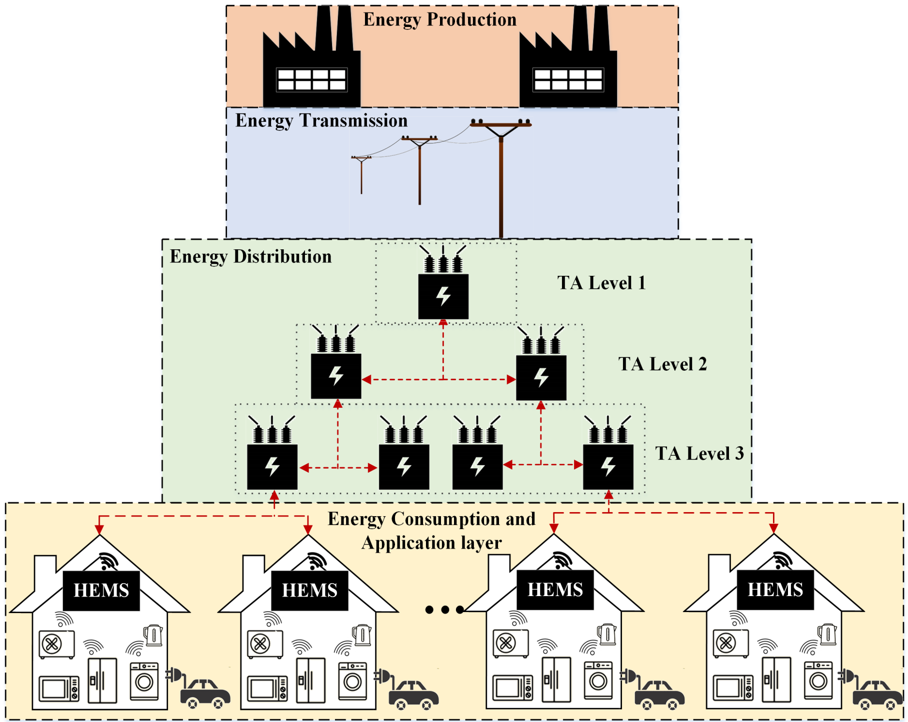

Figure 3.1: Top-down view of our IoT ecosystem.

In this work, we assume that the utility company asks the customers to collaborate on demand management to handle the grid supply and demand at peak times. However, customers have appliances that need to be on during certain times, and they also have thermal loads that can be controlled to maintain a certain level of user satisfaction. To achieve these goals, an intelligent HEMS device is required to control and monitor customer consumption. Our goal is to minimize the cost, maximize customer comfort while reducing the peak-to-average ratio. Let N be the number of customers, where $i \in \mathcal{N} = \{1, 2, ..., N\}$ is the set of customers. Subscript a denotes the appliance number, and $\mathcal{A}_i$ is the set of appliances for customer i, where $a \in \mathcal{A}_i$. The value $|\mathcal{A}_i|$ is the total number of appliances for customer i ($\mathcal{A}_i = \{1, 2, \ldots, |\mathcal{A}_i|\}$). We subdivide the 24-hours period into T equal time slots and $t \in \{1, 2, \ldots, T\}$. An appliance profile may be defined in terms of its nominal pattern of power consumption $\mathbf{L}_a = (l_a^1, \ldots, l_a^{T_a})$, where l_a^t is the energy consumption of appliance a in time slot t, and T_a is the number of time slots in which the appliance a operates. Its optimized operating state during the day is given by the binary vector $\boldsymbol{\tau}_a = (\tau_a^1, \ldots, \tau_a^T)$, where the appliance condition (ON/OFF) for time slot t is given by τ_a^t (i.e., 1 or 0). This operating state is determined by a scheduling and optimization process (described below) that transforms $\mathbf{L}_a$ into $\mathbf{X}_a = (x_a^1, \ldots, x_a^T)$, where x_a^t is the optimized appliance a consumption for time slot t. The customer aggregated demand vector $\boldsymbol{\chi}_i = (\chi_i^1, \ldots, \chi_i^T)$ is sequentially constructed, where χ_i^t is the total optimized demand for time slot t.

3.2.1 Load Categories and Scheduling Approach

We consider three load categories. Essential loads ($\mathcal{A}_E$) are those directly initiated by the user, lacking any HEMS control of their power consumption or profile (e.g., coffee maker). Elastic loads ($\mathcal{A}_{El}$) are those with load profiles whose consumption could be adjusted by HEMS control within any time interval (e.g., HVAC). Such loads have a major impact on customer comfort level. Deferrable loads ($\mathcal{A}_D$) are those whose load profiles are schedulable (e.g., washing machine) within some customer-defined interval. Such loads have a major impact on customer lifestyle and convenience. For each appliance a, we define a binary vector $\mathbf{I}_a = (I_a^1, \ldots, I_a^T)$, where

$$I_a^t = \begin{cases} 1 & \text{if } t_a^s \leq t \leq t_a^f \\ 0 & \text{otherwise} \end{cases} \tag{3.1}$$

denotes the permissible scheduling interval in terms of starting t_a^s and finishing t_a^f time slots of appliance a. This feature permits time constraints to be set. A fundamental constraint is that the permissible interval be greater than the usage time T_a, where

$$|t_a^f - t_a^s| \geq T_a. \tag{3.2}$$

$\mathcal{A}_i$ is composed of distinct subsets and may be represented as:

$$\mathcal{A}_i = \{\mathcal{A}_E, \mathcal{A}_{El}, \mathcal{A}_D\}. \tag{3.3}$$

Appliances may also be categorized by their usage priority, while essential loads are mandatory. For all other loads, priority levels are assigned by the customer via the HEMS, and elastic loads are assumed to have a higher priority than deferrable ones. The appliances priority is denoted by $\mathbf{\Gamma}_i = (\rho_1, \ldots, \rho_M)$ with length of $M = |\mathcal{A}_{El}| + |\mathcal{A}_D|$, whose element ρ_a is appliance a priority coefficient. To allocate the priority coefficients to these appliances, we use the analytic hierarchy process (AHP) [175] in our optimization model.

We implement demand optimization, described in the following subsections, within a sequential approach. This approach is illustrated in the flowchart provided in Figure 3.2. The sequential scheduling considers the appliance load profiles entered into the demand vector based on their priority. Note that the summation of $\boldsymbol{\chi}_i$ across the time horizon will be almost equal to the summation of the load profile of all the appliances. Based on 3.4, $\Delta \geq 0$ is a value that is used to present the difference between aggregated demand vector and the actual demand of appliances in a house.

$$\sum_{t=1}^{T} \chi_i^t = (\sum_{a=1}^{|A_i|} \sum_{t=1}^{|T_a|} l_a^t) \pm \Delta \tag{3.4}$$

3.2.2 Optimization

The ultimate goal of the proposed optimization scheme is to minimize the residential energy consumption which is given by $\min f(\mathbf{X}_a)$ and $\min g(\mathbf{X}_a, \boldsymbol{\tau}_a)$ where $f(\mathbf{X}_a)$ and $g(\mathbf{X}_a, \boldsymbol{\tau}_a)$ are used to schedule elastic and deferrable loads, respectively. Each appliance is contributing to this optimization model by minimizing its consumption as explained below. Constraints specific to appliances type, essential, elastic, or deferrable are applied. We optimize $\mathbf{X}_a$ and

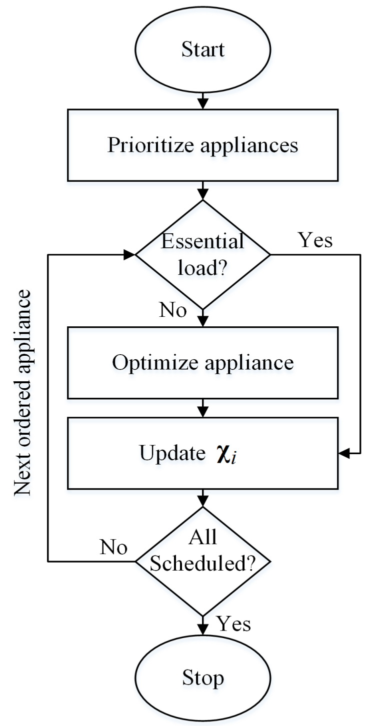

Figure 3.2: The flowchart of the proposed model.

$\boldsymbol{\tau}_a$ by sequentially minimizing the cost of the incremented daily demand, using a general time-of-use price signal $\mathbf{P} = (p^1, \ldots, p^T)$.

3.2.2.1. Elastic Load Model

Elastic devices have a defined operating state $\boldsymbol{\tau}_a$ (i.e., they are not schedulable), but their power consumption $\mathbf{X}_a$ is adjustable. By considering the general form of optimization, we can define a linear programming (LP) optimization model for this load category as

$$\min f(\mathbf{X}_a) = \min \sum_{t=t_a^s}^{t_a^f} p^t (x_a^t + \chi_i^t) \tag{3.5}$$

subject to;

$$\beta \sum_{t=t_a^s}^{t_a^f} log(x_a^t + 1) \geq S_a$$

$$(1-\beta) PPD(x_a^t) \leq D_a, t \in [t_a^s, t_a^f]$$

$$\chi_i^t \leq x_a^t + \chi_i^t \leq Ub^t$$

where p^t is time-of-use pricing signal (known value), x_a^t is appliance a optimized consumption for time slot t (optimization variable), χ_i^t is the aggregated demand vector of customer i at time slot t, and t_a^s and t_a^f are the preferred starting and finishing work time intervals of appliance a. If the appliance is a non-thermal elastic load, $\beta = 1$ (like EV), otherwise $\beta = 0$ (like HVAC). The first constraint is specifically used for non-thermal loads, where S_a is the minimum level of power consumption for electric vehicle that is extracted from [176]. A logarithmic function is used for electric vehicle to guarantee the minimum performance of the device [177]. The second constraint is used for the thermal system and depends on the environment and appliance energy dissipation. The value D_a is the threshold for predicted percentage dissatisfaction (PPD) to ensure customer dissatisfaction remains less than a certain value. We use the PPD function to measure the customer dissatisfaction regarding room temperature [128]. PPD is defined in the ASHRAE standard, and it is governed by the parameters that establish room conditions. There is an indirect relation between PPD and power consumption using predicted mean vote (PMV) formulation (explained in 3.2.3) [84,178]. Finally, the third constraint is used for both thermal and non-thermal loads to bound each time slot between the aggregated demand χ_i^t and the maximum threshold of household usage Ub^t at time slot t. The goal of defining a limitation for each time slot is to prevent peak events and distribute the customer demand evenly throughout the day.

3.2.2.2. Deferrable Load Model

In the case of deferrable load scheduling, the optimization model will manage the load profile through the permissible interval and find the minimum cost. This approach is entirely different from the previous model for elastic devices. In this model, we are using mixed-Integer linear programming (MILP) instead of LP. This model helps us first find the proper usage time for the appliance a and then find the optimized load profile vector. For this optimization, we have

$$\min g(\mathbf{X}_a, \boldsymbol{\tau}_a) = \min \sum_{t=t_a^s}^{t_a^f} p^t \tau_a^t (x_a^t + \chi_i^t) \tag{3.6}$$

subject to;

$$\sum_{t=t_a^s}^{t_a^f} \tau_a^t I_a^t = T_a$$

$$\sum_{\tau_a^t=1 \Rightarrow k=t}^{k+T_a} p^k x_a^k \leq C_a, t_a^s \leq t \leq t_a^f - T_a$$

$$\chi_i^t \leq \tau_a^t (x_a^t + \chi_i^t) \leq Ub^t$$

$$\tau_a^t \in \{0, 1\}$$

where p^t is time-of-use pricing signal, x_a^t is the appliance a consumption at time slot t, χ_i^t is the aggregated demand of customer i at time slot t, τ_a^t is the operating state of appliance a (the ON/OFF condition) at time slot t, and t_a^s and t_a^f are the starting and finishing work time intervals of appliance, respectively. The first constraint is used to find T_a, which is the number of time slots the appliance needs to complete its operation within the permissible interval $\mathbf{I}_a$. The second constraint is used to check the uninterrupted device operation. The constant value C_a is the minimum operation cost for appliance a in its permissible interval (to not allow the optimization to select the high-cost time slots). The notation $\tau_a^t = 1 \Rightarrow k = t$ ensures that if and only if the optimized operating state is equal to one, then the time slot and the summation of cost for the T_a time slots after that (from $k = t$ to $k + T_a$) should be lower than or equal to the minimum cost C_a. The third constraint is used to bound each time slot between the aggregated demand vector and the maximum threshold of household usage at time slot t.

3.2.3 Thermal Model

As mentioned in previous sections, we choose a PPD rate, and with PPD and PMV functions, we calculate the necessary thermal load [84]. To make a map between PPD, PMV, thermal energy, and temperature, we consider the fundamentals of thermal conduction. Room size, wall quality, and inside and outside temperatures directly impact thermal loss. From [179],

$$Q_{power} = C_{room} \times \frac{d\theta_{room}}{dt} \tag{3.7}$$

is used to calculate the thermal power needed to change the room temperature θ_{inside} to the preferred temperature $\theta_{preferred}$ at a specific rate ($\frac{d\theta_{room}}{dt}$), where C_{room} is the room thermal capacity [179]. The power leakage is determined via

$$Q_{leak} = \frac{\theta_{outside} - \theta_{inside}}{R} \tag{3.8}$$

where $\theta_{outside}$ is the outdoor temperature and R is the room thermal resistance. In our model, we use both formulations with regard to ASHRAE standard room temperature.

Figure 3.3 shows that when PPD is equal to 11.68%, we need to consume almost 1.8 kWh to increase the room temperature from $20°C$ to $22.5°C$when the outside temperature is $-10°C$. According to the ASHRAE, standard [128], the optimal temperature range for a room in winter with the optimal PPD ($\leq$ 10%) is between $23°C$and $27°C$which is also observable from Figure 3.3. Therefore, our algorithm keeps the temperature in this range regarding room heating leakage, outside temperature, and inside temperature.

3.2.4 Analytic Hierarchy Process (AHP)

AHP is a decision-making model that is used for ranking the alternatives when we have multi-criteria problems [175]. A pairwise comparison is made between the specified criteria and alternatives with the grades ranging from 1 to 9. The value $r \in \{1, \ldots, 9\}$ shows how

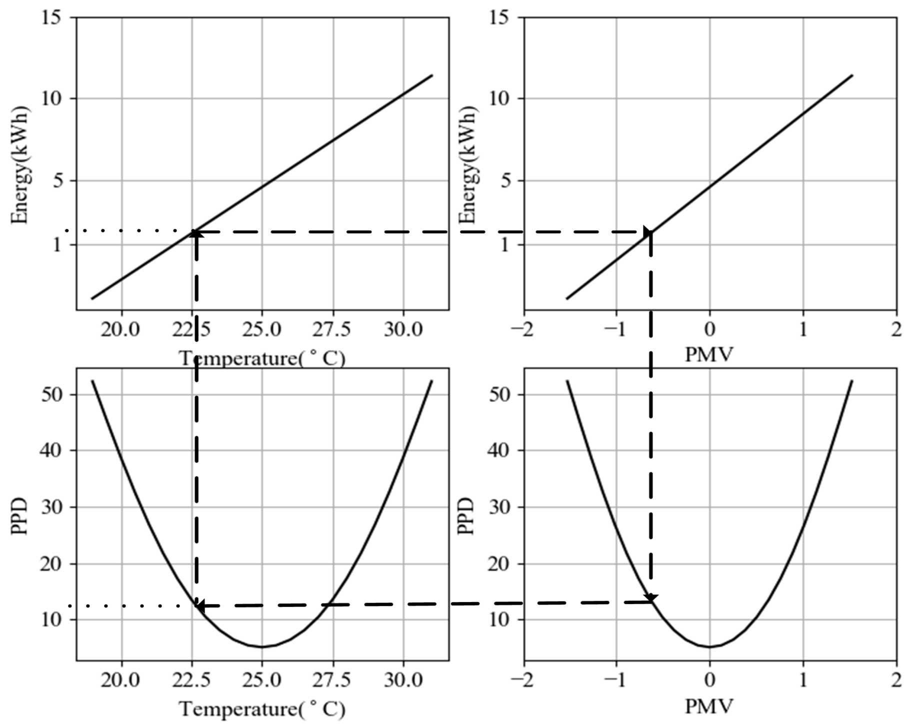

Figure 3.3: Relation between PPD, PMV, temperature and energy [Assumption: $\theta_{outside} = -10°C$].

much more priority an alternative has over the other. Intensity $r = 1$ means they are equal, $r = 2, 3$ shows the moderate condition, $r = 4, 5$ means one is stronger than the other, $r = 6, 7$ one is very strong and $r = 8, 9$ presents the extreme importance of one to the other. Let's assume we have m criteria and n alternatives then, the relative matrix A_k for criteria $k(k \in \{1, \ldots, m\})$ represents the relative rates between alternatives i and $j(\alpha_{ij})$ where $i, j \in \{1 \ldots, n\}$ and it is calculated by $\alpha_{ij} = \frac{r_i}{r_j}$ where $r_i, r_j \in \{1, \ldots, 9\}$.

$$A_k = \begin{bmatrix} \alpha_{11} & \alpha_{12} & \ldots & \alpha_{1n} \\ \alpha_{21} & \alpha_{22} & \ldots & \alpha_{2n} \\ \vdots & \vdots & \ddots & \vdots \\ \alpha_{n1} & \alpha_{n2} & \ldots & \alpha_{nn} \end{bmatrix} = \begin{bmatrix} 1 & \frac{r_1}{r_2} & \ldots & \frac{r_1}{r_n} \\ \frac{r_2}{r_1} & 1 & \ldots & \frac{r_2}{r_n} \\ \vdots & \vdots & \ddots & \vdots \\ \frac{r_n}{r_1} & \frac{r_n}{r_2} & \ldots & 1 \end{bmatrix} \tag{3.9}$$

After filling the matrix, we normalize each relative rate α_{ij} using $\alpha_{ij} = \frac{\alpha_{ij}}{\sum\limits_{i=1}^{n} \alpha_{ij}}$ and to calculate the alternative i's weight in criteria k, we have $w_i^k = \frac{\sum\limits_{i=1}^{n} \alpha_{ij}}{n}$. Then, we extend matrix A_k for other criteria and calculates $w_i^k, \forall i \in \{1, \ldots, n\}, k \in \{1, \ldots, m\}$. After that, we rate the criteria relatively in the same way and multiply the criteria weight w^k with each alternative weight w_i^k and finally the alternative i's priority will be calculated using $\rho_i = \sum\limits_{k=1}^{m} (w^k \times w_i^k)$.

In our model, we have implemented a two-level AHP to fairly prioritize the appliances in our sequential optimization model. We have two criteria ($m = 2$), customer preferences on appliance usage and total appliance consumption, and six deferrable and elastic loads as alternatives ($n = 6$). There might be other criteria and alternatives, but in our case, we found that these are the most important factors that affect appliances scheduling. In our model, the AHP algorithm is implemented in HEMS. Then, each customer can interact with HEMS and rate every two appliances relatively. Note that HEMS has the total consumption information of connected appliances. Finally, HEMS does the AHP computation and finds the weight or priority values of appliances.

3.3 Simulation Results

In this section, we present our simulation results and compare our model, cluster sequential management (CSM), with four other demand management approaches; multi-class appliances scheduling (MAS) [176], autonomous demand-side management (ADM) [57], household energy management (HEM) [95], and multi-objective household appliance optimization (MHO) [107]. To make our implementation close to real-world conditions, we use the dataset of household appliances load profile from [180]. Table 3.1 presents the type of appliances and their total power consumption in a day.

Table 3.1: Types of appliances.

Appliance	Load Type	Energy(kW/day)
Heater	Elastic	25.43
Electric Vehicle	Elastic	26
Freezer	Deferrable	2.07
Washing Machine	Deferrable	1.96
Cloth Dryer	Deferrable	2.47
Dish Washer	Deferrable	1.44
Refrigerator	Essential	3.65
Coffee Maker	Essential	0.19
TV	Essential	2.57
Light	Essential	0.41
Stove	Essential	0.61
PC	Essential	3.93

The simulation environment is Python, and we use the SciPy library to solve MILP and LP optimization models. This simulation is conducted on an Intel i5 CPU with 3.55 GHz clock speed and 16 GB RAM. Also, our algorithm processing time was 10 seconds. Four different scenarios with different mixes of appliances are used for performance evaluation. These are indicated in Table 3.2 and are comprised of (i) 6 essential, 2 elastic (electric vehicle and Heater) and 1 deferrable loads, (ii) 5 essential, 2 elastic (electric vehicle and Heater) and 2 deferrable loads, (iii) 4 essential, 1 elastic (electric vehicle) and 3 deferrable loads, and (iv) 3 essential, 1 elastic (Heater) and 4 deferrable loads. These are defined to compare the sensitivity and effectiveness of five different approaches (CSM, MAS, ADM, HEM, and MHO) with respect to load types. Note that other combinations of loads do not impact the workings of the proposed scheme. Therefore, we choose these four different scenarios to evaluate the performance of our model. In MAS and ADM, all the power consumption is accumulated and distributed through the permissible intervals without considering the priority of appliances on power consumption and customer preferences. However, the authors in MAS have categorized the appliances into different load clusters and optimized each using their specific optimization function while their deferrable loads are non-interruptible. We compare our model with other recent articles HEM and MHO. They have similarities with our model in comfort, cost minimization, and appliance scheduling. Besides these similarities, there are some differences. In HEM [95], the authors have implemented an iterating genetic algorithm (GA) and assumed different load categories with different settings to adjust appliance time usage and comfort level. However, the loads are optimized simultaneously without considering the essential load effects on peak and cost. On the other hand, in MHO [107], their proposed multi-objective model has focused on minimizing cost, peak, and scheduling inconvenience. The authors have determined different orders of these three factors (cost, peak, and scheduling inconvenience) and optimized all the appliances simultaneously. In [107], the effect of the essential loads on the peak consumption and cost has not been considered.

Table 3.2: Load profile scenarios.

Scenarios	Load Type						Total Energy (kW/day)
	Essential		Elastic		Deferrable		
	Qty.	Pct.	Qty.	Pct.	Qty.	Pct.	
Scenario A	6	17.7%	2	80.1%	1	2.2%	64.23
Scenario B	5	16.9%	2	77.8%	2	5.3%	66.11
Scenario C	4	18.5%	1	66.5%	3	15%	39.11
Scenario D	3	16.6%	1	63.6%	4	19.8%	40

To put the appliances in order for our sequential optimization, or in other words, to prioritize them, we used the AHP method explained before. This yielded the priority

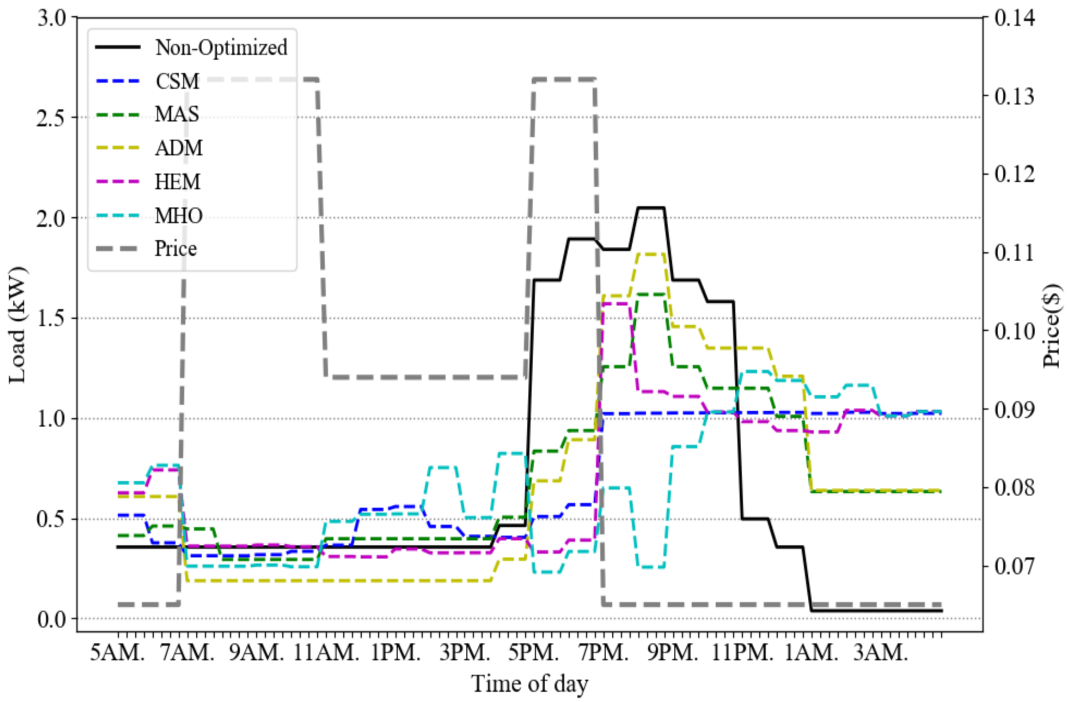

Figure 3.4: time-of-use rate and average energy consumption scheduling in a day of scenario A.

vector $\mathbf{\Gamma}_i = (\rho_1, \ldots, \rho_M)$ for M deferrable and elastic devices. Note that, in this model, elastic loads have higher priority than deferrable ones because their total consumption is higher than deferrable loads. In this simulation, scheduling is performed across a 24-h day subdivided into 96 equal time slots beginning at 5 AM. We use a time-of-use pricing signal based on the Ontario energy board (OEB) [181], with household energy consumption based on an average winter consumption in Ontario, Canada. We assume the customer wants to keep the room temperature within the maximum permissible ASHRAE standard range, and we include provisioning for fully charging an EV. We consider a room size of 118.4 square feet, with $\theta_{outside} = -10°C$ (the average outside temperature in December 2018 in Ontario), and an inside temperature of $\theta_{inside} = 22°C$. We assume a PPD of less than 16%.

Figure 3.4 presents the optimized power consumption of scenario A in six different models: our CSM, versus MAS, ADM, HEM, MHO, and the non-optimized case. Note that for MHO implementation, we choose the order of inconvenience, cost, and the peak optimization (scenario 3 in [107]) that is closer to our proposed architecture. This figure shows the average result of 10 runs. The price signal presents different tiers of time-of-use pricing (off-peak, mid-peak, and on-peak). As observed from the figure, the proposed model reduces the peak consumption by almost 30% more than the MAS, ADM, and HEM, and 15% more than MHO in scenario A.

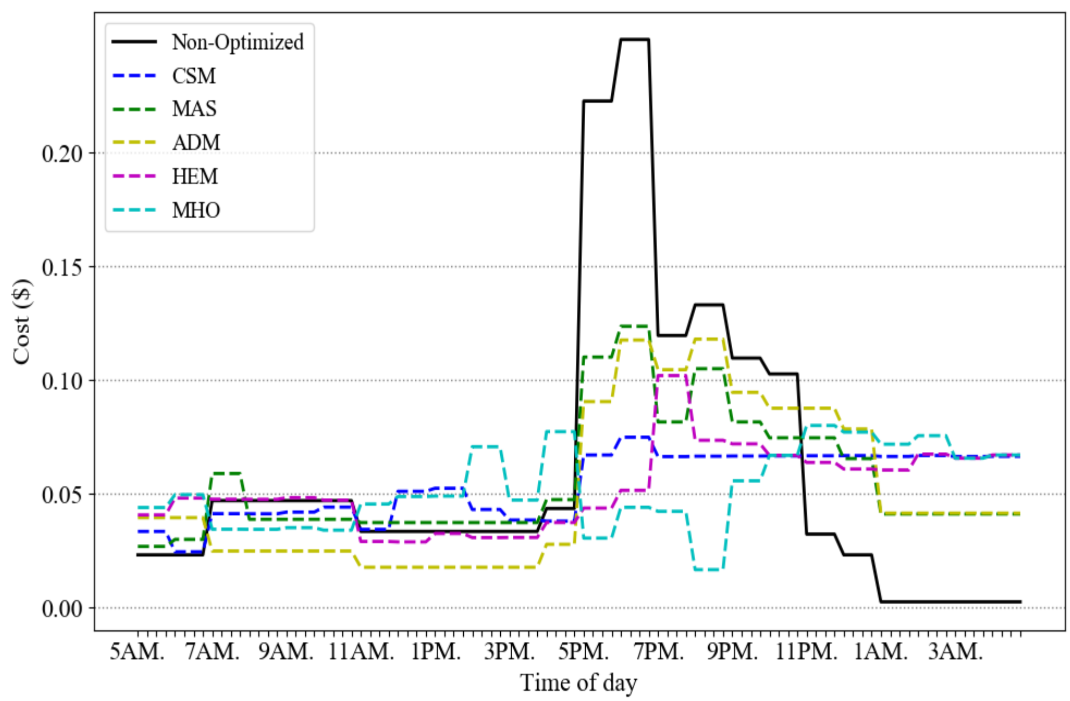

Figure 3.5: Cost changes in different time slots for five models.

Figure 3.5 gives the cost profiles for the demand of Figure 3.4. Due to the flattening impact of our CSM scheme, its overall cost is lower than the other schemes. Figure 3.6 illustrates how the temperature is fluctuating over different time slots in the compared

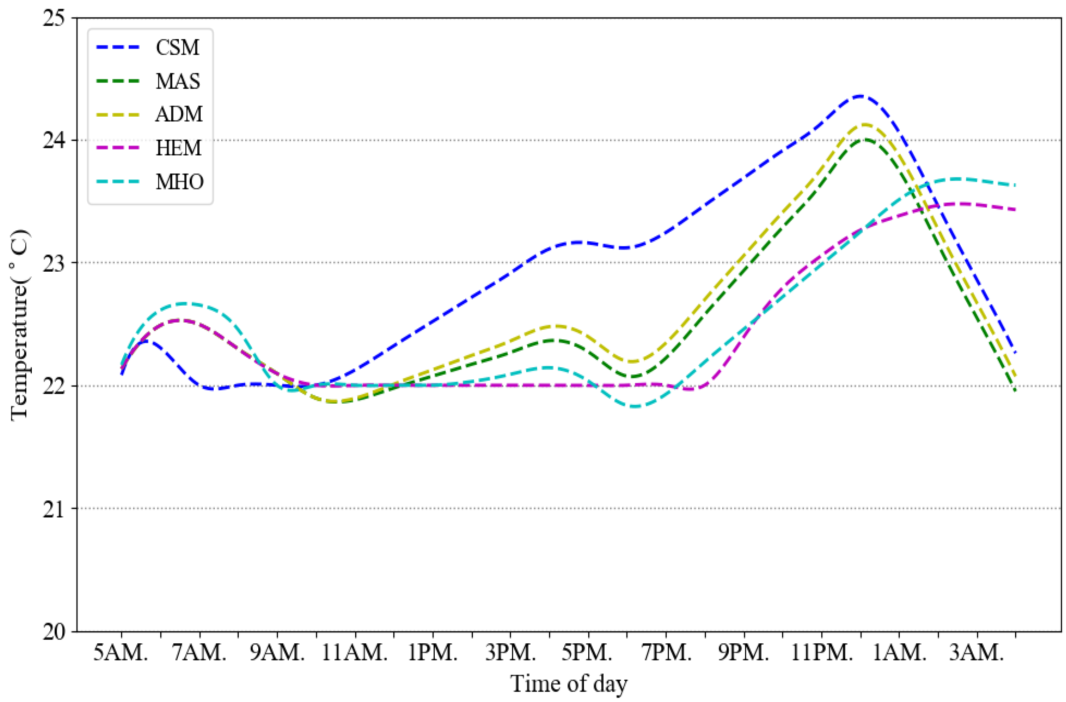

Figure 3.6: Temperature fluctuation in different models.

approaches. The five models consume the same amount of power in a day to keep the room warm, but their temperature is different in different time slots. Our approach is keeping the temperature in ASHRAE standard range and increasing the temperature close to 25°C, which is the best room temperature in winter. The approaches MAS, ADM, and MHO schedule the total energy regardless of thermal comfort formulation but consume the same minimum range of electricity for thermal load during a day.

However, the HEM model has a thermal constraint for setting the minimum and maximum room temperature. Here we set it between 22°C and 25°C, same as our model assumption. CSM and HEM keep the temperature more than 22°C, but our model increases the temperature more (close to 24.35°C to reduce the PPD). Table 3.3 is a summary of the minimum, and maximum temperatures and the averaged PPD in a day for the different approaches. Our CSM approach has the lowest PPD, and though it has a slightly greater temperature excursion than the other approaches while remaining within limits, the temperature variation rate is much less. HEM has a higher PPD than MHO despite having a temperature constraint. The HEM guarantees to keep the temperature in the comfort range (more than $22°C$) and minimize the bill. Therefore, at peak times, it consumes the minimum electricity needed to satisfy the temperature constraint. However, MHO is fluctuating through the times and cooling and warming the house based on the time-of-use pricing signal.

Table 3.3: Results comparison.

Approach	PPD (%)	$T_{min}(°C)$	$T_{max}(°C)$
CSM	11.68	22	24.35
MAS	13.83	21.88	23.99
ADM	13.37	21.89	24.11
HEM	14.27	22	23.46
MHO	13.99	21.83	23.66

As a consequence, the best way for simulating a household thermal comfort is to use a standard satisfaction formulation such as PPD in optimization constraint instead of only considering the temperature range.

To ensure that our approach is robust with regard to parameter choice, we repeat scenario A for 10 days and calculate the cumulative cost for different approaches; the results are presented in Figure 3.7. Our approach is seen to always have less cost than the others. The reason that MAS has a higher cost than ADM is that, in the former, the deferrable loads are non-interruptible, which constrains usage time, but in the latter, they are interruptible and unconstrained. Also, HEM and MHO have almost more accumulated costs than CSM due to the lack of essential load consideration on their scheduling. Moreover, we can assert that within 10 days of consumption, the customer saves almost \$5, and if we extend it to a month, the saving would be \$15. Note that the average cost of electricity bill in Ontario, Canada is \$125 per month [181]. Therefore, the savings of customers would be considerable.

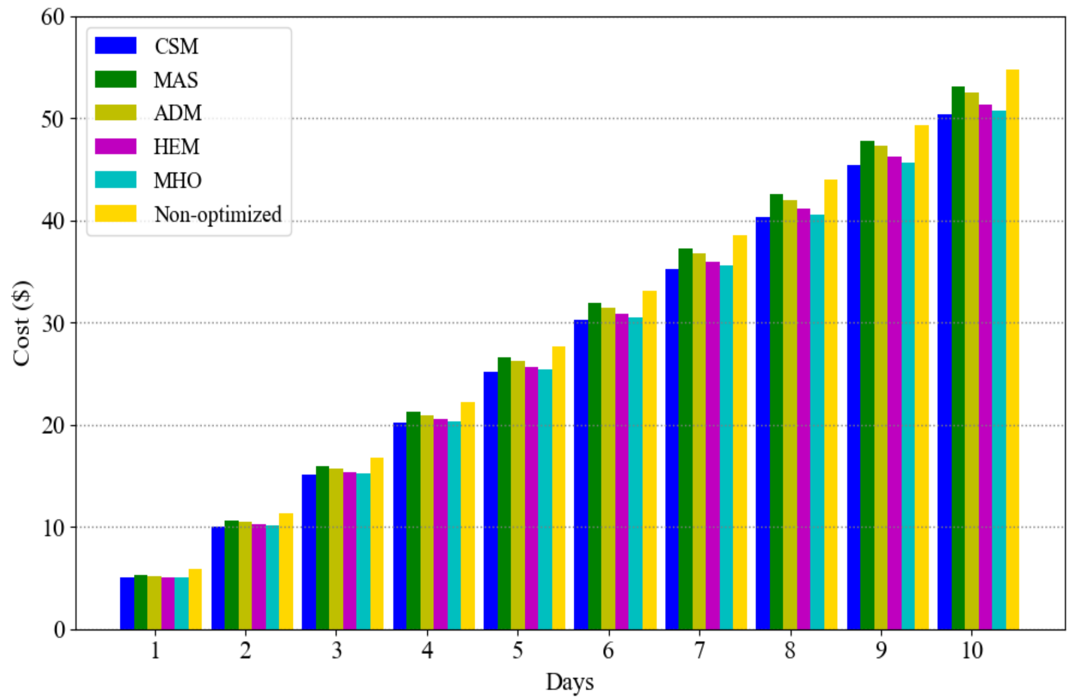

Figure 3.7: Cumulative cost in 10 days.

To present the effect of load clustering and prioritization on our model, Figure 3.8 and Figure 3.9 present the results of different scenarios on the total cost and PAR, respectively. Note that, in each scenario, the total demand is equal between the six approaches.

Based on Figure 3.8, our model has the lowest cost in all the scenarios considered. The usage priority of appliances causes elastic loads, with high consumptions, to be optimized first and then the prioritized deferrable loads to be optimized in the next level. Moreover,

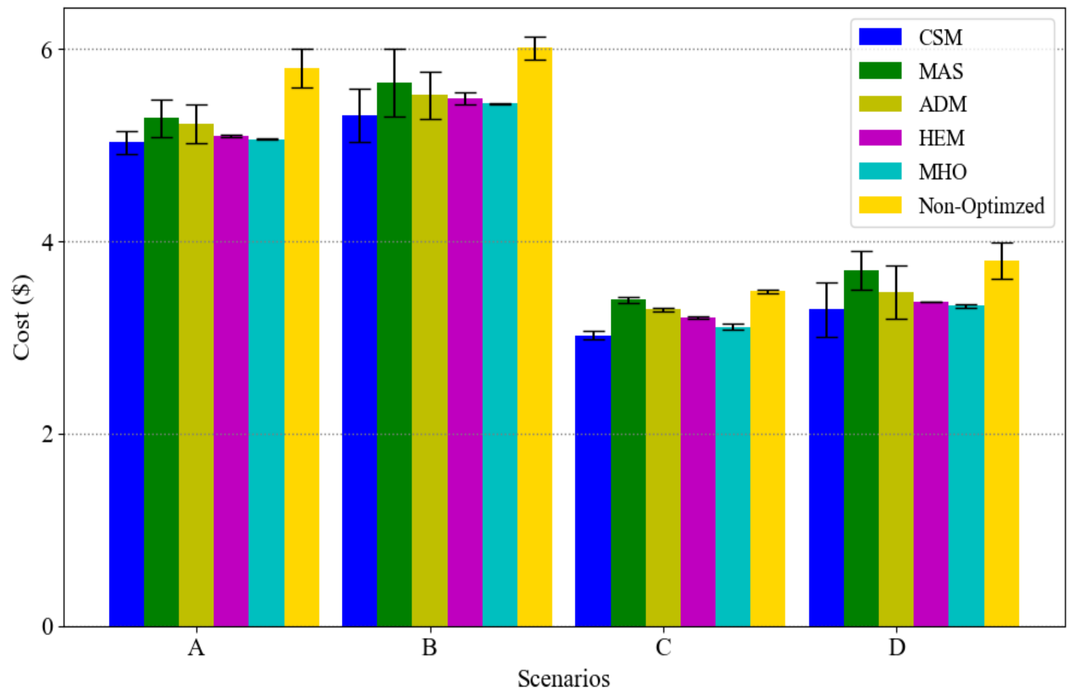

Figure 3.8: Total cost in a winter day on different scenarios with confidential interval.

considering essential loads usage as a lower bound in the optimization model helps reduce the total cost.

Regarding Figure 3.9, the PAR in our model is the minimum in different scenarios, and the reason why ADM has less PAR than MAS in scenarios C and D is due to the interruptible deferrable load assumption in the ADM model (in scenario C and D number of deferrable loads are increased). Moreover, HEM and MHO have less PAR than ADM and MAS because of their optimization models, GA and MILP. Also, it shows that the appliance usage priority and clustering positively affect finding proper time slots for the consumption of the appliance, especially for the elastic load with high demand. Finally, we can assert that we reduced the cost by almost 8%, 6%, 5% and 3%, and decremented PAR almost 34%, 33%, 24% and 17% more than MAS, ADM, HEM and MHO, respectively. The

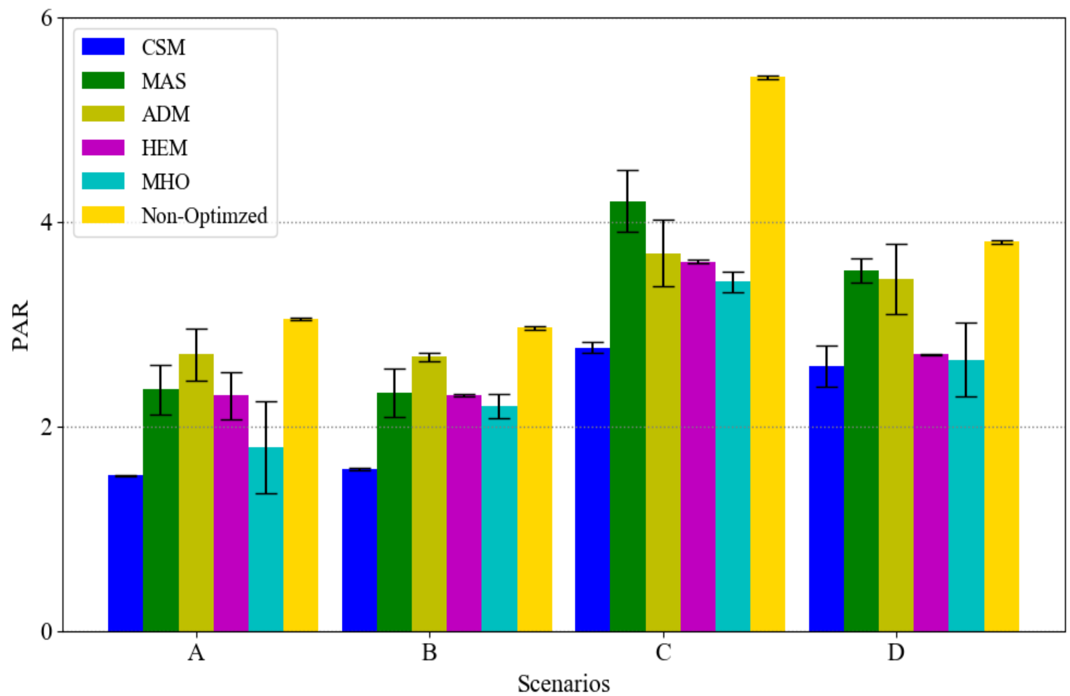

Figure 3.9: PAR on different scenarios with confidential interval.

confidence interval measures the degree of uncertainty of different samples. In Figures 3.8 and 3.9 the intervals are varying due to the different algorithms' sensitivity and behavior in accordance with different types of loads.

3.4 Conclusion

In this chapter, we have presented a multi-objective demand management approach using appliance clustering and prioritization and keeping the customer thermal comfort in ASHRAE standard range. Customer comfort is considered in many aspects, prioritizing appliances for the sequential optimization (the one optimized first will completely satisfy all its constraints), customer comfort on thermal load, electric vehicle state-of-charge, and deferrable loads non-interruptible usage on selected permissible time interval. Our main goals are to flatten the household demand and effectively reduce the cost of the customer while increasing its comfort via elastic and deferrable loads. In this work, we compared our lightweight model with other demand management methods, which have similarities in prioritization, clustering, PAR, and cost management. The loads are nominally the same in different approaches, but they are not treated the same way. Our results illustrated that we smoothed the demand profile, reduced PAR by almost 45% more than the non-optimized case, decreased the electricity bill by almost 13%, kept the room temperature in ASHRAE standard range, and charged electric vehicle more than the desired amount of the customer. The reason is because we discover the nature of the loads and how they should be treated. Note that, this is not a generic system model and in future work we can include more general loads and priority levels. Therefore, to continue our research on energy management, we move from individual customer load management to incentive-based demand control. In the next chapter, we propose a probabilistic demand response approach using a mixed-strategy Stackelberg game between an aggregator and residential customers to deliver demand reduction at peak time slots.

Chapter 4

Stochastic Demand Response Management using Mixed-Strategy Stackelberg Game

4.1 Introduction

Stochastic solutions to the Demand Response (DR) problem enable utility companies to address the uncertainties in customer demand. In other words, stochastic DR solutions have been recently developed considering storage systems, renewable resources, and the electricity market. In this chapter, we present a DR approach for uncertain response of consumers to an incentive-based DR problem. This is a new perspective stochastic DR approach using a mixed-strategy Stackelberg game (MSG) between an aggregator and residential customers during peak load periods (PLP). We use a real dataset collected by a local utility company. We cluster customers based on customer baseline load (CBL), select one reference customer for each cluster, and implement the MSG between those customers and the aggregator. We map the MSG to subgames and prove the equilibrium using mixed-strategy Nash equilibrium (NE). Our results show that the peak load can be shifted to off-peak hours for almost 40%, and players gain monetary rewards in return.

4.2 System Model

We consider a residential area with a distribution system operator (DSO), $N_A = 1$ aggregator, and N_C residential customers/clusters where $i \in \mathcal{N}_C$ and $\mathcal{N}_C = \{1, \ldots, N_C\}$. We define H as the number of time slots within a day and $h \in \mathcal{H}$ where $\mathcal{H} = \{1, \ldots, H\}$. The local aggregator predicts the aggregated customer baseline load vector $\boldsymbol{p} = (p_1, p_2, \ldots, p_H)$ using their load profile and support vector regression (SVR) algorithm. The predicted value is regularly sent to the DSO to monitor the distribution network. The DSO scrutinizes vector $\boldsymbol{p}$ and any time slot with the demand exceeding DSO threshold is detected as PLP and it is added to $\boldsymbol{\tau}_{PLP}$ set, where $\boldsymbol{\tau}_{PLP} \subseteq \mathcal{H}$. PLP is a set of peak load time slots that happens when the network demand is more than a threshold and brings a high cost of supply for the DSO.

Next, the DSO sends $\boldsymbol{\tau}_{PLP}$ set to the aggregator and requests to reduce the local demand of its customers for the given PLP time slots. Then, the aggregator dispatches the $\boldsymbol{\tau}_{PLP}$ set to the local home energy management systems (HEMSs) and ask for load reduction. Individual HEMS estimates the load shed availability (LSA) of customer $\boldsymbol{l}^i = (l_1^i, l_2^i, \ldots, l_H^i)$, which is the maximum available load reduction profile of customer based on its flexible loads [127], and sends it back to the aggregator. Here, for $h \in \boldsymbol{\tau}_{PLP}$ we have $l_h^i \neq 0$ and otherwise $l_h^i = 0$. Afterwards, the aggregator sends the accumulated LSA vector $\boldsymbol{l} = (l_1, l_2, \ldots, l_H)$ to the DSO and it replies with monetary reward profile $\boldsymbol{r} = (r_1, r_2, \ldots, r_H)$ to the aggregator. The reward profile $\boldsymbol{r}$ values are calculated according to the financial policies of DSO. Then, the aggregator initiates the Stackelberg game with HEMSs and updates its reward value $\boldsymbol{k} = (k_1, k_2, \ldots, k_H)$. Here, $\boldsymbol{k}$ and $\boldsymbol{r}$ are the reward profiles generated by the aggregator and DSO respectively for different time slots, and we always have $r_h \geq k_h$ with $k_h, r_h \neq 0$ for $h \in \boldsymbol{\tau}_{PLP}$ and $k_h, r_h = 0$ otherwise.

Then, each customer responds to the aggregator's requests by maximizing its utility function U_c^i shown as below;

$$U_c^i = \sum_{h=1}^{H} k_h \beta_h^i \tag{4.1}$$

subject to;

$$\sum_{h=1}^{H} x_h^i \geq E^i$$

$$0 \leq x_h^i \leq M_h^i$$

$$\beta_h^i = \begin{cases} 1 & \text{if } x_h^i \leq (p_h^i - l_h^i) \\ \frac{(p_h^i - x_h^i)}{l_h^i} & \text{otherwise} \end{cases}$$

where $\boldsymbol{x}^i = (x_1^i, x_2^i, \ldots, x_H^i)$ is the consumption profile of customer i and x_h^i is its power consumption at time slot h. The customer i's baseline load at time slot h is shown as p_h^i and its estimated load shed availability is l_h^i. Therefore, U_c^i gives the total monetary reward of user-i in a day. Constraint $\sum\limits_{i=1}^{H} x_h^i \geq E^i$ gives the customer the ability to shift their deferrable loads to off-peak hours and keep the total optimized consumption almost equal or greater than its minimum total consumption E^i. In addition, $0 \leq x_h^i \leq M_h^i$ is representing the lower and upper bound of customer electricity consumption, and M_h^i is its maximum consumption at time slot h. The term β_h^i helps to fairly calculate reward value for customer i. In the case of reducing more than its LSA, the customer only receives a reward equal to the l_h^i reduction, and this is due to the commitment of aggregator with DSO on reward payment. On the other hand, if the customer consumption is in the range $(p_h^i - l_h^i) < x_h^i \leq p_h^i$ its reward is calculated using $k_h \frac{(p_h^i - x_h^i)}{l_h^i}$ but if the customer consumes more than p_h^i, it will be penalized within the same utility function.

Based on the strategies of customers ($\boldsymbol{x}^i$), the aggregator updates its reward value ($\boldsymbol{k}$) in the iterative leader-follower negotiation. The utility function of an aggregator is calculated within the difference between the monetary reward received from DSO and the customer reward share as follows.

$$U_a = \sum_{h=1}^{H} \Big(r_h \big(1 - \frac{\sum_{i=1}^{N_C} x_h^i}{\sum_{i=1}^{N_C} p_h^i}\big) - \sum_{i=1}^{N_C} k_h \beta_h^i \Big) \tag{4.2}$$

subject to;

$$k_h^{min} \leq k_h \leq k_h^{max}$$

The aggregator aims to maximize U_a with respect to $\boldsymbol{k}$, and k_h^{min} and k_h^{max} are the minimum and maximum boundary for k_h, respectively. In (4.2), the first term represents the incentive value that the aggregator receives from DSO, which is proportional to the total power reduction of customers and the second term denotes the total reward payment of the aggregator to the customers.

4.3 Stochastic Demand Response Management

We introduce a day-ahead stochastic demand response approach to prevent peak load periods and reduce the DSO extra cost of generation. To cope with that, our incentive-based DR model encourages customers to reduce their demand at PLP and give them rewards according to their contribution. This model is a day-ahead power consumption decision-making model with no certainty on the power reduction of customers. The goal is to reduce the demand at PLP by offering a monetary reward to the customers based on their contributions. As illustrated in Figure 4.1, we have a three-level architecture that comprises one DSO, one aggregator, and HEMSs installed at the customer premises. The figure also shows the interconnection of agents and the exchanged demand response information (such as reward value, consumption, baseline load, and their functionalities). The aggregator (the game leader) uses the support vector regression (SVR) model to predict the customers baseline load for the DSO. Additionally, it applies the Silhouette method to

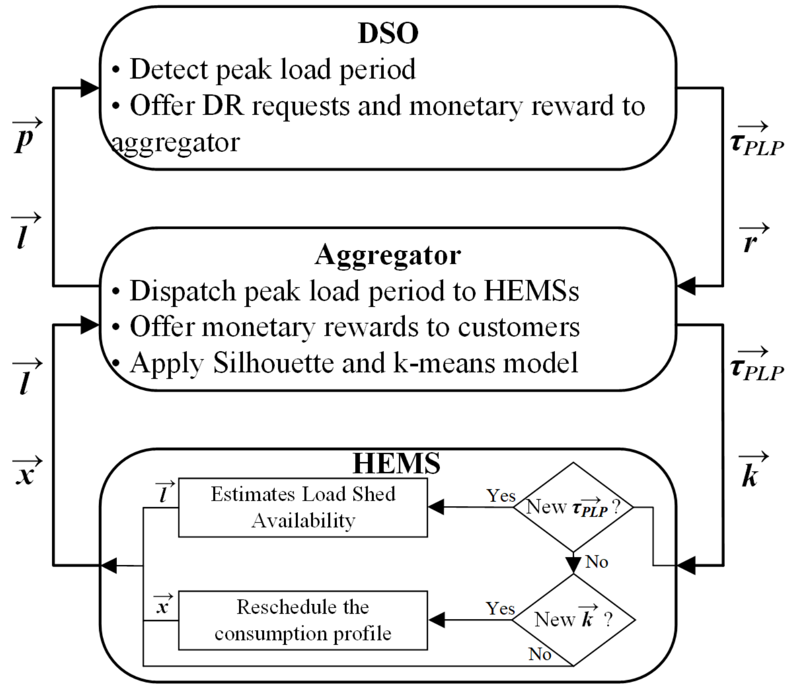

Figure 4.1: Our proposed three-levels architecture.

find the optimal number of clusters and then utilizes the k-means clustering to categorize the customers based on their consumption profile (strategies). The aggregator picks a reference customer from each cluster and plays the game with the reference customers. This approach reduces the processing time and computational resources for seeking all possible strategies and probabilities for all players. All customers in the network share their load with the aggregator regularly for network supervision. To calculate the maximum reward value for customer i, in case of peak load periods, the customer first shares its load shed availability (LSA) with the aggregator and provides an estimation of load reduction. Then, if the aggregator offers new prices $\boldsymbol{k}$ to the customers, customer i reschedules its consumption profile and maximizes (4.1) subject to its constraints to find $\boldsymbol{x}^i$ considering different probabilities (due to mixed-strategy approach) and share it with the aggregator. To this end, the customer who keeps its demand less than the difference of its predicted load and

LSA ($x_h^i \leq p_h^i - l_h^i$), can reach the maximum profit (k_h) according to the constraint in (4.1). The game between the aggregator and the customers repeats until both players and aggregator reach a point that no one can benefit more by changing its strategy. The functions defined in the previous section are used as players' utility functions. Furthermore, to prove the existence of equilibrium point in mixed-strategy Stackelberg game, we present the idea of mapping the game into subgames and prove the mixed-strategy Nash equilibrium in each subgame in the following.

4.3.1 Mixed-strategy Game Definition

Mixed-strategy uses a probability distribution model to allocate random values to players' strategies when there is uncertainty on their reactions. In addition, a game is called Stackelberg when one player's (leader) strategy affects the decision of other players (followers) [58]. Based on the above definition, we model the interaction between the aggregator and customers with a mixed-strategy Stackelberg game because of the uncertainty on the consumption of customers and the leading role of the aggregator in enforcing the reward profile ($\boldsymbol{k}$) to the customers. The strategic form for our finite n-player game may be given by the tuple [182];

$$\Gamma = (\mathcal{N}, \{S^n\}_{n\in\mathcal{N}}, \{U^n\}_{n\in\mathcal{N}}) \tag{4.3}$$

where $\mathcal{N}$ ($\mathcal{N} = \mathcal{N}_A \cup \mathcal{N}_C$) is a finite set of players (in our model it is comprised of N players with $N_C = N - 1$ customers and $N_A = 1$ aggregator whose sets are denoted by $\mathcal{N}_C$ and $\mathcal{N}_A$, respectively), S^n is the space of pure strategies for player $n \in \mathcal{N}$, and U^n is its payoff function. We consider the aggregator as the first player with $n = 1$. We consider Γ as a finite game which means we have a finite number of pure strategies for each player. Therefore, for each $i \in \mathcal{N}_C$ let m_h^i be the number of pure strategies at time slot $h \in \mathcal{H}$, hence $x_h^i \in S_h^i = \{s_1^i, s_2^i, \ldots, s_{m_h^i}^i\}$. Likewise, for the aggregator we have $1 \in \mathcal{N}_A$ and m_h^1 stands for the number of pure strategies of the aggregator at time slot $h \in \mathcal{H}$ and hence, $k_h \in S_h^1 = \{s_1^1, s_2^1, \ldots, s_{m_h^1}^1\}$. Therefore, $\forall n \in \mathcal{N}$ we have $S^n = S_1^n \times S_2^n \times .... \times S_H^n$.

Since we have a finite game, a mixed-strategy equilibrium exists when players choose their strategies probabilistically [183]. Therefore, a mixed-strategy of player n at time $h \in \mathcal{H}$ is denoted by a probability distribution vector $\sigma_h^n = (\rho_1^n, \rho_2^n, \ldots, \rho_{m_h^n}^n)$ over S_h^n. Note that the summation of all the probabilities of player n's strategies at time slot h should be equal to one.

$$\sum_{d=1}^{m_h^n} \rho_d^n = 1 \tag{4.4}$$

If a mixed-strategy played, then the probability distribution over the joint pure strategies $s = (s_{d^1}^1, s_{d^2}^2, \ldots, s_{d^N}^N)(s \in S)$, $\forall n \in \mathcal{N}$ and $d^n \in \{1, \ldots, m_h^n\}$ at time slot h, is $\sigma(s) = (\rho_{d^1}^1, \rho_{d^2}^2, \ldots, \rho_{d^N}^N)$. Based on the above definition, player n's mixed-strategy payoff is calculated as follow [182]:

$$U^n(\sigma) = \sum\nolimits_{s \in S} U^n(s)\sigma(s) \tag{4.5}$$

$$\sigma(s) = \prod_{n \in \mathcal{N}} \rho_{d^n}^n$$

where $U^n(s)$ is the payoff of player n for joint strategies and $\sigma(s) = \prod_{n \in \mathcal{N}} \rho_{d^n}^n$ (this is not the product in mathematics, it presents joint of strategies) is the probability distribution over $s \in S$. Based on the Monte Carlo approach, we allocate different probabilities to the player's pure strategies constrained to (4.4). After calculating (4.5) for player n with different probability values, the highest payoff value will present the player's best strategy with the best probability estimation.

4.3.2 Equilibrium Analysis

In previous works [184–186], authors have presented iterative extensive form definition, coupling Monte-Carlo Tree search sampling with preemptive pruning, and subgame perfect Nash equilibrium by backward induction to prove the equilibrium of mixed-strategy Stackelberg game using NE. Moreover, in [64] the existence of Stackelberg equilibrium (SE) was demonstrated by dividing the game into subgames [187]. To prove the existence of mixed-strategy SE, first, we divide the game into mixed-strategy sub-games (aggregator and customer subgame) according to [64], and then we apply Kakutani fixed point theory [188], we can prove the mixed-strategy NE for each subgame. In addition, by utilizing the Simplex algorithm, we prune the searching area and find the optimal points quicker. Regarding mixed-strategy NE definition in [189, 190], this is a strategy profile with the property that no single player can by opposing unilaterally to another strategy, induce a probability that is strictly preferable.

To formulate the SE based on (4.5), the following assumption should be satisfied for the leader while followers select their best responses. Note that in this model, we have one aggregator ($1 \in \mathcal{N}_A$) and N_C customers ($i \in \mathcal{N}_C$) and this is formulated for a DR event at time slot h.

$$\max \sum_{d=1}^{m_h^1} U_a(s_d^1, s^{-1^*})\rho_d^1 \tag{4.6}$$

subject to;

$$\sum_{d=1}^{m_h^1} \Big(\sum_{i=1}^{N_C} \big(U_c^i(s_d^1, s_{d^i}^{i^*}) - U_c^i(s_d^1, s_{d^i}^i) \big) \Big) \rho_d^1 \geq 0,$$
$$s_{d^i}^i \in S_h^i, d^i = \{1, \ldots, m_h^i\}$$
$$\sum_{d=1}^{m_h^1} \rho_d^1 = 1$$
$$\forall s_d^1 \in S_h^1$$

The pure strategy of the aggregator is s_d^1 where $d \in \{1, \ldots, m_h^1\}$ represents the index of strategies in the set of strategy S_h^1, and s^{-1^*} determines a joint of best response strategy of customers while aggregator selects s_d^1 strategy. The aggregator probability value is presented with ρ_d^1 and $s_{d^i}^{i^*}$ is the pure best strategy of customer i that belongs to the set S_h^i and $d^i \in \{1, \ldots, m_h^i\}$. Equation (4.6) means that for pure followers' strategy s^{-1^*}, we compute via the linear programming (LP) a mixed-strategy $(\rho_1^1, \ldots, \rho_{m_h^1}^1)$ for the leader while playing s^{-1^*} is a best response for the followers and under this constraint $(\rho_1^{1^*}, \ldots, \rho_{m_h^1}^{1^*})$ is the optimal mixed-strategy that maximizes leader's expected utility. To this end, the equilibrium is deduced using the backward induction where the best response of customers i is calculated with the optimization problem (4.7) that guarantees to find the optimal payoff of best strategy $s_{d^i}^{i^*}$ subject to the set A, which represents the constraints in (4.1), and with the initial price s_d^1 from the aggregator.

$$s_{d^i}^{i^*} = \underset{A}{\operatorname{argmax}} \sum_{d^i=1}^{m_h^i} U_c^i(s_d^1, s_{d^i}^i)\rho_{d^i}^i, \forall s_d^1 \in S_h^1 \tag{4.7}$$

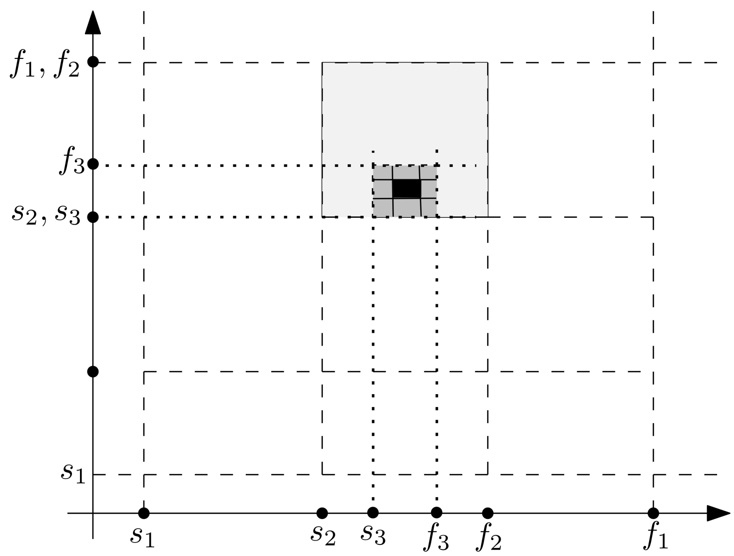

Figure 4.2: The hypothetical Simplex method, to obtains adjacent vertices of the desired set in the sequence.

Now each customer passes its best strategy $s_{d^i}^{i^*}$ to the aggregator subgame, and the aggregator can choose its best response $s_d^{1^*}$ using (4.6). Again this process repeats between the aggregator and customers, where the customers can optimize (4.7) with the new calculated best response of aggregator.

Theorem: A SE exists in the proposed mixed-strategy Stackelberg game, upon the optimal solutions for the customers and the aggregator.

Proof: According to [64] and Kakutani fixed point theory [188], the existence of mixed-strategy NE have to be proven in each subgame to finally prove the SE. Utility function U_c^i is a non-empty, non-negative, continuous, and is defined on a compact subset of Euclidean space [191]. Moreover, U_c^i is concave and using convex programming, we can find its maximum point. Moreover, the optimization in (4.6) is a linear program on $(\rho_1^1, \ldots, \rho_{m_h^i}^1)$ and hence it is convex and also is defined on a compact subset of Euclidean space. Therefore, there exists a solution to (4.6) which is a mixed-strategy SE.

4.3.3 Simplex Algorithm

The Simplex method is a pruning algorithm that starts with a random point and omits points systematically by monitoring the points behavioral algorithm for maximizing the objective function [192]. As it is illustrated hypothetically in Figure 4.2 for two strategies and a given desired levels, which are started at s_{itr} and ended at f_{itr}, $itr = \{1, 2, 3\}$ we may define a simplex algorithm, which is a 2-dimensional generalization of a polytope, and subsimplexes (shaded area in Figure 4.2) to achieve a global maximum. For the simulation, we repeat the game itr times to find accurate strategies by changing the discretization window w_{itr} after each round. For example, a strategy range for one player is changing like;

$$s_{itr} = s_{itr-1} + w_{itr}, f_{itr} = f_{itr-1} - w_{itr}. \tag{4.8}$$

We try to make the window smaller and smaller based on the Simplex method to finally find the highest probability and accurate strategies for the players.

Algorithm 4.1

Initialize number of players, strategies and game iterations
Apply Silhouette method and k-mean clustering to cluster customers based on CBL
Find PLP time slot $h \in \boldsymbol{\tau_{PLP}}$ and LSA $l_h^i, \forall i \in \mathcal{N}_C$
for the number of iterations **do**
    if this is the first iteration **then**
        Specify $\boldsymbol{k}$ based on (4.2).
        Specify $\boldsymbol{x}^i, \forall i \in \mathcal{N}_C$ by maximizing (4.1) and using $\boldsymbol{k}$.
    else
        Update customers and aggregator strategies using $(\boldsymbol{x}^{i^*}, \boldsymbol{k}^*), \forall i \in \mathcal{N}_C$.
    end if
    Apply Simplex algorithm and generate $S^n, \forall n \in \mathcal{N}$.
    Find the combination of strategies S
    Distribute probabilities over combination of strategies using Monte Carlo and (4.4).
    Find $(\boldsymbol{x}^{i^*}, \boldsymbol{k}^*), \forall i \in \mathcal{N}_C$ using mixed-strategy solution (4.5).
end for

4.4 Simulation Results

We implemented the mixed-strategy Stackelberg game (MSG) model on a real residential power consumption dataset that contains the electricity usage of 100 houses in the Ottawa region over a year. The dataset was collected by Hydro Ottawa Company from July 2017 to June 2018. We use Python and MATLAB for data preparation, classification, and game implementation. The results are obtained using a PC with an Intel i5 CPU with 3.55 GHz clock speed and 16 GB RAM. The maximum processing time of the MSG algorithm is 90 seconds. The SVR algorithm is trained with 70% of the data, and the remaining data is used to test the efficacy of our predictions. A day is divided into $H = 24$ time slots. To represent the load profile of customers in different seasons of the year, we select a month in each season as a reference, such as February in winter, May in spring, July in summer, and October in fall. Then, we cluster the customers into groups using k-means and apply the Silhouette method. By doing this, We identify a reference customer from each cluster. As explained before, the reference customer plays in the game as an individual customer. Table 4.1 represents the number of clusters (chosen by Silhouette method) and PLP time slots for different months. For example, in February, the game is played among 6 players, 5 clusters of customers, plus one aggregator. Note that the game is played for each month.

Table 4.1: Summary table for the number of clusters and the peak load period for each month.

Month	**No. of clusters**	**Peak load period (h)**
February	5	7pm-10pm
May	7	7pm-10pm
July	5	5pm-6pm, 8pm-9pm
October	6	5pm-8pm

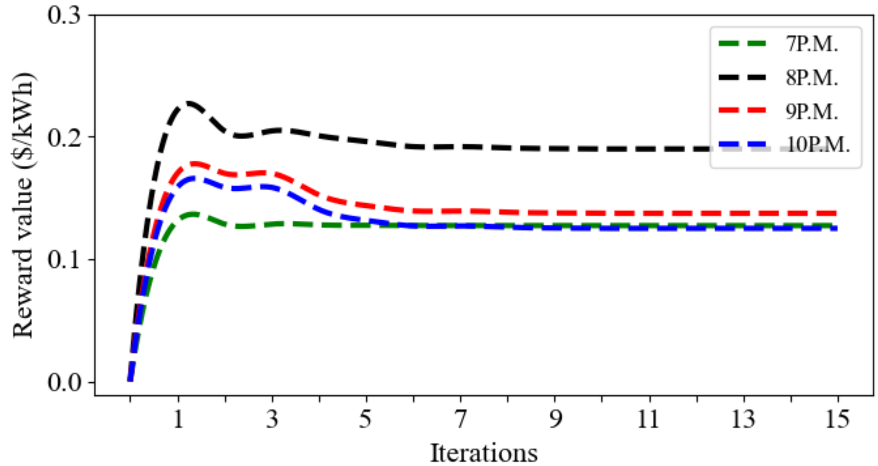

(a)

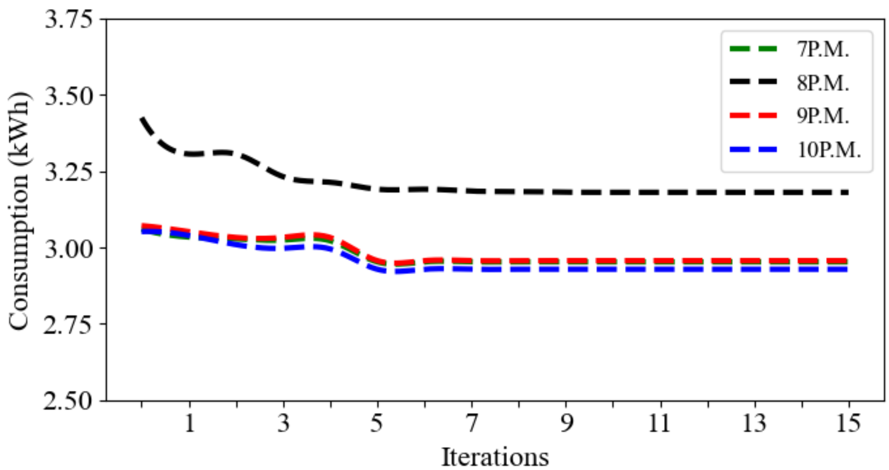

(b)

Figure 4.3: (a) Average reward value of aggregator and (b) accumulated consumption of customers in different iterations in February at peak time slots.

The Silhouette method is applied to find the proper number of clusters for the k-means clustering. It provides a measurement between the points in the cluster and the points in neighbor clusters to discover the optimal number of clusters. We implement k-mean clustering with different numbers of clusters and calculate the average distance between

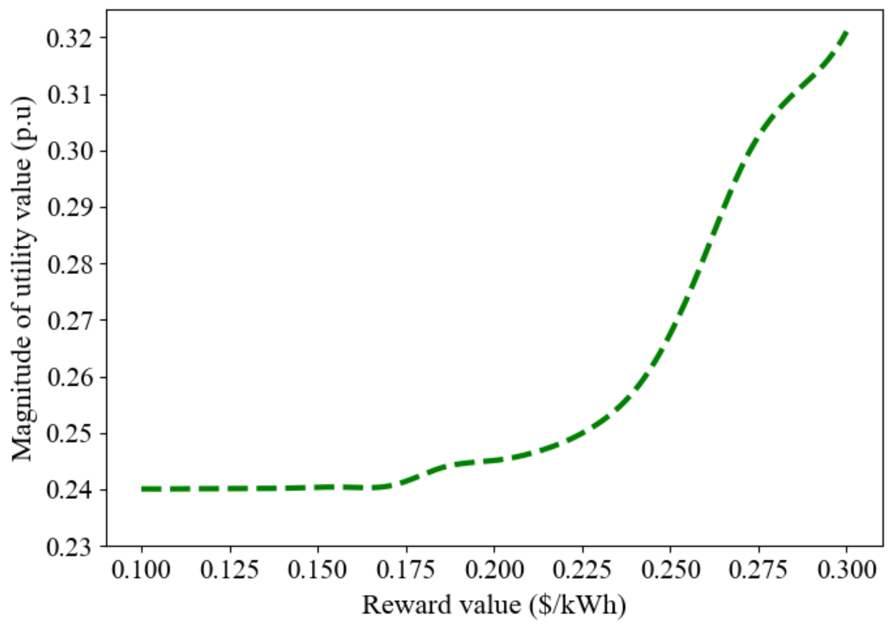

Figure 4.4: Average utility value of aggregator according to varying reward values in February.

point i with other points in the same cluster (a^i), and again the average distance between the point i and other points in neighboring clusters (b^i) [193]. Afterward, the silhouette value is calculated as follows.

$$sil^i = \begin{cases} 1 - \frac{a^i}{b^i} & a^i < b^i \\ 0 & a^i = b^i \\ \frac{b^i}{a^i} - 1 & a^i > b^i \end{cases} \tag{4.9}$$

The Silhouette value has a range of $sil^i \in [-1, 1]$, where 1 means the sample is in the correct cluster, and for sil^i closer to -1, it means the point i is assigned to a wrong cluster. Therefore, we can find the proper number for clustering by implementing the k-mean model for the different number of clusters and calculating the Silhouette values of different points.

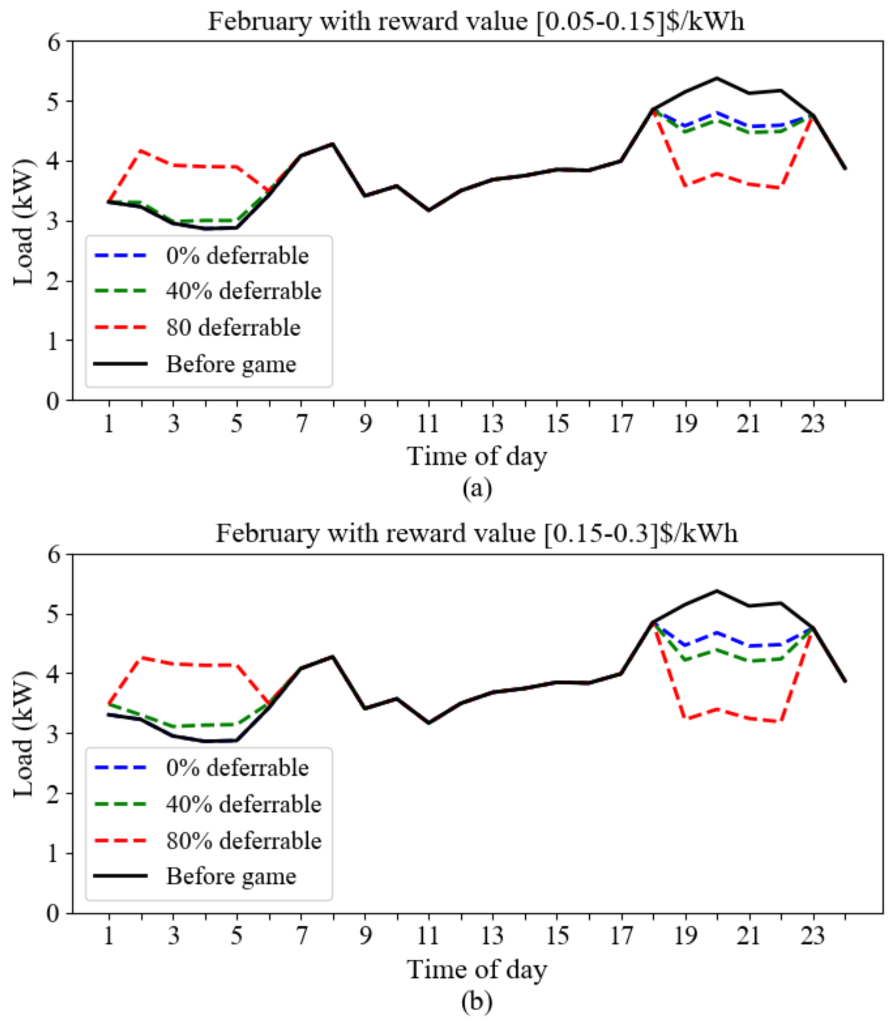

Figure 4.5: Total Demand changes with different percentage of deferrable loads in February.

For the simulation purpose, we assume the customer load shed availability is 40% of their baseline load at each time slot and the range of reward value for the aggregator is $[0.05-0.3]$ $\$/kWh$, which is close to the Ontario time-of-use pricing. Moreover, we consider that almost 20% of customer's load is elastic, such as heating/cooling appliance loads that can be reduced at peak load periods by changing the appliance settings.

Table 4.2: Summary table for load and cost within different ranges of reward price and deferrable loads in February.

Reward value($\$/kWh$)	Deferrable load (%)	Total elastic load (kW)	Total deferrable load (kW)	Saved money (\$)	Total consumption (kW)	Total cost (\$)
0.05-0.15	0	2.27	0	1.87	91.77	12.74
	40		0.43	2.54		
	80		4.02	5.17		
0.15-0.3	0	2.73	0	2.16	91.31	12.6
	40		1.02	4.78		
	80		5.02	8.61		

Figure 4.3.(a) represents the average reward value of aggregator and Figure 4.3.(b) is the accumulated consumption profile of customers through 15 iterations of the game in February with four different peak load period time slots (according to Table 4.1). As expected, customers reduce their consumption more to achieve more monetary rewards with the increase in reward value. To present how the utility value of aggregator is changing with respect to reward, Figure 4.4 shows the averaged utility value of aggregator and its behavior through the varying reward values. As the reward increases, the utility of the aggregator increases either.

4.4.1 Seasonal Peak Reduction Trends

We present the result of demand changes in different seasons with varying percentages of deferrable loads in Figure 4.5 to Figure 4.8. Each figure is representing the results of two different ranges of reward value, $[0.05 - 0.15]\$/kWh$ in figure (a) and $[0.15 - 0.3]\$/kWh$ in figure (b). Figure 4.5 shows the results for February demand profile, Figure 4.6 for May demand profile, Figure 4.7 for July demand profile and Figure 4.8 for October demand profile. The 40% of the deferrable load means only 40% of customers reduce their deferrable loads at peak load period and shift it to the off-peak time slots. We can conclude that by increasing the percentage of deferrable loads, our scheme can shift more loads to off-peak hours and flatten the curve more. Moreover, for the high range of aggregator reward value, the reduction increase is more and more loads can be shifted to off-peak times.

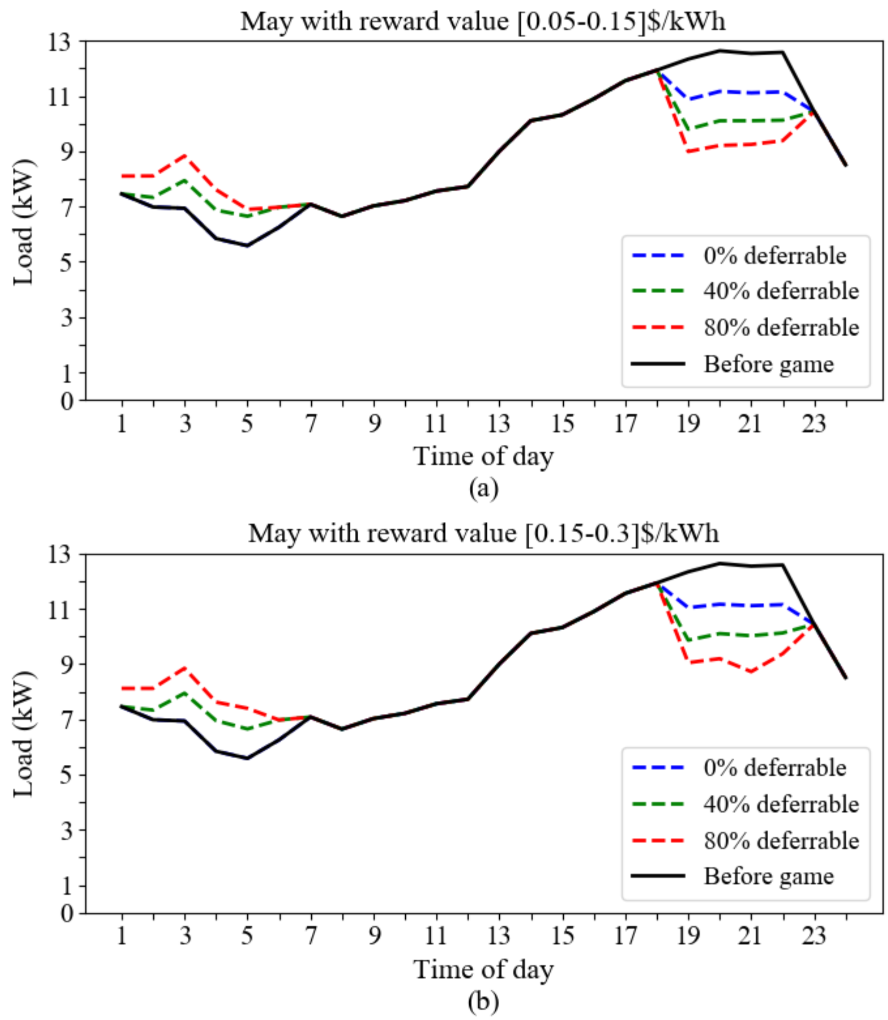

Figure 4.6: Total Demand changes with varying percentage of deferrable loads in May.

In Table 4.2, the results show that for the higher ranges of reward value and deferrable loads, elastic and deferrable loads reduction and saved expenses increase while the total reduction and total cost are almost the same. To scrutinize the reason, we found that in February, the PLP happened at time-of-use off-peak time slots, and shifting the deferrable loads to the minimum consumption time slots, which are time-of-use off-peak hours, does

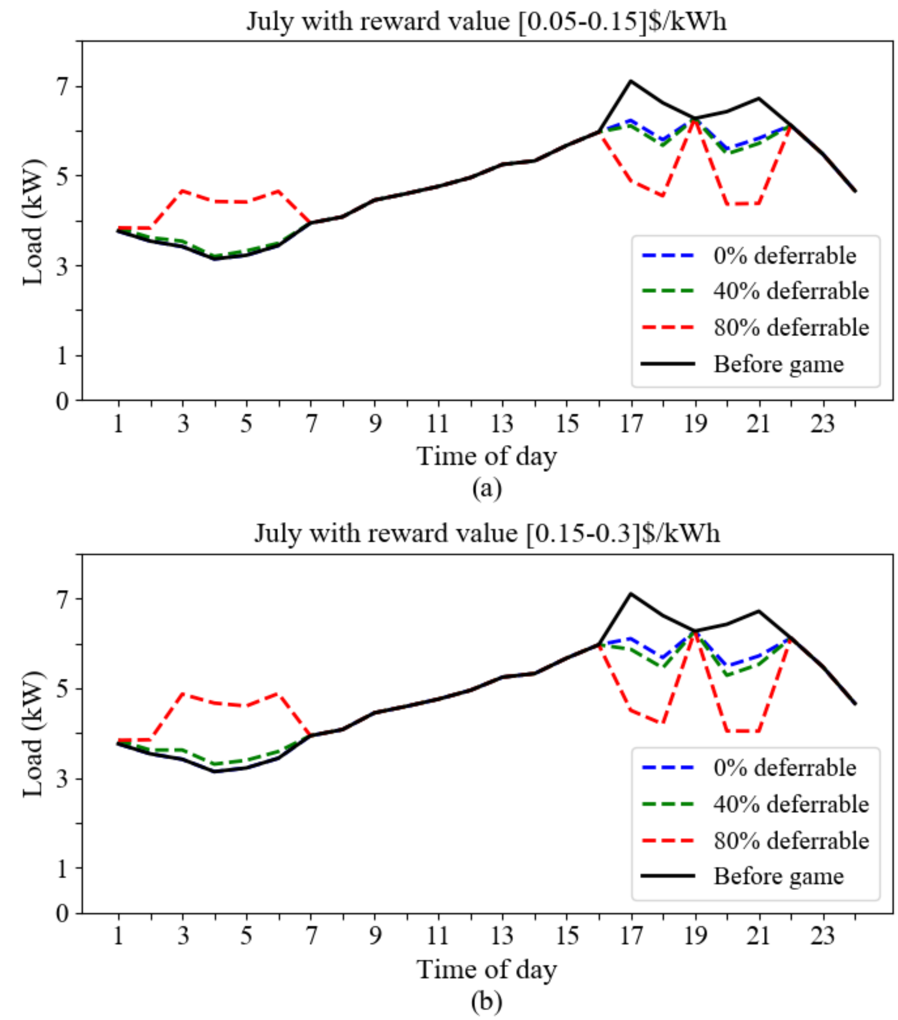

Figure 4.7: Total Demand change with varying percentage of deferrable loads in July.

not have any influence on the total cost. Moreover, only the elastic loads reduce the total consumption, and the deferrable loads are just shifted to other time slots without any reduction.

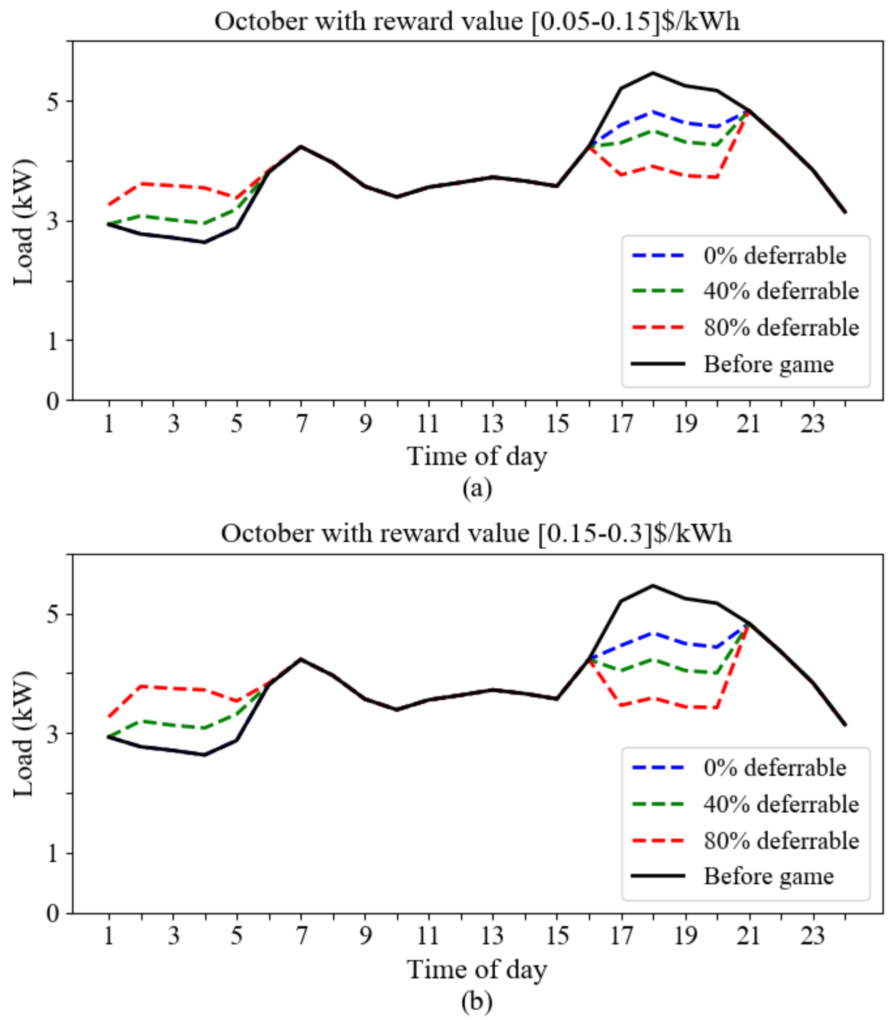

Figure 4.8: Total Demand change with varying percentage of deferrable loads in October.

4.4.2 Comprehensive Comparison and Impact of Clustering

In this section, we investigate the impact of the clustering on customer usage profile during a day at different months, in addition to comparing the output results with two DR models, "Hybrid DR" [74], and "Stochastic Optimization" [194]. The results are presented

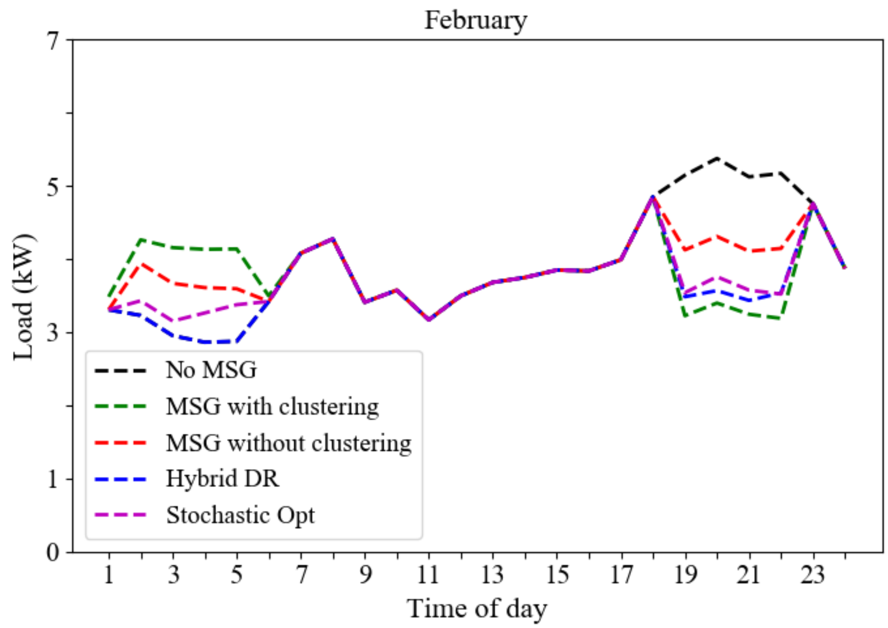

Figure 4.9: The effect of clustering and game model on total demand in February.

in Figure 4.9 to Figure 4.12, noted that "No MSG" refers to the actual demand of the network. Moreover, for "MSG without clustering" condition, we aggregated the usage profile of customers and assumed it as a single player who plays the game with the aggregator (which is a common two-player game solution in the literature [195–197]). To provide a fair comparison between "MSG with clustering", "Hybrid DR" and "Stochastic Optimization", we consider the same initial assumptions and implement the Monte-Carlo algorithm for [74] and [194] to mainly determine the efficiency of our architectural design in the same conditions. Article [74] is an incentive model with a three-level Stackelberg game between power grid operator, retailers, and customers, and [194] is a stochastic demand response optimization model between customers that minimize their cost of electricity usage and shift their controllable loads to off-peak. According to the simulation results, both schemes work close, but "MSG with clustering" reduces the demand and shifts deferrable loads to off-peak hours. The reason would be because of the way of load clustering and the mixed-strategy solution optimal findings. The result shows that in February, May, July, and October, we have almost 37%, 31%, 43%, and 29% peak reduction respectively in comparison to “No MSG”, 23%, 10%, 24%, and 8% reduction with respect to “MSG without clustering”, and almost 10% peak reduction concerning “Hybrid DR” and “Stochastic Optimization”. Moreover, to consider different aspects of comparison, we measured the peak-to-average ratio (PAR). We found out our proposed architecture “MSG with Clustering” is working better with PAR values 1.25, 1.34, 1.28, and 1.27 for months February, May, July, and October respectively, in comparison with “Hybrid DR” that has PAR values 1.33, 1.4, 1.34 and 1.32, and “Stochastic Optimization” that has 1.31, 1.35, 1.34, 1.31. Our scheme is working appropriately due to the mixed equilibrium point of the game, the shift of deferrable loads to off-peak, and the incentive design of the utility function.

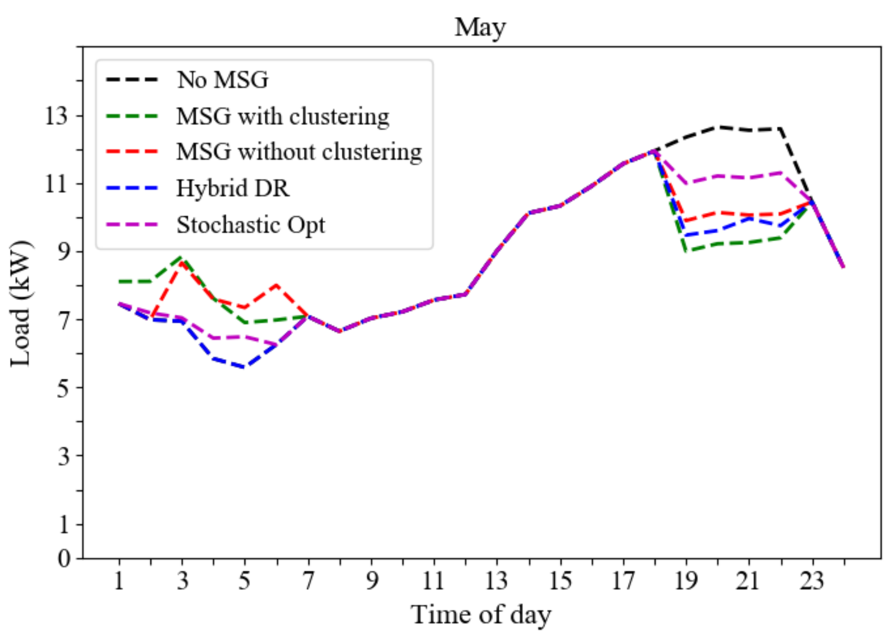

Figure 4.10: The effect of clustering and game model on total demand in May.

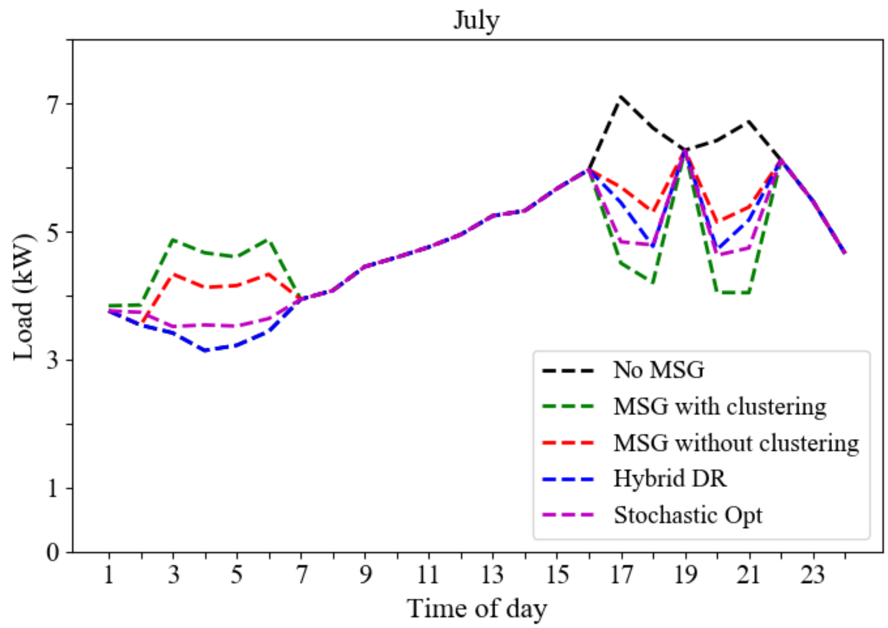

Figure 4.11: The effect of clustering and game model on total demand in July.

4.5 Conclusion

This chapter presented a new perspective demand response approach using a mixed-strategy Stackelberg game between the aggregator and customers to develop stochastic and interactive demand reduction in a residential area. The goal was to engage customers to reduce their consumption at peak load period, keep the total demand less than the DSO threshold, and reward customers for their contributions. The results showed that the proposed scheme brought a significant peak reduction in different months of a year based on real data collected from residential customers. As an outcome, using a stochastic leader-follower game allows the aggregator and customers to select their best strategies, gain significant revenues, and help the network reduce the peak load periods. In the next chapter, we propose an energy blockchain architecture for a demand response model to bring customer privacy, cyber security, and interoperability between the distribution net-

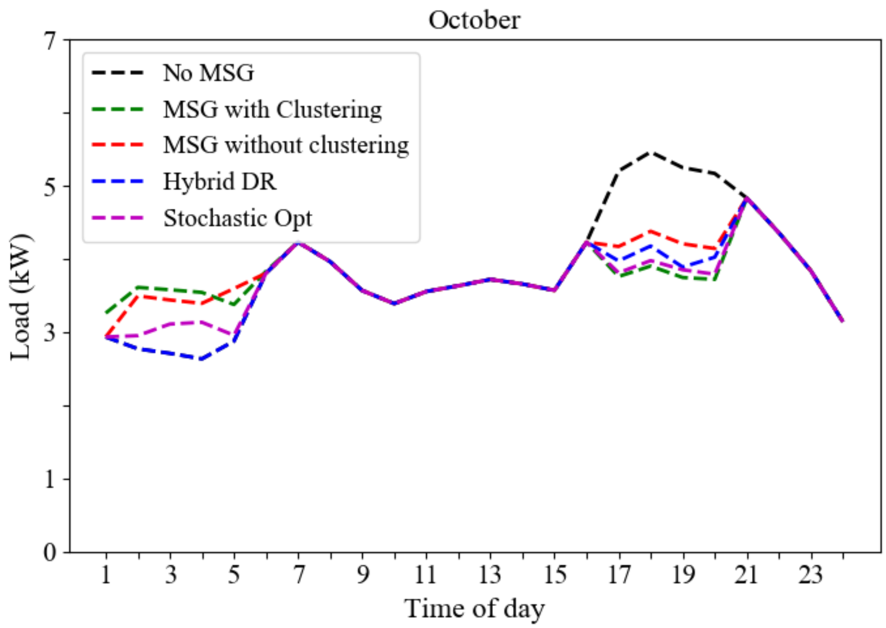

Figure 4.12: The effect of clustering and game model on total demand in October.

work agents. It delivers a real-time and secure automated control among the aggregator and customers.

Chapter 5

Energy Blockchain for Demand Response and Distributed Energy Resource Management

5.1 Introduction

The high impact of demand reduction on the energy grid management and the importance of reducing the loss of distributed energy resources (DER), in addition to the necessity of a secure distributed data storing system, motivate us to propose an energy blockchain solution. This chapter presents a demand response (DR) solution utilizing energy blockchain to reduce demand, save the extra DER, and efficiently incorporate customers block mining ability. In this work, a real dataset of customer demand profiles and photovoltaic (PV) generation in the Ottawa region is used to deploy a DR Stackelberg game between a control agent (CA) and local customers to negotiate demand reduction by integrating the block mining method. This work presents a novel and well-suited consensus algorithm, proof of energy saving (PoES), to incentivize the customers to reduce their demand, discharge their electric vehicle (EV) and maximize their chance for block mining to earn monetary rewards. This results in lower the peak demand, customer bill reduction, and transforms energy savings into monetary rewards. Furthermore, the results show that our proposed consensus algorithm is robust and secure against malicious actions of users.

5.2 System Model

In our system model, the distribution system operator (DSO) intends to offer an incentive-based demand reduction to decrease the demand of customers at the peak to minimize the energy import. To implement this idea, a DR Stackelberg game is designed between the CA and customers to reduce demand using household photovoltaic generation, electric vehicle capacity. Based on Figure 5.1, the DSO sends a DR request to the customers through the CA during peak time slots. The CA is an intelligent agent interacting with customers and reduces the workload of DSO. To provide a trustful and distributed data storage system, the grid transactions (such as game negotiations and DR control signals) are stored on the blockchain where CAs, and DSO are trusted and customers are untrusted nodes of the energy blockchain. There are private blockchains (PBs) in the network where customers are the nodes that can distribute the transactions and blocks through wireless communication. The idea of implementing a private blockchain was to increase the system's sustainability and keep the local area secure from external attacks. Moreover, a private block has the minimum cost of implementation in comparison to other scenarios. Every PB requires a block miner to generate a block of transactions and attaches it to the chain. To pick a miner between the agents, we present proof of energy saving (PoES) consensus algorithm that works similar to the proof of stake (PoS). The node with the highest consensus ratio (energy saving) at a mining event is selected as the miner and generates block. Our consensus algorithm considers the reputation of the node, demand reduction (that is calculated through the Stackelberg game), and available energy for block mining.

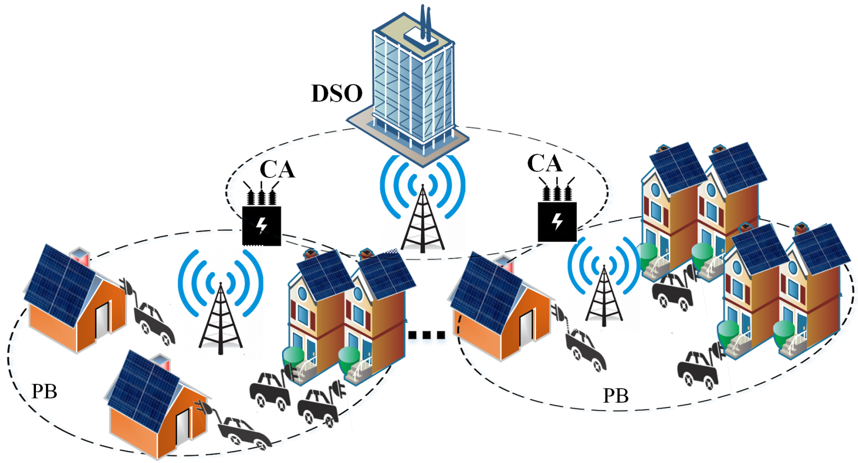

Figure 5.1: Illustration of our demand response architecture and the smart grid.

5.2.1 Proof of Energy Saving Consensus Algorithm

A miner is a node from the network selected through the consensus algorithm. In this work, a consensus mechanism is proposed to use the surplus DER of customers for the block mining operation, which is similar to a storage system that saves energy into monetary resources. In our consensus mechanism, each node has a consensus value measured with availability, reputation, and compliance ratio factors. Therefore, the consensus value for customer i, where $i \in \mathcal{N}_C = \{1, 2, \ldots, N_C\}$, is calculated with the average of three factors (A_i, R_i, ρ_i). 1) **Availability** ($A_i \in [0, 1]$); for mining, a node spends mining energy equal to χ and can supply the energy by PV generation (x_{i1}^{PV}), demand (x_{i1}^{demand}) (that is a part of customer desired consumption) and discharging its EV capacity (x_{i1}^{EV}). The availability is calculated as below.

$$A_i = \frac{(x_{i1}^{PV} + x_{i1}^{demand} + x_{i1}^{EV})}{\chi} \tag{5.1}$$

2) **Reputation** ($R_i \in [0, 1]$); nodes can rank their experience of interacting with other nodes as trusted, untrusted or uncertain according to [144]. A smart contract is an exe-

cution code that runs by all the nodes in the blockchain network to check the transaction validation before being added to the block. Therefore, smart contract can validate a transaction and detect a node with malicious action. In our model, customers with malicious actions lose their reputation value due to the untrusted votes other customers submit. 3) **Compliance Ratio** ($\rho_i \in [0,1]$); this is the ratio of a customer's total electricity reduction to its total requested reduction. The value e is the index of a DR event, and E is the number of events happened in a window of one week, where $e \in \mathcal{E} = \{1, \ldots, E\}$. The value c_i^e is customer i's demand reduction at event e and r_i^e is the amount of demand reduction the CA asks the customer i at event e where we have $\mathbf{c}_i = (c_i^1, c_i^2, \ldots, c_i^E)$, $\mathbf{r}_i = (r_i^1, r_i^2, \ldots, r_i^E)$. The compliance ratio of a customer is defined as follows;

$$\rho_i = \frac{\sum\limits_{e=1}^{E-1} c_i^e + (x_{i2}^{PV} + x_{i2}^{demand} + x_{i2}^{EV})}{\sum\limits_{e=1}^{E} r_i^e}, \tag{5.2}$$

where $\sum\limits_{e=1}^{E-1} c_i^e$ represents the summation of demand reduction until event $(E-1)$ and $\sum\limits_{e=1}^{E} r_i^e$ is the summation of demand request within a week. In other words, the c_i^e for the recent DR event (E) is equal to $c_i^e = x_{i2}^{PV} + x_{i2}^{demand} + x_{i2}^{EV}$. Customer can reduce its demand using PV generation (x_{i2}^{PV}), actual demand reduction (x_{i2}^{demand}) (by shaving or shifting the demand), and discharging EV capacity (x_{i2}^{EV}) to handle the request. Hence, a customer with a considerable history of demand reduction has more chance to be selected as a block miner. By averaging these three factors, the consensus value of customer i would be $arc_i \in [0,1]$, and the customer with the maximum arc value is selected as the block miner in each mining event. This means that miners with high availability, reputation, and compliance factors will be favored. Proof of energy savings (PoES) consumes less energy for block mining than PoW and PoS, while only one node is responsible for the mining process. Moreover, it is a well-suited consensus algorithm for incentive-based DR architectures that consider the combination of reputation and energy contribution to select a miner.

5.2.2 Utility Functions

The DSO predicts the total demand using the support vector regression (SVR) [198] prediction engine and recognizes peak time slots and high-demand situations a day-ahead. Therefore, it sends DR requests (demand reduction signal) to maximize the contribution of customers and minimize the monetary reward paid for compensation according to (5.3). After the DSO initiates the Stackelberg game, the CA starts interacting with customers and allocates different DR requests $r_i^e, \forall i \in \mathcal{N}_C$

$$U_d = \ln{(A + \alpha \sum_{i=1}^{N_C} c_i^e)} - \frac{\beta \sum_{i=1}^{N_C} (\rho_i r_i^e)}{A}, \tag{5.3}$$

subject to;

$$\sum_{i=1}^{N_C} r_i^e \geq G$$
$$r_i^e \geq l_i, \forall i \in \mathcal{N}_C.$$

The value α is the associated DR profit price for the DSO, G is the desired minimum energy reduction of the DSO, l_i is the minimum available DR reduction for customer i, β is the allocated reward value for the customer reduction, c_i^e is the customer i's electricity reduction for the recent event (e), A is the scaling parameter, and ρ_i is customer i's compliance ratio which helps the CA to allocate demand reduction accordingly. In (5.3), the first constraint is used to keep the total DR request more than the minimum reduction threshold, and the second constraint keeps the DR request more than the minimum availability of the customer.

Before the game starts, the customers submit the reputation values and rate each other, but the availability and compliance ratio is calculated during the Stackelberg game due to their dependence on the demand reduction. In this game, customers are the followers, and their goal is to find the best strategy (c_i^e) that maximizes their probability for block mining

(arc_i) and maximizes the profit of EV charging and demand reduction reward at the recent DR event (e). Customers can use their PV generation, demand, and EV capacity for block mining and demand reduction. Moreover, the PV generation is first consumed for mining, then demand, and the surplus is used for EV charging. The customer's utility function is presented as follows.

$$U_c = \gamma(arc_i) + \theta x_{i3}^{EV} + \beta c_i^e, \tag{5.4}$$

subject to;

$$x_{i2}^{PV} + x_{i2}^{demand} + \sigma_i x_{i2}^{EV} \leq r_i^e$$

$$x_{i1}^{PV} + x_{i1}^{demand} + \sigma_i x_{i1}^{EV} = \chi$$

$$x_{i1}^{PV} + x_{i2}^{PV} + \sigma_i x_{i3}^{EV} \leq P_i$$

$$B_i^{min} \leq B_i^{current} + \sigma_i(x_{i3}^{EV} - x_{i1}^{EV} - x_{i2}^{EV}) \leq B_i^{max}$$

$$x_{i1}^{demand} + x_{i2}^{demand} \leq p_i - d_i.$$

The arc_i was represented in the previous section, and γ is the allocated reward for block mining. According to (5.4), the second term maximizes the EV charging profit, and the third term maximizes the reward of demand reduction. The values θ and β are the profit rates of charging EV through PV and the reward value of demand reduction, respectively. In addition, x_{i3}^{EV} represents the extra PV energy used for EV charging. The value P_i is the total PV generation of customer i at the recent DR event, $x_{i1}^{PV}, x_{i1}^{demand}$ and x_{i1}^{EV} are the unknown variables used to find the optimized value of PV, demand, and discharged EV energy allocation for block mining respectively. Moreover, $x_{i2}^{PV}, x_{i2}^{demand}$ and x_{i2}^{EV} are the unknown variables used to show the amount of PV, demand, and discharged EV energy usage for demand reduction, respectively. Note that $c_i^e = x_{i2}^{PV} + x_{i2}^{demand} + x_{i2}^{EV}$ is the reduction strategy of the customer i in the game, and all x are the unknown variables.

Based on (5.4), the first constraint keeps the demand reduction less than CA's DR request (r_i^e), the second provides the required mining energy, the third constraint controls the PV generation (P_i), the fourth monitors the EV charging and discharging and keeps the battery current capacity $B_i^{current}$ between the minimum B_i^{min} and maximum B_i^{max} capacity, and the final constraint keeps the demand reduction $(x_1^{demand} + x_2^{demand})$ always less than the predicted consumption (p_i) minus the essential household demand (d_i) of customer i. The binary value σ_i represents the state of EV, $\sigma_i = 1$ means EV is parked at home, and the customer can discharge/charge it; otherwise, $\sigma_i = 0$. After the game converges, the consensus value of each customer is calculated (according to the above subsection), and the one with the maximum arc_i value is selected as block miner.

The scheme above mainly focuses on the block mining process at DR events, but from the network supervision perspective, the DSO requires real-time demand information of customers to monitor the distribution network. For network supervision, customers send their demand profile to the CA regularly, thus a block mining process is required to store the supervision data on the blockchain. Therefore, for the sake of storing supervision data on the blockchain, customers need to maximize their utility function (5.4) to find the values of $x_{i1}^{PV}, x_{i1}^{demand}, x_{i1}^{EV}$ and x_{i3}^{EV} and exclude other variables and corresponding constraints. Finally, the consensus values are calculated to find the block miner for the network supervision.

5.2.3 Stackelberg Game

The equilibrium strategy for the follower(s) in a Stackelberg game is any strategy that establishes an optimal response to the one adopted by the leader(s) [58]. This model is a forward leader-follower game among the controlling agent (CA) $(1 \in \mathcal{N}_d)$, as a leader, and customers $(i \in \mathcal{N}_C)$ as followers with the total $\mathcal{N} = \mathcal{N}_d \cup \mathcal{N}_C$ number of players. Therefore, a unique equilibrium point exists in our Stackelberg game $\Gamma = (\mathcal{N}, \{S_n\}_{n\in\mathcal{N}}, \{U_n\}_{n\in\mathcal{N}})$, where the set of strategy for player n (S_n) is non-empty, concave and compact in Euclidean space. Moreover, according to (5.3) and (5.4) both utility functions (U_d and U_c) are continuous and differentiable on their set of strategies, and (5.3) is concave which guarantees the game has a maximum and unique strategy. The game initiates by announcing a set of strategies from the CA ($\mathbf{r}^e = (r_1^e, \dots, r_{N_C}^e)$) to the customers, and then, the customers will choose their best response strategy as follows.

$$c_i^{e*} = \underset{C}{\operatorname{argmax}}\, U_c(r_i^e), \forall i \in \mathcal{N}_C \tag{5.5}$$

Let c_i^{e*} be the best response strategy of customer i and $\mathbf{c}^{e*} = (c_1^{e*}, c_2^{e*}, \dots, c_{N_C}^{e}{}^*)$ be the follower's best strategy profile and C represents the constraints in (5.4). The leader will accordingly calculate its best strategy $\mathbf{r}^{e*}$ by;

$$\mathbf{r}^{e*} = \underset{D}{\operatorname{argmax}}\, U_d(\mathbf{c}^{e*}), \tag{5.6}$$

where D represents the constraints in (5.3). These steps repeat till both reach their best responses, that is, they no longer have incentive to change their strategies. Therefore, $(\mathbf{c}^{e*}, \mathbf{r}^{e*})$ would be a Stackelberg equilibrium (SE) set for the game at event e.

5.3 Simulation Results

A critical concern in the block mining process is to estimate the required energy for block generation. The energy usage mainly depends on the number of transactions, the difficulty level of the hash function, and the energy consumption of miner [199, 200]. In a recent work [201], the authors have found that in a small private blockchain network, a miner with a 4 cores CPU and 16 GB RAM processing system requires 1 Watt to process one transaction. Consequently, in our proposed distribution network, the miner (customer) with the same hardware features requires almost $\chi = 3.2$ kW (the mempool size is 3200 transactions) to generate a block. Since we have $N_C = 100$ customers, the CA initiates DR requests by sending 100 individual transactions, and then we run the Stackelberg game for 15 iterations (30 bidirectional transactions) to settle the results. From the network supervision perspective, customers send their demand profiles to the CA every 15 minutes, then they transmit almost 400 monitoring signals (transactions) in one hour, and every eight hours, the block mining process runs to store the data on the blockchain (due to the size of the mempool). Thus, three block minings are required to store 24-hours monitoring data on blockchain that occur at 8 am, 4 pm, and 12 am every day.

To have realistic outputs, a real dataset of customers consumption profiles over a year is used that was collected by Hydro Ottawa Limited, in Ottawa, Ontario. We focus on the customer usage profile in July because the photovoltaic systems have the maximum energy generation in the Ottawa region, and we employed a dataset of PV electricity generation collected by the University of Ottawa SUNLAB during that period [202]. A support vector regression (SVR) model is applied to predict the demand profile of customers a day ahead. To simulate the proposed architecture, Python and MATLAB are used, and assumed that each customer has a PV system (with maximum 4kW capacity), EV (with battery capacity

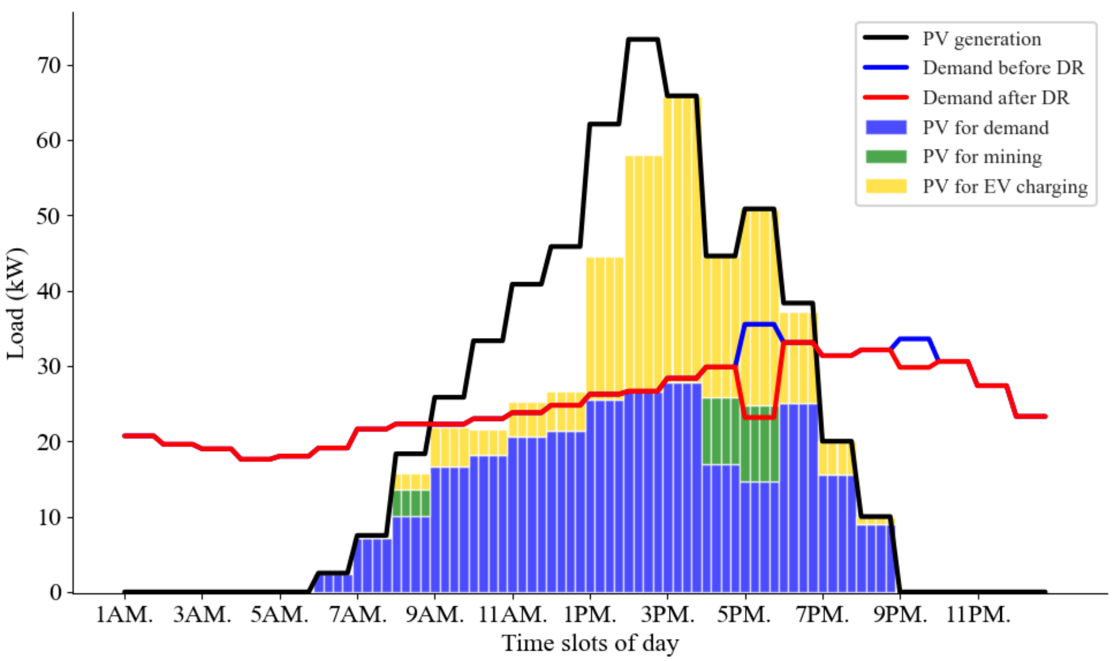

Figure 5.2: Total demand profile and customers allocated resources in a day in July.

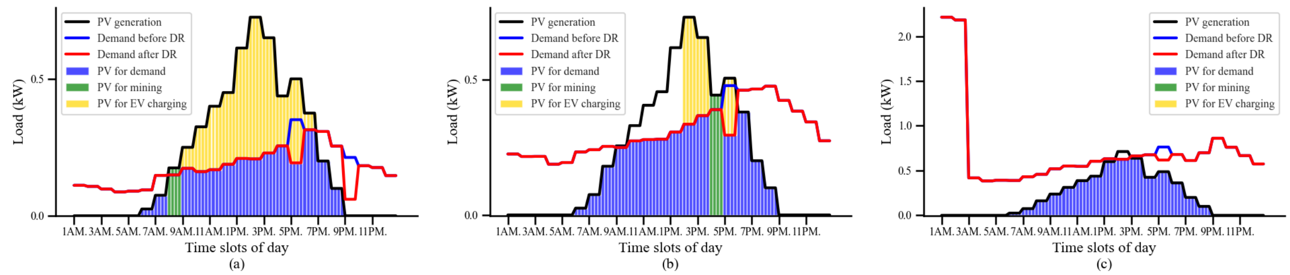

Figure 5.3: Consumption profile of three customers in a day in July that keep EV at home (a) 100%, (b) 50%, and (c) 0% of working hours.

of 40kWh), and a Home Energy Management System (HEMS) with 4 cores CPU and 16 GB RAM for mining and monitoring purpose. To implement a realistic EV pattern of usage, we applied the probability distribution of EV usage taken from [203]. Based on this article, EVs are usually parked at home from 11 pm to 7 am the next day, and only 63% of EVs are parked at home during working hours. For the simulation part, the initial reputation is considered as $R_i = 0.1$, $\forall i \in \mathcal{N}_C$ and the rest of values are $\alpha = 0.2\$/kWh$ (based on dispatching price), $\beta = 0.13\$/kWh$ and $\theta = 0.082\$/kWh$ (based on time-of-use pricing in Ontario), and $\gamma = 5\$$ is the block mining reward.

5.3.1 Impact of Electric Vehicle Usage Pattern

Figure 5.2 denotes the network demand profile before and after DR during a day in July with two DR events at 5 pm and 9 pm. The figure also shows PV generation (dark solid line) and the amount of PV used for demand (blue bars), allocated block mining energy by customers (green bars), and EV charging (yellow bars). Hence, there is a total of five mining processes (3 for monitoring and 2 for DR events) during a day that only three of them (at 8 am, 4 pm, and 5 pm) use the PV generation for the mining process, and the reset (9 pm and 12 am) use EV capacity and demand. Moreover, the peak is reduced by almost 35%. To show more details on load profiles of customers, we selected three

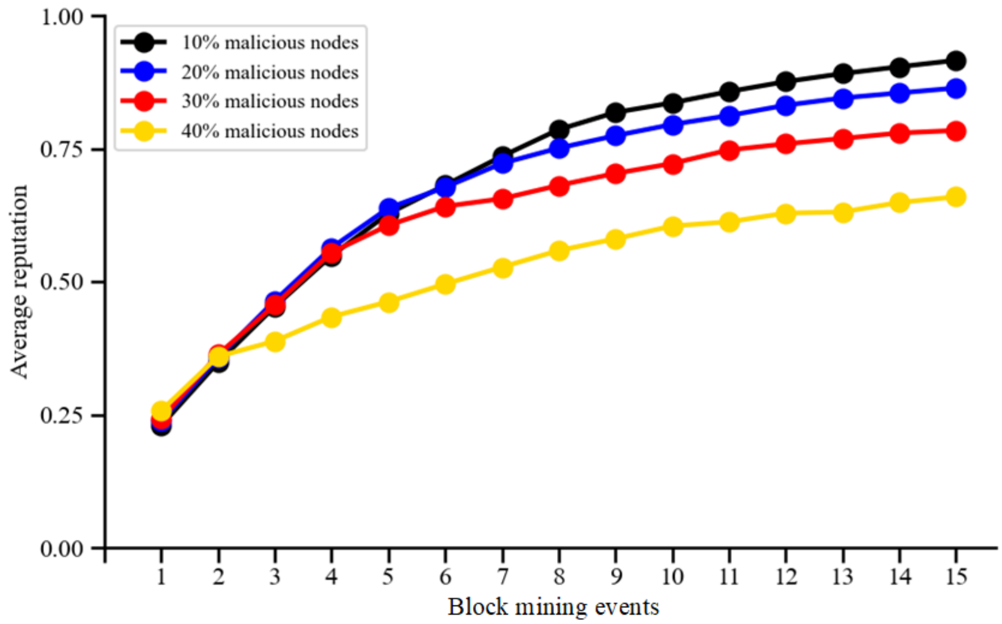

Figure 5.4: Average reputation value during 15 block mining events for different percentage of customers with malicious action.

different customers to keep an EV at home 1) 100% Figure 5.3.(a), 2) 50% Figure 5.3.(b) and 3) zero percent Figure 5.3.(c) of working hours (from 8 am to 8 pm) slots. They have nearly the same PV generation but have different demand profiles. In Figure 5.3.(c), the customer charges its EV during the mid-night (1 am-2 am), and the car is out during the mining events that reduce the chance of the customer to win the block mining. According to Figure 5.3.(a) and (b), customers win the mining at 8 am and 4 pm respectively and charge their EV with PV generation as well. To present more details, Table 5.1 illustrates the output results and profits of five types of customers (keep EV at home for 100%, 70%, 50%, 30%, and 0% of working hours). We found that the customer with 70% of EV at home did not win the block mining because of the inappropriate time slots of keeping EV at home and less demand reduction. But, it charged its EV more than others and increased its charging profit. Then, the customer with 0% EV at home only received the profit of demand reduction. Customers with 100% and 50% EV received the reward of mining, EV charging, and demand reduction. Consequently, the customer who keeps EV at home exactly at mining hours (similar to the customer with 50% EV) and reduces demand equal to the DR request can achieve significant profits and provides EV usage satisfaction during the daytime. Therefore, by keeping EVs at home during mining events, customers can increase the chance to win the block mining and charge EV to enhance the profit values.

Table 5.1: Average earning profit value for different EVs usage.

Working hours EV parked at home (%)	Before DR		After DR		EV charged with PV (kW)	Block mining event	Total profit ($)
	Total demand (kW)	Total cost ($)	Total Demand (kW)	Total cost ($)			
100	17.69	0.68	16.45	0.55	10.26	Event 1	3.96
70	11.25	0.41	10.95	0.38	13.22	-	1.15
50	30.14	1.57	29.41	1.49	3.82	Event 2	3.35
30	16.14	0.58	15.41	0.51	8.05	-	0.68
0	69.22	4.45	68.63	4.39	0	-	0.07

5.3.2 Impact of Malicious Customers

To present our system security and robustness against the users with malicious actions, Figure 5.4. represents that the network average reputation value reduces while the number of users with malicious actions increases. The reputation value is formulated based on article [144] where the blockchain security is guaranteed if the number of malicious nodes doesn't exceed half of the nodes. The reputation algorithm increases the reputation of users when they truthfully submit transactions and successfully mine the block, and it decreases when they send fraudulent information (users can detect the fraudulent transaction using a smart contract). According to our proposed consensus algorithm, the consensus value of customers with malicious action will drop as their reputation values decrease, and their chance to be selected as a block miner will tend to zero. Thus, blockchain privacy and security are guaranteed. Then to clarify how consensus value and reputation of customers change, we applied k-means clustering on 100 customer demand profiles and categorized

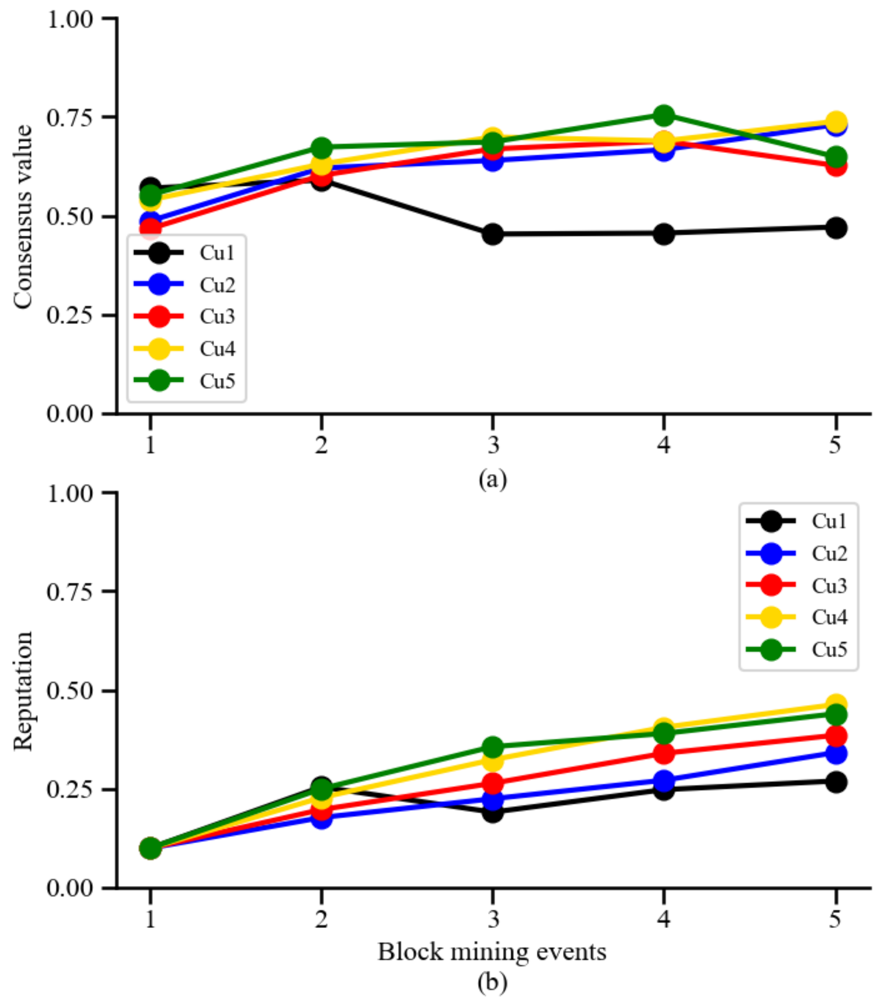

Figure 5.5: (a) Consensus value and (b) reputation values of 5 customers during five events (8 am, 4pm, 5pm, 9pm and 12 am) while customer 1 maliciously acts in event three.

them into five groups. Figure 5.5. shows 5 customers (from different clusters) in five block mining events (defined before). In the beginning, customers had the same reputation value (0.1), and customer 1 was selected as a miner due to its higher demand reduction, and no malicious action was detected among users. Customer 5 was selected as a block miner in the next block mining event and successfully increased its reputation. But at event three, customers detected a fraudulent transaction submission by customer 1, which reduced its reputation and decreased its consensus value accordingly. Then, customers 4, 5, and 4 were selected as block miners for events three, four, and five, respectively. After customer 1 was detected with malicious action, it did not select as a miner in the reset of mining events due to its least reputation, but it still has chances to increase its reputation by acting truthfully and building its history for future events.

5.4 Conclusion

In this chapter, a novel demand response Stackelberg game model is presented that includes a new DER saving mechanism using energy blockchain to develop a collaborative and interactive demand reduction in a residential area. Our main goal was to engage customers to reduce their demand at peak time slots, compete on block mining to win and receive rewards, transform their surplus DER into monetary resources, and incentivize customers to discharge and charge their EVs. In other words, this mining strategy works like a storing mechanism for the DER system that is less expensive and more efficient than installing a battery inside a house. Our results show that the proposed scheme can truly manage the DER resources by efficiently allocating PV resources, demand, and EV to the block mining process and incentivizing customers to discharge EV and reduce their consumption 35% during the peaks. Furthermore, we demonstrated that our proposed consensus algorithm is robust and secure against users with malicious actions. Indeed, this work maximized the chance of block mining for customers and allocated rewards, in addition to maximizing the profit of the DSO by reducing the total demand. To continue this work, the next chapter presents a stochastic Stackelberg game model to monitor customers' uncertain demand response contributions including an energy blockchain architecture to secure energy transactions and system robustness.

Chapter 6

Secure and Robust Demand Response using Stackelberg Game Model and Energy Blockchain

6.1 Introduction

Although demand response (DR) has been studied widely in the smart grid literature, there is still a significant gap in approaches that address security and robustness simultaneously. The need for security and robustness emerges as a vital property, as internet of things (IoT) devices become part of the smart grid; in the form of smart meters, home energy management systems (HEMSs), intelligent transformers, and so on. In this chapter, we use energy blockchain to secure energy transactions among customers and the utility company. In addition, we formulate a mixed-strategy stochastic game model to address uncertainties in DR contributions of agents and achieve optimal demand response decisions. This model utilizes the processing hardware of customers for block mining, stores customer DR agreements as distributed ledgers, and offers a smart contract and consensus algorithm for energy transaction validation. We use a real dataset of residential demand profile and photovoltaic (PV) generation to validate the performance of the proposed scheme. The results show the impact of electric vehicle (EV) discharging and customer demand reduction on increasing the probability of successful block mining and customer profits. Moreover, the results demonstrate the security and robustness of our consensus algorithm on detecting malicious activities.

6.2 System Model

6.2.1 Network Model

As it is shown in Figure 6.1, the electricity grid can be divided into M private blockchains (PBs) comprised of multiple customers. PB groups can be assigned considering geographical and regional situations or power flow constraints of the grid where customers perform as blockchain nodes. The idea of implementing a private blockchain was to increase the system's sustainability and keep the local area secure from external attacks. Moreover, a private block has the minimum cost of implementation in comparison to other scenarios. The distribution system operator (DSO) monitors the energy transactions of the customers through multiple control agents (CAs). Each CA in its PB has a copy of blocks and regularly sends them to the DSO for data storage and monitoring purposes. The CAs are under the authority of DSO, and both are trusted parties in the network while the customers are untrusted. According to Figure 6.1, data synchronization (DS) and PB networks are connected through the wireless communication access points. At the DS, the CAs pass a copy of their local blocks to the DSO, and no CA knows the blocks belonging to its neighbors. The CAs are part of DSO that could be physical units installed in a local area or software-as-a-service (SaaS) on the cloud. The CA failure may happen due to a software or hardware disruption that could be resolved by repairing the unit or debugging the software and returning the CA to a fully functional service. In the meanwhile, another

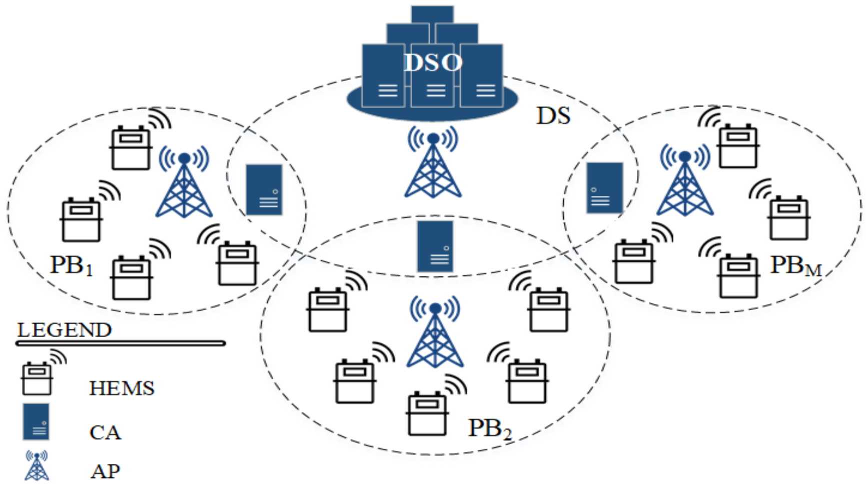

Figure 6.1: The architecture of the proposed energy blockchain, where the distribution system operator (DSO) monitors the energy transactions of the home energy management systems (HEMSs) through multiple control agents (CAs). The data synchronization (DS) and private blockchains (PBs) are connected through the wireless communication access points (APs).

CA (a CA from the neighborhood) takes action and controls the local area. Hence the DSO selects the replaced CA and shares a copy of blocks with the new CA. Moreover, a publisher/subscriber model between the CA and IoT devices such as HEMSs is issued, which enables HEMSs (subscribers) to receive the CA's (publisher) latest updates on DR events [159]. In addition, HEMS controls household energy resources such as photovoltaic, electric vehicle (when it is parked at home), and appliances usages.

In this proposed architecture, we focus on two events, 1) peak load period (PLP) event and 2) network supervision event. The former happens when the demand of the network is more than the DSO threshold and brings a high cost of supply for the network. Then, at PLP the DSO sends DR signals for demand reduction to the customers to control the network demand. The latter is a supervision event that happens regularly for network demand control, and customers submit their consumption to the CA. The block mining process is required to store the DR transactional data and supervision information on the blockchain. Both $\boldsymbol{\tau}_{PLP}$ and $\boldsymbol{\tau}_{Sup}$ are sets of PLP and network supervision time slots for the next 24 hours and we define $h \in \boldsymbol{\tau}_{PLP}$ or $h \in \boldsymbol{\tau}_{Sup}$ where $h \in \mathcal{H}$ and $\mathcal{H} = \{1, 2, ..., H\}$ that H is the number of time slots. The value, N_{Cu} is the number of customers in a PB and $\mathcal{N}_{Cu} = \{1, 2, \ldots, N_{Cu}\}$ is the set of customers where i denotes the customer index and $i \in \mathcal{N}_{Cu}$.

6.2.2 Authentication Technique

We assume that the DSO and CAs are trusted parties and are registered as authenticated nodes in the network. But, HEMSs require an initial registration to prevent malicious activities and fraudulent information submission on the blockchain. The digital signature algorithm (DSA) can be used for node authentication and preventing transactional data tampering [204]. In other words, it provides message integrity and node authentication while guaranteeing message security. Consequently, a new customer in the network is obligated to submit initial information such as identity (ID) number, electric vehicle total capacity, and photovoltaic system maximum capacity. In return, the CA generates public verification key (PK) and secret/private signing key (SK) for HEMS using $keygen(1^{\lambda}) \longrightarrow (PK, SK)$, λ is a security parameter. Thus, every HEMS has a unique public key and secret/private key pair. A HEMS uses SK to sign a $message$ and sends it to the network using the algorithm, $sign(message, SK) \longrightarrow \sigma$, where σ is the HEMS signature. Moreover, the nodes in the network can verify the transaction using the public key of HEMS as $verify(message, \sigma, PK) \longrightarrow (0, 1)$, where 1 if the verification is successful and zero otherwise. In addition, to reduce the rate of malicious activities, a new HEMS has to deposit money to the CA to prevent further malicious activities [146, 148]. The digital signature authentication technique has been used in our designed smart contract, and it is explained in section 6.3.2.

6.3 Blockchain Design

To reveal more details on how the designed energy blockchain works with agents, we summarize our design in four steps. First, HEMSs send a transaction (including consumption information and digital signature) into the network. Next, the smart contract executes to validate and authenticate the transactions. Then, for the block validation, the consensus algorithm initiates to select a block miner. Finally, the selected miner inserts the validated transactions into the blockchain. Note that our designed consensus algorithm, smart contract, and the digital signature algorithm (DSA) guarantee network security and data integrity. In summary, we present a new consensus algorithm and a new smart contract design that are explained in the following sections.

6.3.1 Consensus algorithm - Proof of Energy Saving (PoES)

The required processing hardware for block mining can be satisfied using the computing hardware of customers for transaction validation and block generation. To implement this idea, one customer is needed to be selected as a block miner. As it is shown in Figure 6.1, in a PB, only one HEMS would be a block miner in each round of block generation. Moreover, this idea would allow the DSO to minimize the consensus energy usage by selecting one miner, unlike proof of work (PoW) and proof of stake (PoS), and save money on the block generation process. Additionally, the DSO allocates a portion of mining monetary resources to the customers to incentivize them to compete on block mining selection. To this end, our proposed consensus algorithm, proof of energy saving (PoES), is presented to efficiently use the energy and hardware resources of customers for block mining.

The mempool in the blockchain is a storing architecture that accumulates the transactions temporarily. After the mempool reaches full capacity, it is time to generate a block and save the data on the blockchain. Our proposed consensus algorithm, proof of energy saving (PoES), selects one customer with the higher average value of availability, reputation, and compliance ratio as a block miner. The reasons for choosing these factors are; first to pick a customer with adequate energy (energy resources) to complete the block mining process (Availability). Then, select a high trusted customer as a block miner and prevent further malicious activities (Reputation). Finally, to incentivize customers to increase their DR contribution and maximize the chance to win block mining (Compliance ratio).

1) Availability ($a_h^i \in [0,1]$) presents the ratio of allocated energy for block mining by customer i over the required mining energy (χ) where we have $\boldsymbol{a}^i = (a_1^i, \ldots, a_H^i)$. A customer can supply the block mining energy from its household photovoltaic generation, demand (portion of customer desired consumption), and discharge of electric vehicle at time slot h. The availability is calculated by $a_h^i = \frac{x_h^i + w_h^i + \alpha_h^i e_h^i - b_h^i}{\chi}$ where x_h^i is the customer's consumption from the grid that is shown by vector $\boldsymbol{x}^i = (x_1^i, \ldots, x_H^i)$, w_h^i is the photovoltaic generation, e_h^i is the electric vehicle discharging energy from customer i at time slot h and b_h^i is the customer minimum required demand at time slot h. In addition, α_h^i is a binary value that indicates the electric vehicle status where $\alpha_h^i = 1$ means the electric vehicle of customer i is parked at home (can be discharged) for time slot h, otherwise $\alpha_h^i = 0$. Note that $x_h^i + w_h^i + \alpha_h^i e_h^i$ would be the customer total energy usage at time slot h.

2) Reputation ($r_h^i \in [0,1]$) customers can rank their experience of interacting with others as trusted, untrusted or uncertain according to [144]. Then, $\boldsymbol{r}_h^{-i} = (r_h^1, \ldots, r_h^{i-1}, r_h^{i+1}, \ldots, r_h^{N_{Cu}})$ is the reputation vector that customer i submits for other customers (except itself) at time slot h before the game starts. The reputation increases and decreases by the number of successful and unsuccessful minings and data submission.

3) Compliance Ratio ($c_h^i \in [0,1]$) is the ratio of the total electricity reduction of a customer over its total load shed availability (LSA) (Σl^i) in a time window where we have $\boldsymbol{c}^i = (c_1^i, \ldots, c_H^i)$. We define the compliance ratio of customer i for time slot h as $c_h^i = \frac{\delta^i + (p_h^i - x_h^i)}{\Sigma l^i}$. The value δ^i represents the summation of demand reduction and Σl^i is the summation of load shed availability of customer i in a time window. Moreover, p_h^i is the predicted demand of customer i at time slot h. Customers can reduce their demand using residential photovoltaic generators, decrease their actual demand (by shaving or shifting the demand), and discharging electric vehicle capacity to handle the request. Hence, a customer with a considerable history of demand reduction (DR contribution) has more chance to be selected as a block miner.

By averaging these three coefficients $arc_h^i = \frac{a_h^i + r_h^i + c_h^i}{3}$, ($arc_h^i \in \boldsymbol{arc}^i$), the consensus value of customer i would be $arc_h^i \in [0, 1]$. Finally, the algorithm selects a HEMS with $\max_{\forall i \in \mathcal{N}_{Cu}} \{arc_h^i\}$ as a block miner for time slot h.

6.3.2 Smart Contract

Smart contract is a multistep transaction validation program on blockchain that can stop the disruptive and fake data insertion in a distributed network [158]. After a transaction is submitted, its validity and authenticity must be verified using the smart contract before being added to the mempool. Every agent located in a private blockchain (PB) can execute the smart contract to check the validity of a transaction. However, in this model, only a proportion of HEMSs, who has the reputation value r_h^i more than the trust threshold $\overline{r}$, are allowed to validate the transaction. Note that the CA decides on the trust threshold $\overline{r}$ and shares the value with all customers. In addition, the trust threshold changes over time based on the local average reputation value. These HEMSs are called active nodes, while the idea is to reveal the transaction data only with the trusted nodes (active nodes) in the network to keep the privacy of transactions and reduce the overload.

Algorithm 6.1 shows the steps of our designed smart contract that is executed by active nodes. A transaction contains a_h^i, r_h^i, c_h^i and x_h^i that are signed by HEMS's private key. First, the transaction authenticity is determined using the HEMS public key to validate the message integrity and authentication. Next, the reputation value is checked (r_h^i) to be in a standard range and be equal to the HEMS historical reputation value

rep_h^i. Note that the historical reputation value is a copy of customer i's reputation that is transparent to all HEMSs. The availability value a_h^i has to be equal to one; otherwise, the corresponding HEMS cannot satisfy the mining energy χ. In addition, the compliance ratio c_h^i has to be between 0 and 1, and energy consumption x_h^i has to be more than zero. Note that the transaction information is only transparent to active nodes. To this end, if a transaction successfully passes these steps (smart contract), it will be added to the mempool. Malicious customers may try to deny their submitted energy consumption (x_h^i).

Algorithm 6.1 Smart Contract

1: **Inputs**: $message = (a_h^i, r_h^i, c_h^i, x_h^i)$, PK and σ
2: **if** $verify(message, \sigma, PK) \longrightarrow 1$ **then**
3:     **if** $a_h^i == 1$ and $r_h^i == rep_h^i$ and $0 < c_h^i < 1$ and $x_h^i \geq 0$ **then**
4:         The transaction is accepted and added to the mempool.
5:     **end if**
6: **end if**

In this case, our model penalizes customers by seizing their initial deposit money and reducing their reputation value. Moreover, to discover the optimal energy consumption (x_h^i) for every customer ($i \in \mathcal{N}_{Cu}$), our proposed mixed-strategy Stackelberg game can achieve realistic outcomes while the details are explained in the following section.

6.4 Stochastic Stackelberg Game

6.4.1 Game Model

The DSO monitors the grid regularly and captures the peak load periods day-ahead by analyzing the customer load profile using the support vector regression (SVR) model. Here p_h^i is the customer i's predicted demand for the time slot h, and $\boldsymbol{p}^i = (p_1^i, \ldots, p_H^i)$ is the vector of customer i predicted demand in next 24 hours. As mentioned before, a block generation process is required for both peak load period and network supervision events.

According to Figure 6.2, the DSO passes $\boldsymbol{\tau}_{PLP}$ (in case of DR signal) and $\boldsymbol{\tau}_{Sup}$ (in case of supervision signal) to the CA then the CA passes them to the HEMSs of its local area. In the case of network supervision, DSO asks the CAs to collect the consumption data of customers from the grid ($x_h^i, \forall i \in \mathcal{N}_{Cu}$) regularly. However, for the peak load period, HEMSs reply to the demand reduction signal with their load shed availability vector $\boldsymbol{l}^i = (l_1^i, \ldots, l_H^i)$, and then the CA passes them to the DSO. Load shed availability (LSA) is the desired amount of customer demand reduction for PLP events. Since the DSO has an estimation of local area demand reduction, it offers the demand reduction reward vector $\boldsymbol{d} = (d_1, \ldots, d_H)$ for $\boldsymbol{\tau}_{PLP}$ and mining reward vector $\boldsymbol{q} = (q_1, \ldots, q_H)$ to the CA. Hence, before the game starts, the customers submit the reputation vector $\boldsymbol{r}_h^{-i}$ to the network. At this level, the CA starts the mixed-strategy Stackelberg game and sends the

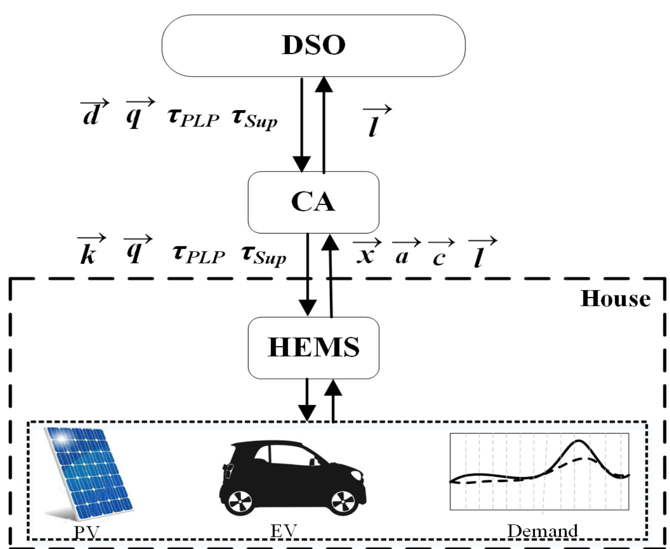

Figure 6.2: Hierarchical architecture and exchange parameters between distribution system operator (DSO), control agent (CA), and home energy management system (HEMS).

vector of prices $\boldsymbol{k}$ and $\boldsymbol{q}$ to the HEMSs. Note that $\boldsymbol{k} = (k_1, \ldots, k_H)$ is the reward price vector that the CA allocates to customers for demand reduction, and we have $d_h > k_h$ where the difference is considered as the CA profit.

$$\begin{cases} d_h, k_h \neq 0 & \text{if } h \in \boldsymbol{\tau}_{PLP} \\ d_h, k_h = 0 & \text{otherwise} \end{cases} \tag{6.1}$$

At the customer level (followers), the customers will receive $\boldsymbol{k}$ (for PLP event) and $\boldsymbol{q}$ from the CA and maximize their utility function (6.2) to increase the profit of demand reduction in case of PLP and allocate energy resources for block mining. According to (6.2), $\boldsymbol{x}^i = (x_1^i, \ldots, x_H^i)$ is the customer i's vector of strategy. The customer shares $\boldsymbol{x}^i$, $\boldsymbol{a}^i$ and $\boldsymbol{c}^i$ with the CA for every DR and supervision transaction. Note that (6.2) can be used for both PLP and supervision events according to $Time = \{\boldsymbol{\tau}_{PLP} \ or \ \boldsymbol{\tau}_{Sup}\}$.

$$U_{Cu}^i = \sum_{h \in Time} \left(q_h arc_h^i + k_h \beta_h^i \right) \tag{6.2}$$

subject to;

$$x_h^i + w_h^i + \alpha_h^i e_h^i \geq b_h^i$$

$$\beta_h^i = \begin{cases} 1 & \text{if } x_h^i \leq (p_h^i - l_h^i) \\ \frac{(p_h^i - x_h^i)}{l_h^i} & \text{otherwise} \end{cases}$$

In (6.2), the first part calculates the customer reward of block mining, and the second part presents the demand reduction profit. The first constraint keeps the summation of consumption from the grid (x_h^i), photovoltaic energy production (w_h^i) and electric vehicle energy discharging (e_h^i) more than the customer i's minimum required energy b_h^i. In addition, α_h^i indicates the electric vehicle status where $\alpha_h^i = 1$ means the electric vehicle of customer i is parked at home for time slot h, otherwise $\alpha_h^i = 0$. Note that the electric vehicle can discharge when its capacity at time slot h is above a certain threshold T_h. $\beta_h^i = 1$ when customer keeps the energy consumption from the grid less than the difference of predicted demand and LSA ($x_h^i \leq p_h^i - l_h^i$), otherwise, if the customer increases the usage ($p_h^i - l_h^i < x_h^i \leq p_h^i$) then $\beta_h^i = \frac{p_h^i - x_h^i}{l_h^i}$. Note that if the customer increases their consumption more than the predicted demand ($x_h^i > p_h^i$) they will be penalized with the same utility function ($\beta_h^i = \frac{p_h^i - x_h^i}{l_h^i}$).

The CA starts the negotiation (the leader-follower game) with customers in case of demand reduction and tries to keep a proportion of demand reduction rewards (d_h) for itself. Therefore, it offers $\boldsymbol{k}$ for PLP event and $\boldsymbol{q}$ for the mining reward to the customers. According to these values, the CA can maximize the utility function (6.3) within strategy vector $\boldsymbol{k} = (k_1, \ldots, k_H)$.

$$U_{CA} = \sum_{h \in \boldsymbol{\tau}_{PLP}} \Big(d_h \big(1 - \frac{\sum_{i=1}^{N_{Cu}} x_h^i}{\sum_{i=1}^{N_{Cu}} p_h^i}\big) - \sum_{i=1}^{N_{Cu}} k_h \beta_h^i \Big) \tag{6.3}$$

subject to;

$$k_h^{min} \leq k_h \leq k_h^{max}$$

Unlike (6.2), (6.3) is only used for the PLP event ($h \in \boldsymbol{\tau}_{PLP}$) while for network supervision $d_h, k_h = 0$. Therefore, the game is only played for PLP event, and for the supervision event, an optimization is solved using (6.2). According to (6.3), the first part calculates the profit value of the CA which is proportional to the total power consumption of customers ($\sum_{i=1}^{N_{Cu}} x_h^i$) over their predicted demand ($\sum_{i=1}^{N_{Cu}} p_h^i$) and the second part presents the monetary reward that the CA allocates to demand reduction of customers. The constraint keeps the offered DR reduction price between a lower bound k_h^{min} and upper bound k_h^{max}. The negotiation between the CA and HEMSs repeats till both sides reach an equilibrium point that no one has incentives to change their strategies.

6.4.2 Mixed-strategy Stackelberg Game and Equilibrium Analysis

Stackelberg game is widely used in demand response research where one player is a leader, and its strategy affects the decision of other players (followers) [58]. In addition, due to the uncertain reaction of customers (followers) to demand response conditions, a stochastic model is usually used to find their best responses. The mixed-strategy game model is a stochastic solution that employs a probability distribution model to allocate random values to the strategies of players in different situations [182]. Based on the definitions, we use the mixed-strategy Stackelberg game to model the interaction between the control agent (CA) and customers. Our finite n-player game is defined as follows;

$$\Gamma = (\mathcal{N}, \{S^n\}_{n \in \mathcal{N}}, \{U^n\}_{n \in \mathcal{N}}) \tag{6.4}$$

where $\mathcal{N}$ ($\mathcal{N} = \mathcal{N}_{CA} \cup \mathcal{N}_{Cu}$) is a finite set of players and N is total number of players while we have $N_{Cu} = N - 1$ customers and $N_{CA} = 1$ with the sets of $\mathcal{N}_{Cu}$ and $\mathcal{N}_{CA}$, respectively. In addition, S^n is the space of pure strategies, and U^n is the utility function for player $n \in \mathcal{N}$. The Γ is a finite game while we have finite number of pure strategies for players. Therefore, for each customer $i \in \mathcal{N}_{Cu}$, m_h^i is the number of pure strategies at time slot $h \in \mathcal{H}$ and we have $x_h^i \in S_h^i = \{s_1^i, s_2^i, \dots, s_{m_h^i}^i\}$. For the CA we also have m_h^1 number of pure strategies at time slot $h \in \mathcal{H}$ and space of strategy, $k_h \in S_h^1 = \{s_1^1, s_2^1, \dots, s_{m_h^1}^1\}$.

According to [183], and based on our finite game, a mixed-strategy equilibrium exists when the players choose their strategies probabilistically. Thus, a mixed-strategy of player n at time h is presented by a probability distribution vector $\sigma_h^n = (\rho_1^n, \rho_2^n, \dots, \rho_{m_h^n}^n)$ over S_h^n. Hence the summation of the probabilities of player n's different strategies at time slot h is equal to one.

$$\sum_{d=1}^{m_h^n} \rho_d^n = 1 \tag{6.5}$$

For a mixed-strategy game, the probability distribution over the joint pure strategies $s = (s_{d^1}^1, s_{d^2}^2, \dots, s_{d^N}^N)(s \in S)$, $\forall n \in \mathcal{N}$ and $d^n \in \{1, \dots, m_h^n\}$, is $\sigma(s) = (\rho_{d^1}^1, \rho_{d^2}^2, \dots, \rho_{d^N}^N)$.

Therefore, player n's mixed-strategy payoff value is found as;

$$U^n(\sigma) = \sum\nolimits_{s \in S} U^n(s)\sigma(s) \tag{6.6}$$
$$\sigma(s) = \prod_{n \in \mathcal{N}} \rho^n_{d^n}$$

where $U^n(s)$ is the utility function of player n for joint strategies $s \in S$ and $\sigma(s) = \prod_{n \in \mathcal{N}} \rho^n_{d^n}$ is the joint of its probability distribution. We apply the Monte Carlo model to allocate probabilities to the pure strategies of players based on (6.5). After calculating (6.6) for player n, the highest payoff value would be selected as the best result, and its related strategy would be the best response.

Several works have proven the existence of mixed-strategy Stackelberg equilibrium [184–186]. Following these studies, to prove the existence of Stackelberg equilibrium (SE), first, we divide the game into mixed-strategy sub-games [64, 187], and then based on the Kakutani fixed point theory [188] the mixed-strategy NE can be proven for each subgame. Moreover, by using the Simplex algorithm [192], we can prune the searching area and find the optimal points in a short time. To find SE based on (6.6), the assumption below has to be satisfied for the CA while customers select their best responses.

$$\sum_{d=1}^{m^1_h} U_{CA}(s^1_d, s^{-1^*})\rho^1_d \tag{6.7}$$

subject to;

$$\sum_{d=1}^{m^1_h} \Big(\sum_{i=1}^{N_{Cu}} \big(U^i_{Cu}(s^1_d, s^{i^*}_{d^i}) - U^i_{Cu}(s^1_d, s^i_{d^i}) \big) \Big) \rho^1_d \geq 0$$
$$\sum_{d=1}^{m^1_h} \rho^1_d = 1$$
$$\forall s^1_d \in S^1_h$$

s^1_d is the pure strategy of the CA while $s^1_d \in S^1_h$. Note that s^{-1^*} is a joint of customers' best response strategy when the CA selects strategy s^1_d. The value ρ^1_d is the probability of the CA and $s_{d^i}^{i^*}$ is the pure best strategy of customer i where $s_{d^i}^{i^*} \in S_h^i$. Equation (6.7) represents that for s^{-1^*}, we calculate a mixed-strategy for the CA via the linear programming (LP) and under the constraints, $(\rho_1^{1^*}, \ldots, \rho_{m_h^1}^{1^*})$ would be the optimal mixed-strategy that maximizes the CA utility function.

The equilibrium is found using the backward induction that first calculates the best response of customers $(s_{d^i}^{i^*}, \forall i \in N_{Cu})$ using (6.8) subject to A (which represents the constraints in (6.2)) for all customers, based on the initial price of the CA as s_d^1 strategy.

$$s_{d^i}^{i^*} = \underset{A}{\operatorname{argmax}} \sum_{d^i=1}^{m_h^i} U_{Cu}^i(s_d^1, s_{d^i}^i)\rho_{d^i}^i, \ \forall s_d^1 \in S_h^1 \tag{6.8}$$

Then, customers pass their best strategies to the CA subgame and the CA can find its best response $s_d^{1^*}$ using (6.7). This process repeats between the CA and customers, and customers calculate (6.8) with the best response of CA .

Theorem: There is a Stackelberg equilibrium in our presented mixed-strategy Stackelberg game based on the optimal solutions of the customers and CA.

Proof: According to Kakutani fixed point theory [188] the existence of mixed-strategy NE have to be proven in each subgame (while we divided the Stackelberg game into subgames) to prove the SE for the whole game. Utility function U_{Cu}^i is non-empty, non-negative, continuous, and it is defined on a compact subset of Euclidean space [191]. Furthermore, U_{CA}^i is concave, and we can find its maximum point. Moreover, (6.7) is a linear optimization on the CA's probability distribution while it is concave and is defined on a compact subset of Euclidean space. Thus, we can assert that there is an optimal point in (6.7) which is a mixed-strategy Stackelberg equilibrium.

6.5 Security and Privacy Functionality

This section determines our proposed model's data consistency and security for different attacks and how we confront them. Sybil attack happens when the attacker defines itself with multiple identities. However, this attack easily fails due to the identical public keys the CA defines for the HEMSs. The appending attack occurs when a registered node in the network tries to submit a fraudulent transaction on the blockchain [147]. Due to our defined smart contract algorithm, any invalid availability, reputation, compliance ratio, and consumption data can be detected. Sometimes a malicious node tries to modify a submitted transaction data or the block information, which is called data forgery [158,159]. The Block information cannot be forged due to the hash pointer feature, and the attack could be easily detected with the digital signature. The data spoofing attack can change the identity of HEMS [159], but in our scheme, the identity of HEMS is known due to its initial registration within the CA. In case of repudiation, [159], the malicious nodes try to deny their submitted energy consumption values. Then, our model will punish the customer by seizing their deposit money and reducing their reputation value. The authentication attack occurs when one node tries to forge another node's identity [159]. Based on our architecture, the private key of a HEMS is unique, and no one knows that; therefore, a malicious HEMS cannot fake another HEMS's identity. For the man in the middle attack, a destructive node could attempt to change the concept of transactions in the middle of the transmission lines. However, no-fault and forged data could be added to the block within the digital signature and smart contract. The denial of service attack happens when a node sends multiple transactions to the CA and keeps it busy to finally make it out of order. In our architecture, only registered nodes are allowed to submit one transaction in response to the CA's signal, and additional transactions are ignored. The last studied attack in this document is the 51% attack that happens when 51% of customers become attackers and generate fake data and store it on the blockchain [147]. According to [205], proof of stake (PoS) consensus algorithm confronts 51% attack using the voting process. The CA can recognize the fraud settlements at the execution time, and in return, seizes their deposit money, reduces their reputation, and puts them on the blacklist to not being selected as a miner or active node for a time window. Therefore, our consensus algorithm (PoES) can prevent 51% attack due to its active nodes transaction validation (voting system).

6.6 Simulation Results

The required energy for the block mining process depends on the number of transactions and the hash function difficulty level of the miner. There are different articles [199,200,206] worked on mining energy, and in article [201], the authors found that for a small private blockchain network, a miner with specific hardware features (4 cores CPU and 16 GB RAM) requires 1 Watt to process one transaction. A version of the proposed energy blockchain application is implemented using the Hyper-Ledger Fabric platform. Consequently, in our proposed architecture with the same hardware features, we need almost $\chi = 3.2$ kW (the size of mempool is 3200 transactions). Following we have $N_{Cu} = 100$ customers, the CA launches the DR game model by sending 100 initial transactions, and the Stackelberg game repeats for 15 iterations (30 bidirectional transactions) to settle. In the case of network supervision, customers share their consumption with the CA every 15 minutes. Then, they transmit almost 400 monitoring signals (transactions) in one hour, and according to the mempool size, three block minings are needed to save the 24-hours monitoring data on the blockchain.

A real dataset of 100 household load profiles over a year, collected by Hydro Ottawa Limited, and a photovoltaic energy generation dataset, collected by the University of Ottawa SUNLAB [202], are selected for our model evaluation. Due to the high irradiation of the sun on photovoltaic systems in July in the Ottawa region, we selected the load profile of users in July. We also employed the support vector regression (SVR) model to predict the profile of customers for the next 24 hours. The proposed architecture is implemented in Python and MATLAB, and we supposed that each customer has a photovoltaic system

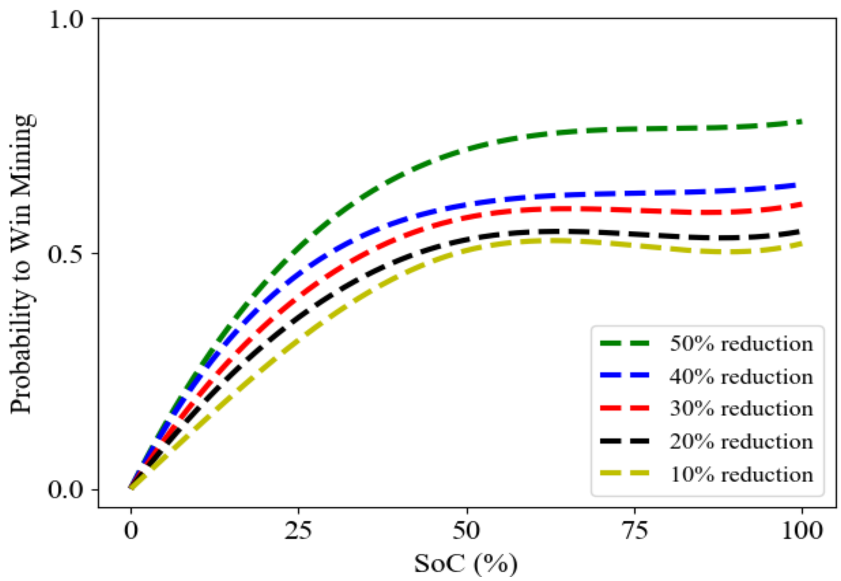

Figure 6.3: The average probability value of block mining with respect to state-of-charge (SoC) and different demand reduction percentages.

(capacity of 4 kW), an electric vehicle (with battery capacity of 40 kWh, maximum discharging power 5 kW), and a HEMS (with 4 cores CPU and 16 GB RAM) for mining and monitoring scheme. The initial reputation is same for all customers $r_h^i = 0.1, \forall i \in \mathcal{N}_c$. We have $d_h = 0.3\$/kWh$ (based on dispatching price) and $q_h = 3\$$ as the block mining reward.

6.6.1 Effect of Electric Vehicle on Customer Decision

We assumed that every customer has an electric vehicle with a battery capacity of 40 kWh that could be fully charged in 8 hours at home and has a maximum discharging power of 5 kW. According to the dataset, the average demand value of a customer would be 1.5 kWh at the peak time. Then, for some fixed percentage of demand reduction and various state-of-charge (SoC) of battery, the probability of winning the block mining varies as shown in

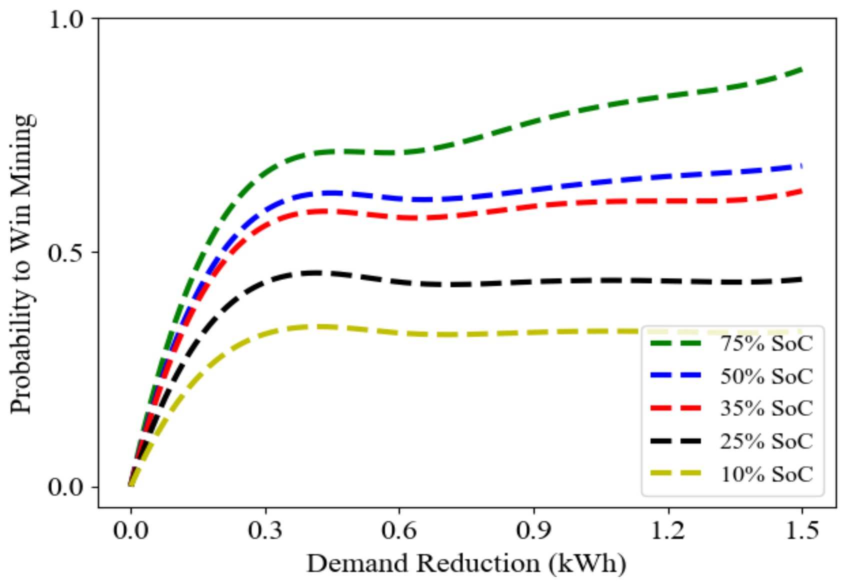

Figure 6.4: The average probability value of block mining with respect to demand reduction and different state-of-charge (SoC).

Figure 6.3. An electric vehicle does not discharge its capacity while its SoC is equal to or less than $T_h = 20\%$ (8 kWh). We observe that 35% is an optimal point to start discharging with the maximum power. From zero percent of SoC to 35% (14 kWh), the probability mounts with a uniform slope because of the increase in demand reduction. However, for the SoC more than 35%, the probability to win the block mining raises more than 0.5 for different percentages of demand reduction, which means it is now more probable to win the block mining. Additionally, by reducing the demand more than 50% of customer baseline load, the winning probability will increase. Next, we considered different percentages of SoC to determine the probability of winning the block mining while the demand reduction is growing. Figure .6.4 presents that the average probability increases significantly while the demand reduction is more than 0.3 kWh, and when the SoC is more than 35%, the probability moves beyond 0.5 that is promising to win block mining.

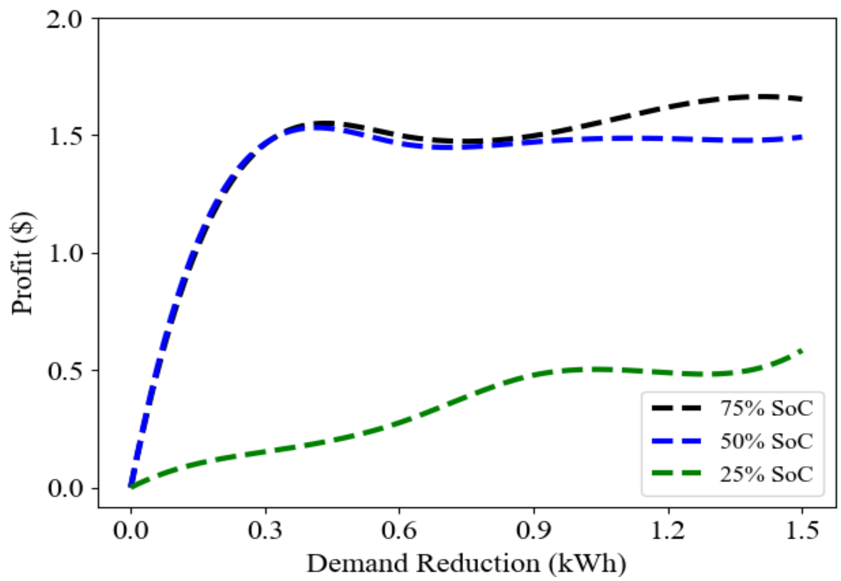

Figure 6.5: The average profit value of customers with respect to demand reduction and different state-of-charge (SoC).

We also observed the average profit of customers, including the mining profit and demand reduction in Figure 6.5 while the demand reduction of the customer and the electric vehicle state-of-charge are increasing. The figure explains that with the SoC of more than 50% (or more than 35%), the profit jumps to 1.5$ per day. That means it is more probable for a customer to win the mining and gain more profit when the SoC is more than 50% and demand reduction is more than 0.3 kWh.

To determine the effect of electric vehicle discharging on customers average reputation value, Figure 6.6 displays the reputation changes for three types of customers, Inactive (does not discharge EV), Moderate (discharge 50% of maximum discharging capacity), and Greedy (discharges the maximum discharging capacity) over 15 continuous block mining events. Note that, in this experiment, the demand reduction is fixed (0.4 kWh) between the customers. The reputation of the greedy customer increases more which explains that

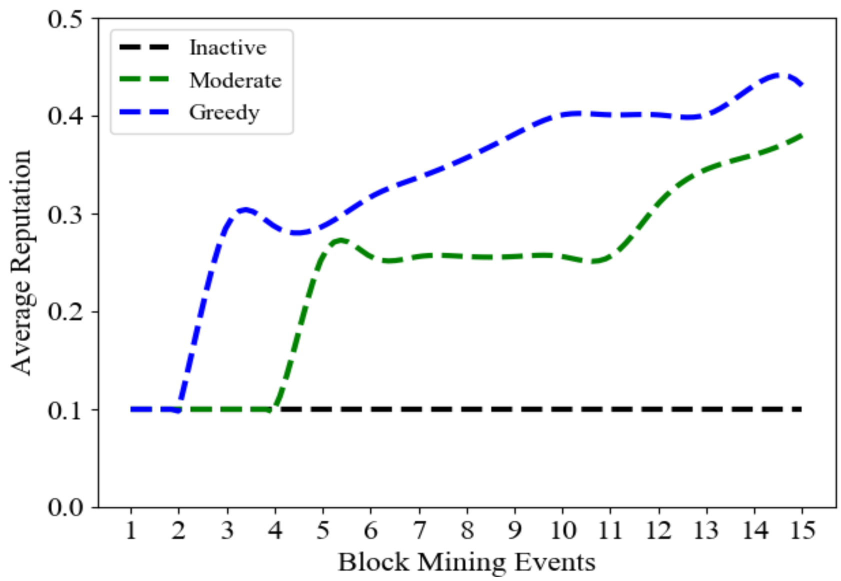

Figure 6.6: The average reputation value of three different types of customers (inactive, moderate, and greedy) in 15 continuous mining events.

it wins more block mining events in comparison. Therefore, we conclude that electric vehicles have significant effects on raising the chance of customers to win the block mining and increase their comfort to gain more profit and save their DER into monetary resources.

6.6.2 Blockchain Performance

According to Figure 6.7, we selected 10, 20, 50, and 70 customers out of 100 customers as active nodes for smart contract transaction validation. Then, we found that with the increase of malicious nodes and numbers of active nodes in the network, the average probability value of detecting the malicious activity decreases smoothly. For example, if half of the customers are malicious and 10 customers are active nodes, our model can detect those with the probability of more than 0.5 and defeat the 51% attack. To present the suited

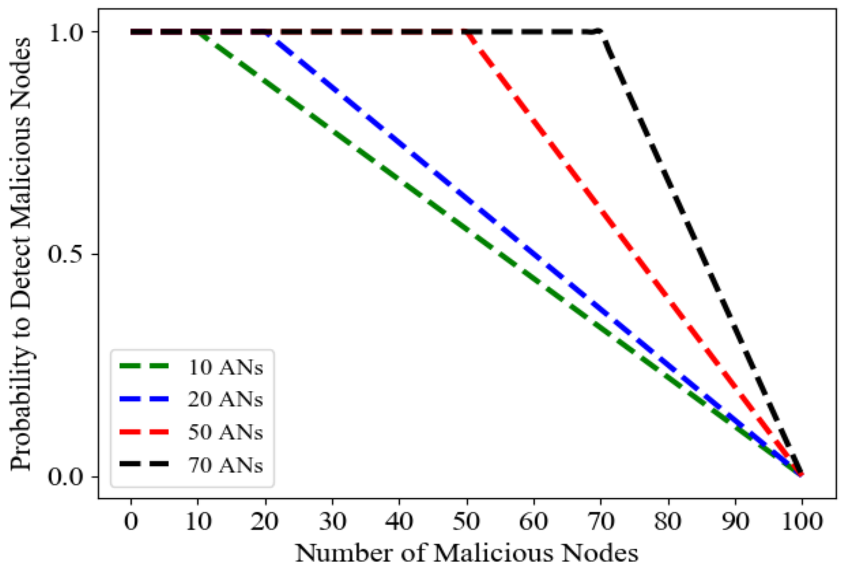

Figure 6.7: The average probability of detecting malicious nodes with different active nodes while the numbers of malicious customers are increasing.

number of active nodes for secure transaction validation, Figure 6.8 shows the maximum and the minimum required numbers of active nodes for a network with 100 customers. Accordingly, with the increase of the average reputation value of customers in the network, the number of active nodes decreases because the network is further trusted. Moreover, with the decrease of active nodes, the network can save on the energy used for smart contract transaction validation.

6.7 Conclusion

In this chapter, we presented a secure and robust DR model that uses the mixed-strategy Stackelberg game integrated with energy blockchain. The advantages of the proposed so-

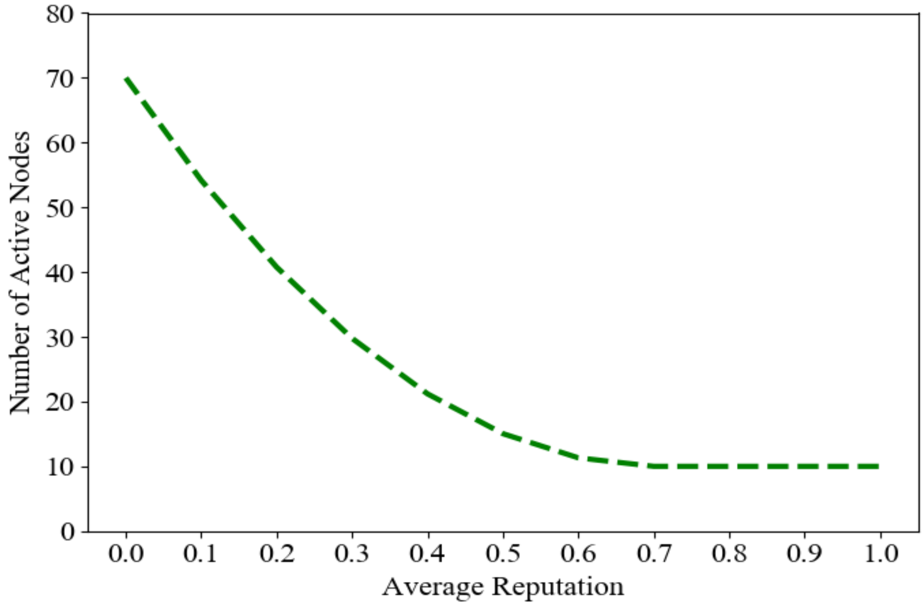

Figure 6.8: The minimum required number of active nodes with respect to the network average reputation value.

lution are; involving customers in a probabilistic game model to control their demand at peak periods, maximize DR profit for customers, increase the winning probability for block mining, invest the surplus energy resources into monetary resources, and use the distributed processing hardware of the customers for the block mining. We defined the proof of energy saving (PoES) as a consensus algorithm to select the block miner considering the reputation, availability, and compliance ratio. We proved the existence of the Stackelberg equilibrium point using Kakutani fixed point theory. The results presented the relation between the average probability value of block mining and DR contribution and showed this probability raises by increasing demand reduction and electric vehicle state-of-charge. We illustrated the average probability of detecting malicious nodes with different active nodes, where the proposed energy blockchain model with only 10 active nodes can defeat 51% attack. We studied the probability of winning the block mining and showed that with more than 20% demand reduction and 35% SoC, the probability of block mining goes beyond 0.5. The outcomes showed that the model provides a secure and robust demand response solution by defeating malicious activities and security attacks.

Chapter 7

Conclusion and Future Work

7.1 Concluding Remarks

Smart grid technologies modernize the monitoring, supervision, and control services in the electricity system. Solutions have been proposed to enhance the efficiency of electricity usage and ensure grid robustness and flexibility. A distributed energy resource management system (DERMS) is a crucial application in the smart grid that is used to efficiently control the electrical loads of customers in the distribution network and minimize electricity losses. Demand response (DR), demand side management (DSM), and distributed energy resources (DER) are solutions embedded in the DERMS concept.

In this thesis, we developed demand management solutions to increase the distribution network efficiency and reduce the need for electricity sources outside the grid. We utilized optimization and game models to control the demand of distribution networks. Our proposed solutions provide clustered sequential management, mixed-strategy Stackelberg game, and energy blockchain for stochastic demand response for DSM, DR, and DER control.

First, we proposed a DSM optimization model for the residential customer to distribute demand over the time horizon, considering their comfort and different appliances. The fundamental difference between the proposed model and existing mechanisms is the design of lightweight mixed-integer linear programming (MILP) and linear programming optimization models in addition to considering thermal comfort jointly with prioritized appliance scheduling. In our proposed approach, every house has a home energy management system (HEMS) that can prioritize appliances and implement MILP and linear programming optimization techniques to minimize customer bills and maximize thermal comfort. The model can improve network efficiency and customer satisfaction as well. The results showed that we smoothed the demand profile, reduced the peak-to-average ratio, reduced the cost to the customer while increasing their comfort, satisfied the room temperature, and charged electric vehicles more than the desired value. The proposed scheme was described in chapter 3, and it was published in [207].

Second, we considered a demand response model that manages the electricity usage in the distribution network and is implemented between the utility company and customers. This model is a unique stochastic DR solution, expressed by game-theoretical analysis using a mixed-strategy Stackelberg game due to the unpredictable reaction of customers to the demand response offers. We designed the interaction between the aggregator and customers as a new perspective on incentive-based demand response architecture. We found the mixed equilibrium point of the game by dividing the mixed-strategy Stackelberg game into mixed-strategy subgames and proving the existence of a Stackelberg equilibrium. Another important factor is the operational significance of the algorithm, which employs k-means clustering and the Silhouette model to find the optimal number of players (as distinct from customers) in the game. This is intimately connected with the probabilistic nature of the game, as we design the interaction between the aggregator and customers via the mixed-strategies. The results show that our scheme successfully flattens the peak, shifts deferrable loads to off-peak hours, and finds the optimal demand response strategy for the network. The scheme was presented in chapter 4 and it was published in [208].

Third, we developed a demand response Stackelberg game played between the control agent (CA) and customers to design a novel demand response solution integrated with energy blockchain. Our model incentivized customers to maximize their demand reduction profit value, charge and discharge electric vehicles efficiently, and maximize their chance to gain rewards through block mining. We designed an energy blockchain to store the energy transaction data securely and use the surplus household energy for block mining to reduce the waste of energy. We proposed a novel consensus algorithm, proof of energy saving (PoES), that selects a block miner by considering the historical reputation, adequacy of energy resources, and demand response contribution among participants. The results showed that the proposed scheme could manage the DER by efficiently allocating photovoltaic resources, demand, and electric vehicles to the block mining process and incentivizing customers to discharge electric vehicles and reduce their consumption during the peaks. We also demonstrated that our proposed consensus algorithm is robust and secure against malicious users. The proposed scheme was described in chapter 5, and it was published in [209].

Fourth, and unlike our previous work, we implemented an incentive-based leader-follower stochastic demand response model using blockchain to determine the random energy consumption of customers during peak hours and effectively control the block mining. This model is a mixed-strategy Stackelberg game played between the CA and customers. For the mixed-strategy Stackelberg game, we proved the existence of the equilibrium point of the game based on the optimal solutions of the customers and CA. The blockchain architecture in this work enables a secure, robust, and reliable distributed energy management system while the processing and computational cost of the crypto algorithm is distributed across the network. We also designed smart contract and authentication schemes using the digital signature algorithm, public-private keys, and smart contract for energy transaction authentication and validation to reduce cyber security attacks. The simulation results show that the proposed architecture is secure and robust against different cyber security attacks. The scheme was presented in chapter 6 and it was submitted into [210].

Our hierarchical architecture can efficiently handle the situation where the users do not comply with the demand response request. In this case, the aggregator has a contingency reserve that can compensate the promised contribution, but if the aggregator fails, the DSO should supply the electricity from other reserves in the market that offer high prices. In return, the DSO charges the aggregator for the electricity cost including the penalty, and also the aggregator charges customers as well. Therefore, the system never fails because there are enough contingency reserves.

Most people think that blockchain is an energy-hungry platform that consumes a lot of electricity for block generation and consensus algorithms. However, there are different types of blockchain platforms with different energy consumption. Based on a system requirement, a user can select a public, conservative or private blockchain which has the highest and lowest consumption, respectively. Moreover, the consensus algorithm mechanism and difficulty level of Hash generation are other parameters that can be managed to minimize the blockchain energy consumption.

7.2 Future Work

The increase in electricity consumption, the high cost of energy generation, and limited energy resources become the main driving force for researchers to look into DERMS solutions. The essential requirement for implementing DERMS is to provide a low-latency connection with an acceptable quality of services, such as high-speed channels with minimum interruption, congestion, and error. To this end, implementing DERMS technology on 5G and recently 6G communication networks can provide high bandwidth and trustable connections network. They are suitable backbones for running smart grid applications on top. The smart grid applications include demand response control, pricing signal management, distributed energy generation monitoring, vehicle-to-grid, and grid-to-vehicle controlling signals. To this end, more investigations are needed to integrate the communication and data exchange control with the algorithms proposed in this thesis.

Security is a significant concern in the smart grid that can reduce customers' trust, damage the network equipment, and waste the energy of resources. Blockchain is a fully functional data exchange platform that can confront security concerns such as the loss, forgery, and theft of data while managing data storage and user privacy. To this end, a comprehensive design of smart contracts, consensus algorithms, and authentication and authorization techniques are required to defeat various security attacks and provide user privacy on the blockchain.

According to the studied blockchain articles, blockchain is a practical solution for energy trading problems while it gives the prosumers the ability to interact and control their demand and supply. They can offer price and energy quantity directly. To improve the profit of prosumers, an autonomous energy trading model could assist them in selecting a proper bidding price and quantity to maximize their benefit. The financial exchange could be done through the blockchain cryptocurrency to eliminate the third party from future works.

The use of DER in a power grid can provide effective energy control and reduce the energy generation and waste of generated renewable resources. For example, residential photovoltaic systems usually generate a significant amount of energy in the morning, which is usually wasted due to inefficient usage. This extra generation could be used for home-to-the-grid solutions such as charging electric vehicles, storing extra energy in the local batteries, and selling energy into the grid or to neighbors. Users can charge their vehicles at their neighbor's charging place while the homeowners are not using them.

Due to increasing electric vehicle use, the distribution network requires intelligent solutions to monitor and control these vehicles' energy consumption (grid-to-vehicle) and efficiently use their mobile battery resources for energy management (vehicle-to-grid). However, predictive models and machine learning solutions can help determine their possible attitudes in different situations. Within intelligent applications, the utility company would be able to control network supply and demand by offering incentive prices for charging and discharging in over and under-generation conditions. From electric vehicle drivers' perspective, a smart application is needed to inform them about available charging spots and electricity prices to drive with confidence and no concern about energy requirements.

References

[1] M. Erol-Kantarci and H.T. Mouftah. Energy-efficient information and communication infrastructures in the smart grid: A survey on interactions and open issues. *IEEE Communications Surveys and Tutorials*, 17(1):179–197, 2014.

[2] National Institute of Standards and Technology (NIST). NIST framework and roadmap for smart grid interoperability standards, release 3.0. http://dx.doi.org/10.6028/NIST.SP.1108r3, 2014.

[3] M.E El-Hawary. The smart grid—state-of-the-art and future trends. *Electric Power Components and Systems*, 42(3-4):239–250, 2014.

[4] K. Rose, R.E. Burns, and R.J. Graniere. Summary of key state issues of Federal Energy Regulatory Commission (FERC) orders 888 and 889, 1997.

[5] US Energy Information Administration. Electricity generation, capacity, and sales in the United States. https://www.eia.gov/energyexplained/electricity/electricity-in-the-us-generation-capacity-and-sales.php, 2020.

[6] P. Palensky and D. Dietrich. Demand side management: Demand response, intelligent energy systems, and smart loads. *IEEE Transactions on Industrial Informatics*, 7(3):381–388, 2011.

[7] A. Basit, G.A.S. Sidhu, A. Mahmood, and F. Gao. Efficient and autonomous energy management techniques for the future smart homes. *IEEE Transactions on Smart Grid*, 8(2):917–926, 2015.

[8] Independent Electricity System Operator (IESO) Company. Peak tracker for global adjustment class A. http://www.ieso.ca/peaktracker, 2021.

[9] The GridWise Architecture Council. GridWise transactive energy framework version 1.1. https://www.gridwiseac.org/pdfs/pnnl_22946_gwac_te_framework_july_2019_v1_1.pdf, 2019.

[10] Independent Electricity System Operator (IESO) Company. Settlement process. https://www.ieso.ca/en/Sector-Participants/Settlements/Settlement-Process, 2021.

[11] J. Reilly and G. Joos. Integration and aggregation of distributed energy resources–operating approaches, standards and guidelines. *25th International Conference and Exhibition on Electricity Distribution (CIRED)*, 1:45–51, 2019.

[12] G. Benetti, D. Caprino, Marco L. Della V., and T. Facchinetti. Electric load management approaches for peak load reduction: A systematic literature review and state of the art. *Sustainable Cities and Society*, 20:124–141, 2016.

[13] M. Rastegar, M. Fotuhi-Firuzabad, and M. Moeini-Aghtaie. Improving direct load control implementation by an inititative load control method. *18th IEEE Electric Power Distribution Conference*, 1:1–5, 2013.

[14] A.H. Mohsenian-Rad, V.WS. Wong, J. Jatskevich, and R. Schober. Optimal and autonomous incentive-based energy consumption scheduling algorithm for smart grid. *IEEE Innovative Smart Grid Technologies Conference (ISGT)*, 1:1–6, 2010.

[15] J. Vuelvas, F. Ruiz, and G. Gruosso. Limiting gaming opportunities on incentive-based demand response programs. *Applied Energy*, 225:668–681, 2018.

[16] P. Olivella-Rosell, P. Lloret-Gallego, Í. Munné-Collado, R. Villafafila-Robles, A. Sumper, S. Ottessen, J. Rajasekharan, and B.A. Bremdal. Local flexibility market design for aggregators providing multiple flexibility services at distribution network level. *Energies*, 11(4):822–841, 2018.

[17] S.H. Madaeni and R. Sioshansi. The impacts of stochastic programming and demand response on wind integration. *Energy Systems*, 4(2):109–124, 2013.

[18] M.H. Yaghmaee, M. Samadi, and A.L. Garcia. Personalized pricing: A new approach for dynamic pricing in the smart grid. *4th IEEE Smart Energy Grid Engineering Conference (SEGE)*, 1:46–51, 2016.

[19] I. Lampropoulos, W.L. Kling, P.F. Ribeiro, and J. van den Berg. History of demand side management and classification of demand response control schemes,. *IEEE Power and Energy Society General Meeting*, 2013.

[20] W. Saad, Z. Han, H.V. Poor, and T. Basar. Game-theoretic methods for the smart grid: An overview of microgrid systems, demand-side management, and smart grid communications. *IEEE Signal Processing Magazine*, 29(5):86–105, 2012.

[21] M. Ghorbanian, S.H. Dolatabadi, P. Siano, I. Kouveliotis-Lysikatos, and N.D. Hatziargyriou. Methods for flexible management of blockchain-based cryptocurrencies in electricity markets and smart grids. *IEEE Transactions on Smart Grid*, 11(5):4227–4235, 2020.

[22] M. Sun and J. Zhang. Research on the application of blockchain big data platform in the construction of new smart city for low carbon emission and green environment. *Computer Communications*, 149:332–342, 2020.

[23] J. Li, Z. Zhou, J. Wu, J. Li, S. Mumtaz, X. Lin, H. Gacanin, and S. Alotaibi. Decentralized on-demand energy supply for blockchain in internet of things: A microgrids approach. *IEEE Transactions on Computational Social Systems*, 6(6):1395–1406, 2019.

[24] S.A. Boyer. SCADA: supervisory control and data acquisition. *International Society of Automation, ACM*, 2009.

[25] J. Figueiredo and J. da Costa. A SCADA system for energy management in intelligent buildings. *Energy and Buildings*, 49:85–98, 2012.

[26] W.R. Cassel. Distribution management systems: Functions and payback. *IEEE Transactions on Power Systems*, 8(3):796–801, 1993.

[27] US Energy Independence and Security Act (EISA). Public law 110–140—dec. 19, 2007. https://www.govinfo.gov/content/pkg/PLAW-110publ140/pdf/PLAW-110publ140.pdf, 2007.

[28] M. Erol-Kantarci and H.T. Mouftah. Wireless sensor networks for cost-efficient residential energy management in the smart grid. *IEEE Transactions on Smart Grid*, 2(2):314–325, 2011.

[29] F.A. Rahimi and S. Mokhtari. Distribution management system for the grid of the future: A transactive system compensating for the rise in distributed energy resources. *IEEE Electrification Magazine*, 6(2):84–94, 2018.

[30] IEEE Power and Energy Society. IEEE guide for distributed energy resources management systems (DERMS) functional specification. https://ieeexplore.ieee.org/document/9447316, 2021.

[31] A. Renjit, A. O'Connell, D. Zandt, and B. Seal. Evaluating the value of DERMS: Methods and mitigation to increase feeder hosting capacity. *25th International Conference and Exhibition on Electricity Distribution (CIRED)*, 1:1–5, 2019.

[32] Smart Electric Power Alliance. Distributed energy resource management system (DERMS) requirements version 2.0. https://sepapower.org/resource/distributed-energy-resource-management-system-derms-requirements/, 2019.

[33] S. Nowak, N. Tehrani, M.S. Metcalfe, W. Eberle, and L. Wang. Cloud-based DERMS test platform using real-time power system simulation. *IEEE Power and Energy Society General Meeting (PESGM)*, 1:1–5, 2018.

[34] F. Katiraei, R. Iravani, N. Hatziargyriou, and A. Dimeas. Microgrids management. *IEEE Power and Energy Magazine*, 6(3):54–65, 2008.

[35] J. Wang, C. Chen, and X. Lu. Guidelines for implementing advanced distribution management systems-requirements for DMS integration with DERMS and microgrids. Argonne National Lab.(ANL), Argonne, IL (United States), 2015.

[36] P. Dehghanian, M. Fotuhi-Firuzabad, S. Bagheri-Shouraki, and A.A. Kazemi. Critical component identification in reliability centered asset management of power distribution systems via fuzzy AHP. *IEEE Systems Journal*, 6(4):593–602, 2011.

[37] V.N. Coelho, M.W. Cohen, I.M. Coelho, N. Liu, and F.G. Guimarães. Multi-agent systems applied for energy systems integration: State-of-the-art applications and trends in microgrids. *Applied Energy*, 187:820–832, 2017.

[38] P. Asmus. Microgrids, virtual power plants and our distributed energy future. *The Electricity Journal*, 23(10):72–82, 2010.

[39] D.E. Olivares, A. Mehrizi-Sani, A.H. Etemadi, C.A. Cañizares, R. Iravani, M. Kazerani, A.H. Hajimiragha, O. Gomis-Bellmunt, M. Saeedifard, and R. Palma-Behnke. Trends in microgrid control. *IEEE Transactions on Smart Grid*, 5(4):1905–1919, 2014.

[40] H. Haddadian and R. Noroozian. Multi-microgrids approach for design and operation of future distribution networks based on novel technical indices. *Applied Energy*, 185:650–663, 2017.

[41] S.DJ. McArthur, E.M. Davidson, V.M. Catterson, A.L. Dimeas, N.D. Hatziargyriou, F. Ponci, and T. Funabashi. Multi-agent systems for power engineering applica-

tions—part I: Concepts, approaches, and technical challenges. *IEEE Transactions on Power systems*, 22(4):1743–1752, 2007.

[42] M.R. Khan, R. Jidin, and J. Pasupuleti. Multi-agent based distributed control architecture for microgrid energy management and optimization. *Energy Conversion and Management*, 112:288–307, 2016.

[43] M.T. Miller, M.B. Johns, E. Sortomme, and S.S. Venkata. Advanced integration of distributed energy resources. *IEEE Power and Energy Society General Meeting*, 1:1–2, 2012.

[44] A. Bani-Ahmed, M. Rashidi, and A. Nasiri. Decentralised resilient autonomous control architecture for dynamic microgrids. *IET Generation, Transmission and Distribution*, 13(11):2182–2189, 2019.

[45] B. Zhou, W. Li, K.W. Chan, Y. Cao, Y. Kuang, X. Liu, and X. Wang. Smart home energy management systems: Concept, configurations, and scheduling strategies. *Renewable and Sustainable Energy Reviews*, 61:30–40, 2016.

[46] B. Mahapatra and A. Nayyar. Home energy management system (HEMS): Concept, architecture, infrastructure, challenges and energy management schemes. *Energy Systems*, 1:1–27, 2019.

[47] S. Aman, Y. Simmhan, and V. Prasanna. Energy management systems: state of the art and emerging trends. *IEEE Communications Magazine*, 51(1):114–119, 2013.

[48] M. Shakeri, M. Shayestegan, H. Abunima, S. Reza, M. Akhtaruzzaman, A. Alamoud, K. Sopian, and N. Amin. An intelligent system architecture in home energy management systems (HEMS) for efficient demand response in smart grid. *Energy and Buildings*, 138:154–164, 2017.

[49] D. Han and J. Lim. Design and implementation of smart home energy management systems based on ZigBee. *IEEE Transactions on Consumer Electronics*, 56(3):1417–1425, 2010.

[50] R. Ford, M. Pritoni, A. Sanguinetti, and B. Karlin. Categories and functionality of smart home technology for energy management. *Building and Environment*, 123:543–554, 2017.

[51] H. Dinh, J. Yun, D. Kim, K. Lee, and D. Kim. A home energy management system with renewable energy and energy storage utilizing main grid and electricity selling. *IEEE Access*, 8:49436–49450, 2020.

[52] L.D. Collins and R.H. Middleton. Distributed demand peak reduction with non-cooperative players and minimal communication. *IEEE Transactions on Smart Grid*, 10(1):153–162, 2017.

[53] A. Carreiro, H. Jorge, and C. Antunes. Energy management systems aggregators: A literature survey. *Renewable and Sustainable Energy Reviews*, 73:1160–1172, 2017.

[54] B. Chai, J. Chen, Z. Yang, and Y. Zhang. Demand response management with multiple utility companies: A two-level game approach. *IEEE Transactions on Smart Grid*, 5(2):722–731, 2014.

[55] N. Hajj and M. Awad. A game theory approach to demand side management in smart grids. *Intelligent Systems' 2014, Springer*, 807-819, 2015.

[56] F. Viani and M. Salucci. A user perspective optimization scheme for demand-side energy management. *IEEE Systems Journal*, 12(4):3857–3860, 2017.

[57] A.H. Mohsenian-Rad, V.WS. Wong, J. Jatskevich, R. Schober, and A. Leon-Garcia. Autonomous demand-side management based on game-theoretic energy consumption scheduling for the future smart grid. *IEEE Transactions on Smart Grid*, 1(3):320–331, 2010.

[58] T. Basar and G. Jan Olsder. Dynamic Noncooperative Game Theory. *Society for Industrial and Applied Mathematics*, 2:77-160, 1998.

[59] M. Yu and S.H. Hong. A real-time demand-response algorithm for smart grids: A stackelberg game approach. *IEEE Transactions on Smart Grid*, 7(2):879–888, 2015.

[60] E. Nekouei, T. Alpcan, and D. Chattopadhyay. Game-theoretic frameworks for demand response in electricity markets. *IEEE Transactions on Smart Grid*, 6(2):748–758, 2014.

[61] S. Maharjan, Q. Zhu, Y. Zhang, S. Gjessing, and T. Basar. Dependable demand response management in the smart grid: A Stackelberg game approach. *IEEE Transactions on Smart Grid*, 4(1):120–132, 2013.

[62] J. Chen, B. Yang, and X. Guan. Optimal demand response scheduling with Stackelberg game approach under load uncertainty for smart grid. *3th IEEE International Conference on Smart Grid Communications (SmartGridComm)*, 1:546–551, 2012.

[63] F.L. Meng and X.J. Zeng. A stackelberg game-theoretic approach to optimal real-time pricing for the smart grid. *Soft Computing*, 17(12):2365–2380, 2013.

[64] J. Fattahi, D. Wright, and H. Schriemer. An energy internet DERMS platform using a multi-level Stackelberg game. *Sustainable Cities and Society*, 60:102–128, 2020.

[65] M. Tavakkoli, S. Fattaheian-Dehkordi, M. Kasmaei, M. Liski, and M. Lehtonen. Bonus-based demand response using Stackelberg game approach for residential end-users equipped with HVAC system. *IEEE Transactions on Sustainable Energy*, 12(1):234–249, 2020.

[66] S. Abapour, B. Mohammadi-Ivatloo, and M.T. Hagh. A Bayesian game theoretic based bidding strategy for demand response aggregators in electricity markets. *Sustainable Cities and Society*, 54:101–130, 2020.

[67] S. Pal, S. Thakur, R. Kumar, and B.K. Panigrahi. A strategical game theoretic based demand response model for residential consumers in a fair environment. *International Journal of Electrical Power and Energy Systems*, 97:201–210, 2018.

[68] A. Khalid, N. Javaid, A. Mateen, M. Ilahi, T. Saba, and A. Rehman. Enhanced time-of-use electricity price rate using game theory. *Electronics*, 8(1):48, 2019.

[69] R. Tang, H. Li, and S. Wang. A game theory-based decentralized control strategy for power demand management of building cluster using thermal mass and energy storage. *Applied Energy*, 242:809–820, 2019.

[70] Q. Lu, S. Lü, and Y. Leng. A Nash-Stackelberg game approach in regional energy market considering users' integrated demand response. *Energy*, 175:456–470, 2019.

[71] M. Motalleb, P. Siano, and R. Ghorbani. Networked Stackelberg competition in a demand response market. *Applied Energy*, 239:680–691, 2019.

[72] H. Huang, Y. Cai, H. Xu, and H. Yu. A multiagent minority-game-based demand-response management of smart buildings toward peak load reduction. *IEEE Transactions on Computer-Aided Design of Integrated Circuits and Systems*, 36(4):573–585, 2016.

[73] N. Aguiar, A. Dubey, and V. Gupta. Network-constrained Stackelberg game for pricing demand flexibility in power distribution systems. *IEEE Transactions on Smart Grid*, 12:4049 – 4058, 2021.

[74] B. Xu, J. Wang, M. Guo, J. Lu, G. Li, and L. Han. A hybrid demand response mechanism based on real-time incentive and real-time pricing. *Energy*, 231:120940, 2021.

[75] L. Chen, N. Liu, C. Li, and J. Wang. Peer-to-peer energy sharing with social attributes: A stochastic leader-follower game approach. *IEEE Transactions on Industrial Informatics*, 17(4):2545–2556, 2020.

[76] S. Abapour, B. Mohammadi-Ivatloo, and M. Tarafdar-Hagh. Robust bidding strategy for demand response aggregators in electricity market based on game theory. *Journal of Cleaner Production*, 243:118–134, 2020.

[77] H. Rashidizadeh-Kermani, M. Vahedipour-Dahraie, M. Shafie-khah, and J.P Catalão. Stochastic programming model for scheduling demand response aggregators considering uncertain market prices and demands. *International Journal of Electrical Power and Energy Systems*, 113:528–538, 2019.

[78] H. Yang, J. Zhang, J. Qiu, S. Zhang, M. Lai, and Z.Y. Dong. A practical pricing approach to smart grid demand response based on load classification. *IEEE Transactions on Smart Grid*, 9(1):179–190, 2016.

[79] C.P. Mediwaththe and D.B. Smith. Game-theoretic demand-side management robust to non-ideal consumer behavior in smart grid. *25th IEEE International Symposium on Industrial Electronics (ISIE)*, 1:702–707, 2016.

[80] C.P. Mediwaththe and D.B. Smith. Game-theoretic electric vehicle charging management resilient to non-ideal user behavior. *IEEE Transactions on Intelligent Transportation Systems*, 19(11):3486–3495, 2018.

[81] P.A. Apostolopoulos, E.E. Tsiropoulou, and S. Papavassiliou. Demand response management in smart grid networks: A two-stage game-theoretic learning-based approach. *Mobile Networks and Applications*, 26(2):548–561, 2021.

[82] H. Pourbabak, T. Chen, and W. Su. The Energy Internet. *Woodhead Publishing*, 3-19, 2019.

[83] E. Guelpa and V. Verda. Demand response and other demand side management techniques for district heating: A review. *Energy*, 219:119440, 2021.

[84] J. Vasudevan and K.S. Swarup. Price based demand response strategy considering load priorities. *6th IEEE International Conference on Power Systems (ICPS)*, 1:1–6, 2016.

[85] P. Huang and Y. Sun. A collaborative demand control of nearly zero energy buildings in response to dynamic pricing for performance improvements at cluster level. *Energy*, 174:911–921, 2019.

[86] J.M. Lujano-Rojas, C. Monteiro, R. Dufo-Lopez, and J.L. Bernal-Agustín. Optimum residential load management strategy for real time pricing (RTP) demand response programs. *Energy Policy*, 45:671–679, 2012.

[87] R. Karthikeyan and A.K. Parvathy. Real time energy optimization using cyber physical controller for micro-smart grid applications. *IEEE 5th International Conference on Recent Trends in Information Technology (ICRTIT)*, 1:1–6, 2016.

[88] S.L. Arun and M.P. Selvan. Intelligent residential energy management system for dynamic demand response in smart buildings. *IEEE Systems Journal*, 12(2):1329–1340, 2017.

[89] D. Li, W.Y. Chiu, H. Sun, and H.V. Poor. Multiobjective optimization for demand side management program in smart grid. *IEEE Transactions on Industrial Informatics*, 14(4):1482–1490, 2017.

[90] M.B. Rasheed, N. Javaid, A. Ahmad, M. Awais, Z.A. Khan, U. Qasim, and N. Alrajeh. Priority and delay constrained demand side management in real-time price environment with renewable energy source. *International Journal of Energy Research*, 40(14):2002–2021, 2016.

[91] Y. Liu, C. Yuen, R. Yu, Y. Zhang, and S. Xie. Queuing-based energy consumption management for heterogeneous residential demands in smart grid. *IEEE Transactions on Smart Grid*, 7(3):1650–1659, 2015.

[92] S.M. Ali, M. Naveed, F. Javed, N. Arshad, and J. Ikram. DeLi2P: A user centric, scalable demand side management strategy for smart grids. *4th IEEE International Conference on Smart Cities and Green ICT Systems (SMARTGREENS)*, 1:1–9, 2015.

[93] R. Rana, J. Fattahi, and H. Schriemer. Multi-dimensional energy consumption scheduling for event based demand response. *25th International Conference on Electricity Distribution*, 1:2251–2256, 2019.

[94] M. Tahir and S.K. Mazumder. Event-and priority-driven coordination in next-generation grid. *IEEE Journal of Emerging and Selected Topics in Power Electronics*, 4(4):1186–1194, 2016.

[95] X. Jiang and C. Xiao. Household energy demand management strategy based on operating power by genetic algorithm. *IEEE Access*, 7:96414–96423, 2019.

[96] M.R. Alam, M. St-Hilaire, and T. Kunz. Cost optimization via rescheduling in smart grids—a linear programming approach. *IEEE 13th International Conference on Smart Energy Grid Engineering (SEGE)*, 1:1–6, 2013.

[97] S.L. Arun and M.P. Selvan. Dynamic demand response in smart buildings using an intelligent residential load management system. *IET Generation, Transmission and Distribution*, 11(17):4348–4357, 2017.

[98] I. Ihsane, L. Miègeville, N. Aït-Ahmed, and P. Guérin. Real-time management model for residential multi-class appliances. *9th IEEE PES Asia-Pacific Power and Energy Engineering Conference (APPEEC)*, 1:1–6, 2017.

[99] S. Shah, R. Khalid, A. Zafar, S.M. Hussain, H. Rahim, and N. Javaid. An optimized priority enabled energy management system for smart homes. *31st IEEE International Conference on Advanced Information Networking and Applications (AINA)*, 1:1035–1041, 2017.

[100] A. Sinha and M. De. Load shifting technique for reduction of peak generation capacity requirement in smart grid. *1st IEEE International Conference on Power Electronics, Intelligent Control and Energy Systems (ICPEICES)*, 1:1–5, 2016.

[101] V.K. Tumuluru and D.H. Tsang. A two-stage approach for network constrained unit commitment problem with demand response. *IEEE Transactions on Smart Grid*, 9(2):1175–1183, 2016.

[102] L. Yu, D. Xie, C. Huang, T. Jiang, and Y. Zou. Energy optimization of HVAC systems in commercial buildings considering indoor air quality management. *IEEE Transactions on Smart Grid*, 10(5):5103–5113, 2018.

[103] H. Wang, K. Meng, F. Luo, Z.Y. Dong, G. Verbič, Z. Xu, and K.P. Wong. Demand response through smart home energy management using thermal inertia. *23th IEEE Australasian Universities Power Engineering Conference (AUPEC)*, 1:1–6, 2013.

[104] R. Raza, N.U Hassan, and C. Yuen. Determination of consumer behavior based energy wastage using IoT and machine learning. *Energy and Buildings*, 220:110–138, 2020.

[105] W. Guo, J. Wen, F. Luo, and Y. Zheng. Peak load reduction by thermostatically controlled load dispatch with thermal comfort model. *10th IEEE International Conference on Advances in Power System Control, Operation and Management (APSCOM)*, 1:1–5, 2015.

[106] M. Tasdighi, H. Ghasemi, and A. Rahimi-Kian. Residential microgrid scheduling based on smart meters data and temperature dependent thermal load modeling. *IEEE Transactions on Smart Grid*, 5(1):349–357, 2013.

[107] Z. Yahia and A. Pradhan. Multi-objective optimization of household appliance scheduling problem considering consumer preference and peak load reduction. *Sustainable Cities and Society*, 55:102–137, 2020.

[108] R. Kyoho, T. Goya, W. Mengyan, T. Senjyu, A. Yona, T. Funabashi, and C.H. Kim. Optimal operation of thermal generating units and smart houses considering transmission constraints. *10th IEEE International Conference on Power Electronics and Drive Systems (PEDS)*, 1:1225–1230, 2013.

[109] G. Huang, J. Yang, and C. Wei. Cost-effective and comfort-aware electricity scheduling for home energy management system. *IEEE International Conferences on Big Data and Cloud Computing (BDCloud), Social Computing and Networking*

(SocialCom), Sustainable Computing and Communications (SustainCom)(BDCloud-SocialCom-SustainCom), 1:453–460, 2016.

[110] M. Akorede, H. Hizam, and E. Pouresmaeil. Distributed energy resources and benefits to the environment. *Renewable and sustainable energy reviews*, 14(2):724–734, 2010.

[111] M. Rehmani, M. Reisslein, A. Rachedi, M. Erol-Kantarci, and M. Radenkovic. Integrating renewable energy resources into the smart grid: Recent developments in information and communication technologies. *IEEE Transactions on Industrial Informatics*, 14(7):2814–2825, 2018.

[112] M. Sadeghi, S. Mollahasani, and M. Erol-Kantarci. Power loss-aware transactive microgrid coalitions under uncertainty. *Energies*, 13(21):5782, 2020.

[113] K. Wang, Z. Ouyang, R. Krishnan, L. Shu, and L. He. A game theory-based energy management system using price elasticity for smart grids. *IEEE Transactions on Industrial Informatics*, 11(6):1607–1616, 2015.

[114] A.R. Ahmadi, I. Martinez, B. Stojkovska, T. Manandhar, and S. Georgiopoulos. UK power networks providing power services from distributed energy resources to transmission system operator via a centralised DERMS platform. *25th International Conference and Exhibition on Electricity Distribution (CIRED)*, 1:1–5, 2019.

[115] A. Bouallaga, R. Kadri, V. Albinet, A. Davigny, F. Colas, V. Courtecuisse, A. Merdassi, X. Guillaud, and B. Robyns. Advanced metering infrastructure for real-time coordination of renewable energy and electric vehicles charging in distribution grid. *20th International Conference and Exhibition on Electricity Distribution (CIRED) Workshop*, 1:1–6, 2014.

[116] D. Wang, B. De Wit, S. Parkinson, J. Fuller, D. Chassin, C. Crawford, and N. Djilali. A test bed for self-regulating distribution systems: Modeling integrated renewable energy and demand response in the GridLAB-D/MATLAB environment. *3rd IEEE PES Innovative Smart Grid Technologies (ISGT)*, 1:1–7, 2012.

[117] C. Chen, S. Duan, T. Cai, B. Liu, and G. Hu. Smart energy management system for optimal microgrid economic operation. *IET Renewable Power Generation*, 5(3):258–267, 2011.

[118] A. Chaouachi, R. M Kamel, R. Andoulsi, and K. Nagasaka. Multiobjective intelligent energy management for a microgrid. *IEEE Transactions on Industrial Electronics*, 60(4):1688–1699, 2012.

[119] S. Das and M. Basu. Day-ahead optimal bidding strategy of microgrid with demand response program considering uncertainties and outages of renewable energy resources. *Energy*, 190:116441, 2020.

[120] A.G. Zamani, A. Zakariazadeh, S. Jadid, and A. Kazemi. Stochastic operational scheduling of distributed energy resources in a large scale virtual power plant. *International Journal of Electrical Power and Energy Systems*, 82:608–620, 2016.

[121] D. Zhang, S. Li, P. Zeng, and C. Zang. Optimal microgrid control and power-flow study with different bidding policies by using powerworld simulator. *IEEE Transactions on Sustainable Energy*, 5(1):282–292, 2013.

[122] D. Arcos-Aviles, J. Pascual, L. Marroyo, P. Sanchis, and F. Guinjoan. Fuzzy logic-based energy management system design for residential grid-connected microgrids. *IEEE Transactions on Smart Grid*, 9(2):530–543, 2016.

[123] R. Bahmani, H. Karimi, and S. Jadid. Stochastic electricity market model in networked microgrids considering demand response programs and renewable energy sources. *International Journal of Electrical Power and Energy Systems*, 117:105606, 2020.

[124] F. Wang, X. Ge, P. Yang, K. Li, Z. Mi, P. Siano, and N. Duić. Day-ahead optimal bidding and scheduling strategies for DER aggregator considering responsive uncertainty under real-time pricing. *Energy*, 213:118765, 2021.

[125] B. Hussain, A. Khan, N. Javaid, Q.U. Hasan, S. A Malik, O. Ahmad, A.H. Dar, and A. Kazmi. A weighted-sum PSO algorithm for HEMS: A new approach for the design and diversified performance analysis. *Electronics*, 8(2):180, 2019.

[126] C. Vivekananthan, Y. Mishra, G. Ledwich, and F. Li. Demand response for residential appliances via customer reward scheme. *IEEE Transactions on Smart Grid*, 5(2):809–820, 2014.

[127] J. Fattahi, M. Samadi, M. Erol-Kantarci, and H. Schriemer. Transactive demand response operation at the grid edge using the IEEE 2030.5 standard. *Engineering*, 6(7):801–811, 2020.

[128] Atlanta: American Society of Heating Refrigerating and Air conditioning Engineering. ANSI/ASHRAE standard 55. thermal environmental conditions for human occupancy. https://www.ashrae.org/technical-resources/bookstore/thermal-environmental-conditions-for-human-occupancy, 2013.

[129] I. Ullah and D.H. Kim. An improved optimization function for maximizing user comfort with minimum energy consumption in smart homes. *Energies*, 10(11):1818, 2017.

[130] K. Ma, S. Hu, J. Yang, X. Xu, and X. Guan. Appliances scheduling via cooperative multi-swarm PSO under day-ahead prices and photovoltaic generation. *Applied Soft Computing*, 62:504–513, 2018.

[131] A.R. Jordehi. Binary particle swarm optimisation with quadratic transfer function: A new binary optimisation algorithm for optimal scheduling of appliances in smart homes. *Applied Soft Computing*, 78:465–480, 2019.

[132] L. Wang, Z. Wang, and R. Yang. Intelligent multiagent control system for energy and comfort management in smart and sustainable buildings. *IEEE Transactions on Smart Grid*, 3(2):605–617, 2012.

[133] D. Mahmood, N. Javaid, N. Alrajeh, Z.A. Khan, U. Qasim, I. Ahmed, and M. Ilahi. Realistic scheduling mechanism for smart homes. *Energies*, 9(3):202, 2016.

[134] B. Li, S. Gangadhar, S. Cheng, and P.K. Verma. Predicting user comfort level using machine learning for smart grid environments. *2nd IEEE Innovative Smart Grid Technologies (ISGT) Conference*, 1:1–6, 2011.

[135] A. Miglani, N. Kumar, V. Chamola, and S. Zeadally. Blockchain for internet of energy management: Review, solutions, and challenges. *Computer Communications*, 151:395–418, 2020.

[136] B. Bhushan, A. Khamparia, K. Sagayam, S. Sharma, M. Ahad, and N. Debnath. Blockchain for smart cities: A review of architectures, integration trends and future research directions. *Sustainable Cities and Society*, 61:102360, 2020.

[137] Scribd. Insight into the world of blockchain by cybrosys technologies - cryptocurrency - Bitcoin. https://www.scribd.com/document/375428377/Insight-into-the-world-of-blockchain-by-cybrosys-technologies, 2020.

[138] Z. Liu, N.C. Luong, W. Wang, D. Niyato, P. Wang, Y.C. Liang, and D.I. Kim. A survey on blockchain: A game theoretical perspective. *IEEE Access*, 7:47615–47643, 2019.

[139] V. Buterin. A next-generation smart contract and decentralized application platform. https://blockchainlab.com/pdf/Ethereum_white_paper-a_next_generation_smart_contract_and_decentralized_application_platform-vitalik-buterin.pdf, 2015.

[140] G. Xu, Y. Liu, and P.W. Khan. Improvement of the DPoS consensus mechanism in blockchain based on vague sets. *IEEE Transactions on Industrial Informatics*, 16(6):4252–4259, 2019.

[141] P. Siano, G. De Marco, A. Rolán, and V. Loia. A survey and evaluation of the potentials of distributed ledger technology for peer-to-peer transactive energy exchanges in local energy markets. *IEEE Systems Journal*, 13(3):3454–3466, 2019.

[142] M.B. Mollah, J. Zhao, D. Niyato, K.Y. Lam, X. Zhang, A.M. Ghias, L.H. Koh, and L. Yang. Blockchain for future smart grid: A comprehensive survey. *IEEE Internet of Things Journal*, 8(1):18–43, 2020.

[143] C. Qiu, H. Yao, X. Wang, N. Zhang, F.R. Yu, and D. Niyato. AI-chain: Blockchain energized edge intelligence for beyond 5G networks. *IEEE Network*, 34(6):62–69, 2020.

[144] A. Asheralieva and D. Niyato. Reputation-based coalition formation for secure self-organized and scalable sharding in IoT blockchains with mobile-edge computing. *IEEE Internet of Things Journal*, 7(12):11830–11850, 2020.

[145] Y. Lewenberg, Y. Bachrach, Y. Sompolinsky, A. Zohar, and J.S. Rosenschein. Bitcoin mining pools: A cooperative game theoretic analysis. *Proceedings of the International Conference on Autonomous Agents and Multiagent Systems*, 1:919–927, 2015.

[146] V. Dedeoglu, R. Jurdak, G. D Putra, A. Dorri, and S. Kanhere. A trust architecture for blockchain in IoT. *Proceedings of the 16th EAI International Conference on Mobile and Ubiquitous Systems: Computing, Networking and Services*, 1:190–199, 2019.

[147] A. Dorri, S. Kanhere, R. Jurdak, and P. Gauravaram. LSB: A lightweight scalable blockchain for IoT security and anonymity. *Journal of Parallel and Distributed Computing*, 134:180–197, 2019.

[148] J. Kang, Z. Xiong, D. Niyato, D. Ye, D.I. Kim, and J. Zhao. Toward secure blockchain-enabled internet of vehicles: Optimizing consensus management using reputation and contract theory. *IEEE Transactions on Vehicular Technology*, 68(3):2906–2920, 2019.

[149] S. Rouhani and R. Deters. Data trust framework using blockchain technology and adaptive transaction validation. *IEEE Access*, 9:90379–90391, 2021.

[150] C.L. Bastian-Pinto, F.V. Araujo, L.E. Brandão, and L.L. Gomes. Hedging renewable energy investments with Bitcoin mining. *Renewable and Sustainable Energy Reviews*, 1:110–121, 2020.

[151] R. Shan and Y. Sun. Bitcoin mining to reduce the renewable curtailment: A case study of CAISO. *United States Association for Energy Economics (USAEE)*, 1:1–9, 2019.

[152] M.U. Hassan, M.H. Rehmani, and J. Chen. VPT: Privacy preserving energy trading and block mining mechanism for blockchain based virtual power plants. *arXiv preprint arXiv:2102.01480*, 2021.

[153] M. Moniruzzaman, A. Yassine, and R. Benlamri. Blockchain-based mechanisms for local energy trading in smart grids. *16th IEEE International Conference on Smart Cities: Improving Quality of Life Using ICT and IoT and AI (HONET-ICT)*, 1:110–114, 2019.

[154] C. Liu, K.K. Chai, X. Zhang, and Y. Chen. Peer-to-peer electricity trading system: smart contracts based proof-of-benefit consensus protocol. *Wireless Networks*, 1:1–12, 2019.

[155] T. Jiang, H. Fang, and H. Wang. Blockchain-based internet of vehicles: Distributed network architecture and performance analysis. *IEEE Internet of Things Journal*, 6(3):4640–4649, 2018.

[156] R. Jin, X. Zhang, Z. Wang, W. Sun, X. Yang, and Z. Shi. Blockchain-enabled charging right trading among EV charging stations. *Energies*, 12(20):3922, 2019.

[157] C. Liu, K.K. Chai, E.T. Lau, and Y. Chen. Blockchain based energy trading model for electric vehicle charging schemes. *International Conference on Smart Grid Inspired Future Technologies*, 1:64–72, 2018.

[158] J. Kang, R. Yu, X. Huang, M. Wu, S. Maharjan, S. Xie, and Y. Zhang. Blockchain for secure and efficient data sharing in vehicular edge computing and networks. *IEEE Internet of Things Journal*, 6(3):4660–4670, 2018.

[159] S.M. Danish, K. Zhang, H.A. Jacobsen, N. Ashraf, and H.K. Qureshi. BlockEV: Efficient and secure charging station selection for electric vehicles. *IEEE Transactions on Intelligent Transportation Systems*, 22(7):4194–4211, 2020.

[160] A. Al-Obaidi and H. Farag. Decentralized quality of service based system for energy trading among electric vehicles. *IEEE Transactions on Intelligent Transportation Systems*, 1:1–10, 2021.

[161] L. Luo, J. Feng, H. Yu, and G. Sun. Blockchain-enabled two-way auction mechanism for electricity trading in internet of electric vehicles. *IEEE Internet of Things Journal*, 2:1–10, 2021.

[162] C. Pop, T. Cioara, M. Antal, I. Anghel, I. Salomie, and M. Bertoncini. Blockchain based decentralized management of demand response programs in smart energy grids. *Sensors*, 18(1):162–176, 2018.

[163] Y. Jiang, K. Zhou, X. Lu, and S. Yang. Electricity trading pricing among prosumers with game theory-based model in energy blockchain environment. *Applied Energy*, 271:115239, 2020.

[164] P. Gallo, S. Longo, F. Montana, E.R. Sanseverino, and G. Sciume. Blockchain-based DR logic: A trade-off between system operator's and customer's needs. *20th IEEE Mediterranean Electrotechnical Conference (MELECON)*, 1:576–581, 2020.

[165] K. Suankaewmanee, P.S. Ng, and D. Niyato. Distributed, scalable, and transparent data management framework for energy market: A blockchain approach. *IEEE/ACM 5th International Conference on Internet-of-Things Design and Implementation (IoTDI)*, 1:272–275, 2020.

[166] M.K. AlAshery, Z. Yi, D. Shi, X. Lu, C. Xu, Z. Wang, and W. Qiao. A blockchain-enabled multi-settlement quasi-ideal peer-to-peer trading framework. *IEEE Transactions on Smart Grid*, 12(1):885–896, 2020.

[167] S. Saxena, H. Farag, A. Brookson, H. Turesson, and H. Kim. A permissioned blockchain system to reduce peak demand in residential communities via energy trading: A real-world case study. *IEEE Access*, 9:5517–5530, 2020.

[168] M.L. Di Silvestre, P. Gallo, E.R. Sanseverino, G. Sciume, and G. Zizzo. Aggregation and remuneration in demand response with a blockchain-based framework. *IEEE Transactions on Industry Applications*, 56(4):4248–4257, 2020.

[169] K. Chatterjee, A. Goharshady, R. Ibsen-Jensen, and Y. Velner. Ergodic mean-payoff games for the analysis of attacks in crypto-currencies. *arXiv preprint arXiv:1806.03108*, 2018.

[170] A. Sapirshtein, Y. Sompolinsky, and A. Zohar. Optimal selfish mining strategies in Bitcoin. *International Conference on Financial Cryptography and Data Security*, 1:515–532, 2016.

[171] C. Dong, Y. Wang, A. Aldweesh, P. McCorry, and A. van Moorsel. Betrayal, distrust, and rationality: Smart counter-collusion contracts for verifiable cloud computing. *Proceedings of the 2017 ACM SIGSAC Conference on Computer and Communications Security*, 1:211–227, 2017.

[172] A. Asgaonkar and B. Krishnamachari. Solving the buyer and seller's dilemma: A dual-deposit escrow smart contract for provably cheat-proof delivery and payment for a digital good without a trusted mediator. *1st IEEE International Conference on Blockchain and Cryptocurrency (ICBC)*, 1:262–267, 2019.

[173] G. Bigi, A. Bracciali, G. Meacci, and E. Tuosto. Validation of decentralised smart contracts through game theory and formal methods. *Springer*, 142-161, 2015.

[174] M. Aazam, S. Zeadally, and K.A. Harras. Deploying fog computing in industrial internet of things and industry 4.0. *IEEE Transactions on Industrial Informatics*, 14(10):4674–4682, 2018.

[175] T.L. Saaty. Decision making with the analytic hierarchy process. *International Journal of Services Sciences*, 1(1):83–98, 2008.

[176] J.W. Lee and D.H. Lee. Residential electricity load scheduling for multi-class appliances with time-of-use pricing. *11th IEEE Global Communications Conference (GLOBECOM) Workshops*, 1:1194–1198, 2011.

[177] R.E. Tudoroiu, M. Zaheeruddin, S.M. Radu, and N. Tudoroiu. Real-time implementation of an extended Kalman filter and a PI observer for state estimation of rechargeable Li-Ion batteries in hybrid electric vehicle applications—A case study. *Batteries*, 4(2):19, 2018.

[178] J.A. Orosa and A.C. Oliveira. A new thermal comfort approach comparing adaptive and PMV models. *Renewable Energy*, 36(3):951–956, 2011.

[179] M.B. Wilson, R. Luck, and P.J. Mago. A first-order study of reduced energy consumption via increased thermal capacitance with thermal storage management in a micro-building. *Energies*, 8(10):12266–12282, 2015.

[180] A. Reinhardt, P. Baumann, D. Burgstahler, M. Hollick, H. Chonov, M. Werner, and R. Steinmetz. On the accuracy of appliance identification based on distributed load metering data. *2nd IEEE Sustainable Internet and ICT for Sustainability (SustainIT) Conference*, 1:1–9, 2012.

[181] Ontario Energy Board. Electricity rates. `http://www.oeb.ca/rates-and-your-bill/electricity-rates`, 2020.

[182] B. Chatterjee. An optimization formulation to compute nash equilibrium in finite games. *IEEE Proceeding of International Conference on Methods and Models in Computer Science (ICM2CS)*, 1:1–5, 2009.

[183] L.B. Cunningham, R. Baldick, and M.L. Baughman. An empirical study of applied game theory: Transmission constrained Cournot behavior. *IEEE Transactions on Power Systems*, 17(1):166–172, 2002.

[184] D. Korzhyk, V. Conitzer, and R. Parr. Solving Stackelberg games with uncertain observability. *10th International Conference on Autonomous Agents and Multiagent Systems (AAMAS)*, 1:1013–1020, 2011.

[185] J. Marecki, G. Tesauro, and R. Segal. Playing repeated Stackelberg games with unknown opponents. *Proceedings of the 11th International Conference on Autonomous Agents and Multiagent Systems*, 2:821–828, 2012.

[186] V. Conitzer. On Stackelberg mixed strategies. *Synthese*, 193(3):689–703, 2016.

[187] J. Watson. Strategy: An Introduction to Game Theory. *W.W. Norton*, 183–199, 2008.

[188] S. Kakutani. A generalization of Brouwer's fixed point theorem. *Duke Mathematical Journal*, 8(3):457–459, 09 1941.

[189] H. Peters. Game theory: A multi-leveled approach. *Springer*, 197-209, 2015.

[190] P.J. Reny. On the existence of pure and mixed strategy Nash equilibria in discontinuous games. *Econometrica*, 67(5):1029–1056, 1999.

[191] S. Tadelis. Game theory: An introduction. *Princeton University Press*, 101-123, 2013.

[192] R.K. Arora. Optimization: algorithms and applications. *CRC Press*, 93-133, 2015.

[193] P.J. Rousseeuw. Silhouettes: A graphical aid to the interpretation and validation of cluster analysis. *Journal of Computational and Applied Mathematics*, 20:53–65, 1987.

[194] Z. Wang, U. Munawar, and R. Paranjape. Stochastic optimization for residential demand response with unit commitment and time of use. *IEEE Transactions on Industry Applications*, 57(2):1767–1778, 2021.

[195] Y. Qiu, D. Haley, T. Chan, and L. Davis. Game theoretic framework for studying WBAN coexistence: 2-player game analysis and n-player game estimation. *IEEE Australian Communications Theory Workshop (AusCTW)*, 1:53–58, 2016.

[196] C. Wu, H. Mohsenian-Rad, and J. Huang. Vehicle-to-aggregator interaction game. *IEEE Transactions on Smart Grid*, 3(1):434–442, 2011.

[197] A. Tzavellas, P. Nguyen, P. Ribeiro, and W. Kling. A game theory approach for coordinating multiple virtual synchronous generators. *IEEE Grenoble Conference*, 1:1–6, 2013.

[198] I. Steinwart and A. Christmann. Support vector machines. *Springer Science and Business Media*, 1-19, 2008.

[199] V. De Maio, R. Brundo Uriarte, and I. Brandic. Energy and profit-aware proof-of-stake offloading in blockchain-based VANETs. *Proceedings of the 12th IEEE/ACM International Conference on Utility and Cloud Computing*, 1:177–186, 2019.

[200] J. Yang, A. Paudel, and H.B. Gooi. Compensation for power loss by a proof-of-stake consortium blockchain microgrid. *IEEE Transactions on Industrial Informatics*, 17(5):3253–3262, 2020.

[201] J. Sedlmeir, H.U. Buhl, G. Fridgen, and R. Keller. Recent developments in blockchain technology and their impact on energy consumption. *arXiv preprint arXiv:2102.07886*, 2021.

[202] University of Ottawa SUNLAB Group. Photovoltaic testing at Ottawa region. http://sunlab.eecs.uottawa.ca/facilities/solar-test-sites/, 2018.

[203] Z. Wang, P. Jochem, and W. Fichtner. A scenario-based stochastic optimization model for charging scheduling of electric vehicles under uncertainties of vehicle availability and charging demand. *Journal of Cleaner Production*, 254:119886, 2020.

[204] W. Diffie and M. Hellman. New directions in cryptography. *IEEE Transactions on Information Theory*, 22(6):644–654, 1976.

[205] E.G. Julie, J.J.V. Nayahi, and N. Jhanjhi. Blockchain Technology: Fundamentals, Applications, and Case Studies. *CRC Press*, 14-21, 2020.

[206] K.J. O'Dwyer and D. Malone. Bitcoin mining and its energy footprint. *Proceeding 25th IET Irish Signals System Conference (ISSC)*, 1:280–285, 2014.

[207] M. Samadi, J. Fattahi, H. Schriemer, and M. Erol-Kantarci. Demand management for optimized energy usage and consumer comfort using sequential optimization. *Sensors*, 21(1):130–146, 2021.

[208] M. Samadi, H. Kebriaei, H. Schriemer, and M. Erol-Kantarci. Stochastic demand response management using mixed-strategy Stackelberg game. *IEEE Systems Journal*, 2022.

[209] M. Samadi, H. Schriemer, S. Ruj, and M. Erol-Kantarci. Energy blockchain for demand response and distributed energy resource management. *12th IEEE International Conference on Communications, Control, and Computing Technologies for Smart Grids (SmartGridComm)*, 1:425–431, 2021.

[210] M. Samadi, S. Ruj, H. Schriemer, and M. Erol-Kantarci. Energy blockchain for demand response and distributed energy resource management. *IEEE Internet of Things Journal*, 2022.

[211] J.F. Nash. Equilibrium points in n-person games. *Proceedings of the National Academy of Sciences*, 36(1):48–49, 1950.

[212] Ankur A. Kulkarni. Stackelberg game. https://www.sc.iitb.ac.in/~ankur/docs/SC631Notes/SC631_2014_Lecture23.pdf, 2014.

[213] R. Johari. Lecture notes — MS&E 246: Lecture 7 Stackelberg games — Stanford University. http://web.stanford.edu/~rjohari/teaching/notes/246_lecture7_2007.pdf, 2007.

APPENDICES

Appendix A

Game Theory

Game is an optimal decision-making solution between the agents, that defines as follows;

$$\Gamma = (\mathcal{N}, \{S^n\}_{n\in\mathcal{N}}, \{U^n\}_{n\in\mathcal{N}}) \tag{A.1}$$

where $\mathcal{N} = \{1, \ldots, N\}$ a finite set of N players who play in the game, S^n is the space of pure strategies for player $n \in \mathcal{N}$ that are the possible moves of players in the game, and U^n represents the utility function for player n [189].

- **Cooperative and non-cooperative game.** In a cooperative game, players have information about strategies of each other and choose their strategies accordingly. However, in a non-cooperative game, players choose their strategies individually without any information about others' decisions [189].

- **Simultaneous and sequential game.** In a simultaneous game, all players choose their strategies simultaneously, but in the sequential game, some players choose their strategies first, and then the rest choose their strategies accordingly. Note that the leader-follower (Stackelberg game) game is a sequential game.

- **Pure strategy and mixed strategy game.** In a pure strategy game, the player selects one strategy with probability equal to one as a final decision. However, in a mixed strategy (random strategy) game, the player could have different strategies with different probability values (the summation of probabilities is equal to one) for their final decision.

- **Nash equilibrium (NE).** Nash equilibrium happens when all the players want to improve their profits and choose their best responses (BR). A game reaches a NE point when no player has incentives to change their strategy to get a better payoff value [211]. NE tells us that an optimal point exists in the game where all players are satisfied. The mathematical definition of BR is defined as follows.

$$U^n(S^{n^*}, S^{-n^*}) \geq U^n(S^n, S^{-n^*}), \forall n \in \mathcal{N} \tag{A.2}$$

  where S^{n^*} is the player n's set of best response (best strategies) and S^{-n^*} is the set of best response for other players. To prove the existence of NE in a game model, the terms of the Kakutani theorem [110] have to be satisfied. These terms are presented in the following.

  1. S^n is a compact and convex set in Euclidean space.
  2. $U^n(s^n)$ is non-empty for all $s^n \in S^n$.
  3. For all $s^n \in S^n, U^n(s^n)$ is a continuous and convex set.

  where $s^n \in S^n$ is a pure strategy of player n.

- **Stackelberg game.** Stackelberg game is a sequential game model that one player (as a leader) has the power to choose the first movement, and all other players (as followers) move after that [58]. This loop repeats till there is no temp for players to change their strategies, and the resulting pair of strategies is called Stackelberg equilibrium (SE). For a two players Stackelberg game model, player one (as a leader) selects s^1 strategy as the first move, then player 2 (as a follower) chooses s^2 using;

$$s^2 = \underset{s^2 \in S^2}{\operatorname{argmax}}\, U^2(s^1, s^2). \tag{A.3}$$

Because s^2 is found by s^1 (dependent to s^1 strategy), it is shown as $s^2(s^1)$. Then player 1 updates its strategy s^1 using;

$$s^1 = \underset{s^1 \in S^1}{\operatorname{argmax}} U^1(s^1, s^2(s^1)). \tag{A.4}$$

These steps repeat till there is no incentive for players to change their strategies. Finally, the best responses of players 1 and 2, s_1^* and s_2^*, would be the equilibrium outcome [212,213]. Moreover, the existence of Stackelberg equilibrium (SE) could be demonstrated by dividing the game into subgames (leader and follower subgames) [187] and then proving the NE for each subgame.